DYNAMIC ANALYSIS OF UNDERGROUND CYLINDERS SUBJECTED TO EARTHQUAKE EXCITATIONS

Thesis for the Degree of Ph. D.

MICHIGAN STATE UNIVERSITY

PAIBOON CHOWCHUVECH

1973

This is to certify that the

thesis entitled

DYNAMIC ANALYSIS OF UNDERGROUND
CYLINDERS SUBJECTED TO EARTHQUAKE EXCITATIONS

presented by

Paiboon Chowchuvech

has been accepted towards fulfillment
of the requirements for

PH.D. degree in Civil Engineering

Robert K. Wen
Major professor

Date November 1, 1973

O-7639

ABSTRACT

DYNAMIC ANALYSIS OF UNDERGROUND CYLINDERS
SUBJECTED TO EARTHQUAKE EXCITATIONS

By

Paiboon Chowchuvech

An analytical study is made of the dynamic response of buried cylinders subjected to horizontal and vertical earthquake excitations. The problem is assumed to be one of plane strain, the axis of the cylinder being perpendicular to the plane. Both the cylinder and the soil are assumed to have linear stress-strain relationships.

A typical column of "free field" soil at a large distance horizontally from the cylinder is modelled by a series of springs and dashpots which is excited by the bedrock earthquake accelerations. The responses of the free field soil are used as inputs to a "cylinder-soil composite". The latter represents the cylinder and the soil in its vicinity within which the cylinder-soil interaction is considered significant. Within the region of the cylinder-soil composite, the soil is idealized by two-dimensional finite elements and, immediately around the cylinder, by radial springs. The cylinder is represented by either a lumped mass, continuous flexibility model or an infinitely rigid model.

Analyses based on both the modal analysis method and direct integration are programmed in FORTRAN for a numerical solution of the problem on the CDC 6500 System of Michigan State University.

Response analysis and parametric studies were made. It was found that the response of the flexible cylinder case would converge to that of a rigid one as the stiffness of the flexible cylinder is increased. The rigid case requires much less computer time. Curves are given which show quantitative relationships between the cylinder stiffness and the convergence of the lowest five frequencies to those of the rigid cylinder case. The response of the cylinder depends on the bedrock accelerations and the free field soil displacements and velocities. It was found that the free field displacement inputs dominated the response. It was found that the modal analysis as formulated required a high degree of computational precision and the inclusion of higher modes. To alleviate these computational difficulties, it is suggested that the free field displacement inputs be decomposed into a uniform part and a deviatory part.Effects on the frequencies due to variation of a number of modelling parameters are also considered. These parameters include: the number of cylinder nodes, the distance of the boundary of the cylinder-soil composite away from the cylinder, and the width of the soil represented by radial springs.

DYNAMIC ANALYSIS OF UNDERGROUND CYLINDERS SUBJECTED TO EARTHQUAKE EXCITATIONS

By

Paiboon Chowchuvech

A THESIS

Submitted to
Michigan State University
in partial fulfillment of the requirements
for the degree of

DOCTOR OF PHILOSOPHY

Department of Civil Engineering

1973

ACKNOWLEDGMENTS

The auther would like to express his sincere gratitude to Dr. R.K. Wen who helped him so many times, in so many ways, during the past five years both in the author's personal life and his academic development. The completion of this thesis is due to him for freely providing help, guidance and advice. Thanks are also expressed to the other members of the guidance committee: Dr. J.L. Lubkin who offered valuable suggestions on computer usage; Dr. W.A. Bradley who inspird him as a teacher; and Dr. J.S. Frame who, knowing the author's home country personally, took special interest in his welfare.

The author will always be indebted to his wife, Karen, whose love, help and companionship sustained him through the rigor of preparing a thesis.

This thesis is dedicated to the author's parents, Mr. Viboon and Mrs. Sumana Chowchuvech, who loved and cared for him in the early years, and provided the opportunity for an education that led to his doctoral program.

TABLE OF CONTENTS

Page

LIST OF TABLES

LIST OF FIGURES

Figure		Page

LIST OF SYMBOLS

A_r = area of one unit depth of the cylinder wall;

[A] = displacements transformation matrix;

[B] = strain interpolation function matrix;

b_i, b_j, b_m = constants involving coordinates of triangular finite elements nodes;

[B'] = force transformation matrix;

[C] = damping matrix;

C_i = compressive dashpot constant for the ith interval of the free field soil;

c_i = shear dashpot constant for the ith interval of the free field soil;

[D] = stress-strain relationship matrix;

d_i, d_j, d_m = constants involving coordinates of triangular finite element nodes;

d_{xi}, d_{yi} = horizontal and vertical distances between node i and the center of the cylinder;

D_1, D_2, D_3 = displacements in the x and y directions and rotation at the free end of the released structure;

E = unconstrained elastic modulus of soil;

E_s = constrained elastic modulus of soil;

E_r = elastic modulus of cylinder material in plain strain;

f_i = tangential D'Alembert forces

$F_{x\ total}$, $F_{y\ total}$ = Total forces on the rigid cylinder;

F_{xi}, F_{yi} = forces on the cylinder node i;

$\{F\}$ = translational forces vector in global coordinates;

$\{F_m\}$ = force vector of a cylinder arc in local coordinates;

$[F_{BB}]$ = flexibility matrix of a cylinder arc;

$\{F_R\}$ = vector of moments on the cylinder nodes;

$\{F_{ex}\}$,$\{F_{in}\}$ = forces vector of the exterior and interior nodes;

$\{F_S\}$ = force vector of soil nodes;

$\{F'\}$ = rigid cylinder force vector

F_I, F_S, F_D = inertia, elastic and damping force vector;

F'_{xi} , F'_{yi} = tangential D'Alembert forces for cylinder node i;

F''_{xi} , F''_{yi} = final forces on cylinder node i

$[FLEX]_i$ = flexibility matrix for cylinder node i in global coordinates;

$[FLEX_{local}]_i$ = flexibility matrix in local coordinates

$\{F_{int}\}$ = internal force vector at cylinder cut;

G_s = unconstrained shear modulus of soil;

I_r = moment of inertia of one unit depth of cylinder wall;

K_i = compression spring constant for free field;

k_i = shear ,, ,, ,, ,, ;

$[K]$ = matrix for eigenproblem;

K_c = total spring force on rigid cylinder;

l_i = length of ith interval of free field soil column;

m_i = i^{th} mass of free field;

$[M_I]$ = mass matrix of the interior nodes;

$[M_{in}]$ = mass matrix of interior nodes of finite element quadrangle;

M_{rigid} = total mass of all the cylinder nodes;

M = moment on rigid cylinder;

$\{M_0\}_i$ = modal moment vector;

nr = number of cylinder nodes;

ni = number of interior nodes of the cylinder-soil composite;

m_s = mass density of soil;

m_r = mass density of cylinder material;

P1 = shear spring constant of packing soil;

P2 = compression spring constant of packing soil;

$\{P\}$ = applied force vector;

R = cylinder radius;

$[R_B]$ = coordinate rotation matrix;

$[R^i]$ = rotation matrix for packing soil spring;

$[S]$ = stiffness matrix;

$[S_R^*]$ = translational stiffness matrix;

$[S_m]$ = local stiffness matrix of a cylinder arc;

$[S_{BB}]$ = stiffness matrix of a cylinder arc;

$[S_s]^i$ = global stiffness matrix for member i of the cylinder;

$[S']$ = stiffness matrix for rigid cylinder-soil composite;

$[S_{overall}]$ = stiffness matrix for cylinder nodes (rotation included);

$[S'_{overall}]$ = rearrangement of $[S_{overall}]$;

$[S_p]_{local}$ = local stiffness matrix for a packing soil spring;

$[S_p]^i_{global}$ = global stiffness matrix for a packing soil spring;

$[S_{triangle}]$ = triangular finite element stiffness matrix;

$[S_{quad}]$ = stiffness matrix of finite element quadrangle;

$[S_F^*]$ = modified stiffness matrix for finite element quadrangle;

$[S_{in}]$ = stiffness involving node i and node n;

$[T'_{AB}]$ = transformation matrix for parallel coordinates;

$[T_{AB}]$ = transformation matrix including coordinates rotation;

TH = thickness of packing soil annulation;

t' = thickness of finite element;

t = time instant

$\{U_{ex}\},\{U_{in}\}$ = displacement vector of the exterior node and interior node of the finite element quadrangle;

$\{U\}$ = displacement vector of cylinder node in global coordinates;

$\{U_m\}$ = displacement vector of a cylinder arc in local coordinates;

$\{U_S\}$ = displacement vector of soil nodes;

u_i = horizontal displacement of the ith free field soil mass;

$\ddot{u}_g$ = bedrock horizontal accelerations;

$\{U_B\}$ = displacement vector of the boundary nodes;

$\{u_F\}$ = free field displacement inputs;

$\{U_I\}$ = displacement vector of the interior nodes;

U_{n1},U_{n2} = displacement of the packing soil node n;

U_{i1}, U_{i2} = displacement of cylinder node i;

$U_{x\ rigid}$, $U_{y\ rigid}$ = accelerations of the rigid cylinder;

v = displacement in a triangular finite element;

$\ddot{v}_g$ = bedrock vertical accelerations;

W_d = average width of packing soil area;

X_I = coordinate in the x direction of interior node I;

x = coordinate within a triangular finite element;

$\{X_i\}$ = shape of the ith mode;

$\{\ddot{X}_g\}$ = vector with bedrock horizontal and vertical accelerations alternately placed;

Y_I = coordinate in the y direction of interior node I;

y = coordinate within the triangular finite element;

$\{\sigma\}_d$ = vector of damping stresses;

μ = damping proportionality constant;

$\{\varepsilon\}$ = strain vector;

ν_s = Poisson's ratio of soil;

α = subtending angle;

θ_i = angle to the horizontal of the packing soil spring;

$\alpha_1, \alpha_2, \ldots, \alpha_6$ = constants in the finite element displacement function;

Δ = area of a finite element triangle;

λ_n = damping ratio;

ω_n = circular frequency;

$[\Phi]$ = matrix of modal columns;

Δt = time increment;

$\dot{(\ )}$ = $\frac{d(\ )}{dt}$

$\ddot{(\ )}$ = $\frac{d^2(\ )}{dt^2}$

CHAPTER I

INTRODUCTION

1.1 General

For a variety of reasons, it has been often found desirable or even necessary to build structures underground. Tunnels have been constructed to shorten the distance of travel, culverts to provide drainage, and underground pipes to minimize man's intrusion on the landscape.

There have been extensive experimental and analytical works done on the problem of buried structures. Earlier investigations had concentrated on the statics of the problem. More recently the dynamic response of these structures, particularly under a seismic environment, has been increasingly receiving the attention of civil engineering researchers.

The development has arisen mainly from two causes. The first is the continuing need to construct underground structures (for example, the planned underground oil pipeline across part of the seismic region in Alaska). The other is the advancement of computer technology and the attendant development in numerical methods of structural mechanics.

The problem under consideration is a highly complex one. Past works (see Section 1.3) have been generally concerned with very specific cases. The present study attempts to examine the problem of buried cylinders subject to earthquakes on a broader scope by

using the latest state-of-the-art.

1.2 Objectives and Scope

The objectives of this study are two-fold: to develop a numerical model and solution procedure for the analysis of a buried cylinder subjected to earthquake effects, and to use the method to obtain numerical data in order to gain a clearer understanding of the problem such as the relative importance of the physical parameters as well as the modelling parameters.

The problem is assumed to be one of plane strain, the axis of the cylinder being perpendicular to the plane. Both the cylinder and the soil are assumed to have linear stress-strain relationship. The cylinder and the soil around it is considered to be in contact at all times. A proportional viscous type of damping is assumed. The discrete model developed for the problem consists of two separate parts:

a). A series of springs and dashpots representing a column of soil at a large distance horizontally from the cylinder where the effect of the cylinder inclusion is negligible.

b). A rectangular composite consisting of two -dimensional soil finite elements surrounding a smaller annular area of radial soil springs which in turn circumscribe the cylinder.

The cylinder is represented by either a lumped mass continuous flexibility, or an infinitely rigid model. The composite represents the area in which the cylinder-soil interaction is significant.

The bedrock earthquake motion is transmitted upward through the soil layer of part a), whose motions will be used as inputs to the boundary of part b).

Numerical analyses based on both direct integration and the modal analysis method are formulated and programmed in FORTRAN. Parametric studies and response analysis were made using the programs developed. As the stiffness of the cylinder is increased, the response of the cylinder is found to approach that of a rigid cylinder. The latter case takes much smaller computer time to solve. The response of the cylinder depends on the bedrock accelerations and the displacements and velocities inputs to the boundary of part b). It is found that the influence of the displacements input was predominant. Results from modal analysis suggests that a uniform part of this displacements input should be separated from a deviatory part if the inclusion of the higher modes and the necessity for a high degree of computational precision are to be avoided.

1.3 Related Works

One of the earliest civil engineering treatment of soil structure interaction is in the area of design of culverts to withstand overburden loads. Marston (1)* first formulated the theory for loads on underground conduits. This work was continued by Spangler (2), the result being the well known Iowa Formula which predicts the vertical deflection of culverts. Other methods of design for loads on culverts can be found in (3).

---

*Numbers refer to references listed in the bibliography.

Further works along this line were concerned with the buckling loads of buried pipes and arching. Among the well known findings is the fact that the buried cylinders have several times higher loads at failure than in-air cylinders. Allgood (4) and Clarke (18) provide good references on the current state-of-the-art in the design of buried culverts and pipelines. In all the works cited above, the methods of analysis are semi-empirical in which certain gross approximations were made, based on experimental observations, as to the nature and the distribution of overburden loads on the culverts.

Mow and McCabe (5), using the theory of elasticity, derived expressions for stresses around a thick elastic cylinder in an infinite elastic media during the passage of a plane compressional wave. Robinson (6) used the Fourier frequency analysis for the problem of a plane wave in an elastic half space traversing a buried cylinder. In both of these works, the method of analysis, giving a closed form solution, are not easily adaptable to more complex patterns of loading and/or boundary conditions.

Ang and Chang (7) used a discrete model analogous to a central finite difference approximation to solve the problem of a plane blast wave acting on the ground surface of a half space soil medium surrounding a tunnel. The procedure can also easily incorporate nonlinear soil behavior. However, the discretization pattern must follow a systematic scheme. For a cylindrical tunnel, for example, the domain must be formulated in cylindrical coordinates in order to meet the conditions inherent in the finite difference procedure. Thus it would be difficult to apply this approach to problems with complex

boundaries.

Dawkin (13) studied the problem of a reinforced concrete tunnel protected against stress wave passing through the surrounding rock by a layer of liner-packing system. A lumped mass, lumped flexibility model was used for the tunnel and the packing material is represented by a number of radial massless springs. He found that a minimum of twelve mass nodes are required to reasonably predict the behavior of the system. In the present study the cylinder and the soil in its immediate vicinity will be modelled similar to the above except that the cylinder will have continuous flexibility.

The method of finite element is very easily adaptable to irregularities in material properties or boundary conditions and, as a result, has found many applications involving interaction of soil and structures. Costantino, Wachowski and Barnwell (8) developed a computer program that can treat the problem of a general two-dimensional continuum with irregular soil layers and inclusions subjected to nuclear detonation. Yamada (9, 10) cited the results of some works done in Japan in which the finite element method is applied to the problem of foundation structures and underground tunnels subjected to earthquake. Results pertinent to individual cases are also given. In both the works cited above, the finite elements representing the soil were extended down to bedrock and horizontally to the two side boundaries at a relatively large distance from the inclusions, which made the problem rather large in scope (and expensive to solve). Roller supports were provided at the side boundary nodes. In this study finite elements will also be used,

but only to idealize a smaller area of soil.

Finally, in cases where (i) there is no inclusion in the soil medium, (ii) the ground surface, the rock surface and the boundaries between soil layers with different properties are essentially horizontal, and (iii) the lateral extent of the soil is so large that it exerts only negligible influence on the response, the problem can then be analyzed as a column of soil being excited at the bedrock end. Idriss and Seed (11) solved such a problem using a lumped mass springs and dashpots model and the results were found to be in good agreement with those obtained from closed form solutions. A procedure was also outlined for obtaining equivalent linear parameters for a soil with bilinear characteristics. The result obtained using this procedure was found to be in good agreement with those obtained from the bilinear case. Penzien, Scheffey and Parmelee (12) utilized results obtained from the procedure in (11) as free field inputs in determining the interaction of a bridge and piles system with a moving clay medium.

CHAPTER II

DISCRETE MODEL

2.1 General

In order to keep the computer cost within practical limits for this study, it is necessary that the number of degrees of freedom first be reduced to a manageable size. This is achieved by separating the horizontally infinite soil medium with the embedded cylinder as shown in Figure 2.1a into two different parts as illustrated in Figure 2.1b. The first part consists of that portion of the soil medium far enough from the cylinder that its behavior is essentially the same as that when no cylinder is present in the soil. In such a case, there will not be any interaction between adjacent columns of soil (11) and the behavior of all soil at far enough distance from the cylinder can be studied by considering any one typical soil column, hereafter referred to as the free field soil column. This soil column can be represented by a lumped mass spring-dashpot model as indicated in Figure 2.1b.

The second part, hereafter referred to as the cylinder-soil composite, consists of the cylinder and the soil medium within a distance of B from the sides and from the bottom of the cylinder. This is the region in which the cylinder-soil interaction is considered significant. The cylinder will be represented by a lumped mass, continuous flexibility model, the soil immediately around the cylinder, hereafter referred to as the packing soil, by a number of radial springs and the rest of

the soil by finite elements.

The mass matrix used in this study is of the diagonal "lumped mass" formulation which has been found to yield results with similar degree of accuracy as the "consistent mass" formulation(16). It is also easy to formulate and requires less computational efforts.

2.2 Basic Assumptions

The basic assumptions implied by the discrete model are summarized in the following.

a). The problem is assumed to be one of plane strain. Variation of loading in the axial direction of the cylinder is neglected.

b). If the side and the bottom boundaries of the cylinder-soil composite are taken far enough from the cylinder, wave reflections at these boundaries would be negligible. It is assumed that the feedback between the responses of the free field soil column and those of the cylinder-soil composite is negligible.

c). The stress-strain relationships for both the materials making up the cylinder and the soil are assumed to be linear. For the soil, this linear modulus will be the same as the equivalent linear modulus in (11).

d). Damping is assumed to be of the linearly viscous type. The damping stresses are assumed to be proportional to the strain velocities, i.e.,

$$\{\sigma\}_d = \mu[D]\{\dot{\varepsilon}\} \qquad .....(2\text{-}1)$$

where $\{\sigma\}_d$ denotes the damping stresses, μ is the damping constant, $[D]$ denotes the stress-strain relationship and $\{\dot{\varepsilon}\}$ denotes the strain velocities. This is a frequently used assumption that would render the

damping matrix proportional to the stiffness matrix, i.e.,

$$[C] = \mu\ [S] \qquad .....(2\text{-}2)$$

where $[C]$ denotes the damping matrix and $[S]$ denotes the stiffness matrix.

2.3 Free Field Soil Column

As shown in Figure 2.1b, the free field soil column will be idealized by a series of lumped masses $m_1, m_2, \ldots m_n$, interconnected by springs and dashpots. The spring constants K_i and k_i represent the compressive and shear stiffness properties of the soil between any two masses m_i and m_{i-1}. Likewise the dashpot constants C_i and c_i represent the compressive and shear damping properties. If E and G_s denote the unconstrained modulus of elasticity and the shear modulus of elasticity of the soil, respectively, at level i, then the constrained modulus of elasticity, E_s, at level i will be given by

$$E_s = \frac{E\ (1-\nu_s)}{(1-2\nu_s)\ (1+\nu_s)} \qquad .....(2\text{-}3)$$

where ν_s denotes the soil Poisson's ratio.

The spring constants K_i and k_i will be given by

$$K_i = \frac{E_s}{l_i}$$

$$k_i = \frac{G_s}{l_i} \qquad .....(2\text{-}4a)$$

and the dashpot constants C_i and c_i will be given by

$$C_i = \mu K_i$$
$$c_i = \mu k_i \qquad \text{.....(2-4b)}$$

where μ is the damping constant defined in Eqs.(2-1) and (2-2). The mass, m_i, will be given by

$$m_i = \left(\frac{l_{i+1}}{2} m_s\right) + \left(\frac{l_i}{2} m_s\right) \qquad \text{for } i = 1,2,\ldots,n-1 \qquad \text{.....(2-4c)}$$

and, $$m_n = \frac{l_n}{2} m_s$$

where m_s is the mass per unit volume of the soil.

2.4 Cylinder-Soil Composite

2.4.1 Cylinder

As shown in Figure 2.2, the cylinder is idealized by a lumped mass, continuous flexibility model. The masses are equally spaced around the cylinder with each mass attached to a spring of the packing soil. The mass of a typical mass i is computed simply as the sum of the mass of the cylinder wall segment of length αR (see Figure 2.2) and the mass of the packing soil from the tributary area Al.

It is reasonable to assume that the packing soil spring exerts no rotational constraint on the lumped mass of the cylinder to which it is attached. If the number of the lumped masses on the cylinder is "nr" , the cylinder stiffness would be the 2nr×2nr matrix $[S_R^*]$ which relates the cylinder node forces to node displacements as follows:

$$\{F\} = [S_R^*]\{U\} \qquad .....(2\text{-}5)$$

where, as shown in Figure 2.3, $\{F\} = \{F_1, F_2, \ldots, F_{2nr}\}$ is the translational forces vector, and $\{U\} = \{U_1, U_2, \ldots, U_{2nr}\}$ is the corresponding displacements vector, both in global coordinates. $\{F\}$ and $\{U\}$ are column vectors. (The notation in which $\{F_1, F_2, \ldots F_{2nr}\}$, for example, represents a column vector will be used throughout this investigation).

The procedure to obtain $[S_R^*]$ is described in the following.

a). Local stiffness matrix, $[S_m]$, of a typical arc. Figure 2.4a shows a typical cylinder arc between two mass points A and B. The local stiffness matrix $[S_m]$ is such that

$$\{F_m\} = [S_m]\{U_m\} \qquad .....(2\text{-}6)$$

where $\{F_m\} = \{F_{A1}, F_{A2}, F_{A3}, \vdots F_{B1}, F_{B2}, F_{B3}\}$ is the force vector (moments included) in local coordinates, and $\{U_m\} = \{U_{A1}, U_{A2}, U_{A3}, \vdots U_{B1}, U_{B2}, U_{B3}\}$ is the displacement vector (rotations included) in local coordinates. $[S_m]$ can be partitioned corresponding to nodes A and B:

$$[S_m] = \left[\begin{array}{c|c} S_{AA} & S_{AB} \\ \hline S_{BA} & S_{BB} \end{array}\right] \qquad .....(2\text{-}7)$$

The flexibility matrix , $[F_{BB}]$, for the structure shown in Figure 2.4b can be found, for example, by the principle of minimum strain energy to be:

$$[F_{BB}] = \left[\begin{array}{c|c|c} \frac{R^3(6\alpha-8\sin\alpha+\sin 2\alpha)}{4E_rI_r} + \frac{R(2\alpha+\sin 2\alpha)}{4A_rE_r} & \frac{-R^3(1-\cos\alpha)^2}{2E_rI_r} + \frac{R(1-\cos 2\alpha)}{4A_rE_r} & \frac{-R^2(\alpha-\sin\alpha)}{E_rI_r} \\ \hline -\frac{R^3(1-\cos\alpha)^2}{2E_rI_r} + \frac{R(1-\cos 2\alpha)}{4A_rE_r} & \frac{R^3(2\alpha-\sin 2\alpha)}{4E_rI_r} + \frac{R(2\alpha-\sin 2\alpha)}{4A_rE_r} & \frac{R^2(1-\cos\alpha)}{E_rI_r} \\ \hline \frac{-R^2(\alpha-\sin\alpha)}{E_rI_r} & \frac{R^2(1-\cos\alpha)}{E_rI_r} & \frac{R\alpha}{E_rI_r} \end{array}\right] \quad \ldots\ldots(2\text{-}8)$$

where E_r is the modulus of elasticity of the cylinder material in plain strain, A_r and I_r are the area and the moment of inertia of one unit depth of the cylinder wall, α is the subtending angle and R is the radius of the cylinder.

The stiffness matrix $[S_{BB}]$ in Eq.(2-7) can be calculated as:

$$[S_{BB}] = [F_{BB}]^{-1} = \begin{bmatrix} S_{11} & S_{12} & S_{13} \\ S_{21} & S_{22} & S_{23} \\ S_{31} & S_{32} & S_{33} \end{bmatrix} \quad \ldots\ldots(2\text{-}9)$$

To obtain $[S_{AB}]$ by statics from $[S_{BB}]$, the coordinate transformation matrix $[T_{AB}]$ has to be found first. It may be written as:

$$[T_{AB}] = [R_B][T'_{AB}] \quad \ldots\ldots(2\text{-}10)$$

where $$[R_B] = \begin{bmatrix} \cos\alpha & \sin\alpha & 0 \\ -\sin\alpha & \cos\alpha & 0 \\ 0 & 0 & 1 \end{bmatrix} \quad \ldots\ldots(2\text{-}11)$$

rotates the local coordinates at B to those at A;

and, $$[T'_{AB}] = \begin{bmatrix} 1 & 0 & 0 \\ 0 & 1 & 0 \\ R(1-\cos\alpha) & R\sin\alpha & 1 \end{bmatrix} \qquad .....(2\text{-}12)$$

translates the parallel coordinates from B to A.

Substituting Eq.(2-11) and Eq.(2-12) in Eq.(2-10), we have

$$[T_{AB}] = \begin{bmatrix} \cos\alpha & \sin\alpha & 0 \\ -\sin\alpha & \cos\alpha & 0 \\ -R(1-\cos\alpha) & R\sin\alpha & 1 \end{bmatrix} \qquad .....(2\text{-}13)$$

Then each column of $[S_{AB}]$ is just the static equilibrating force vector at A for each column of $[S_{BB}]$, i.e.,

$$[S_{AB}] = -[T_{AB}][S_{BB}]$$

$$= \left[\begin{array}{c|c|c} -S_{11}\cos\alpha & -S_{12}\cos\alpha & -S_{13}\cos\alpha \\ -S_{21}\sin\alpha & -S_{22}\sin\alpha & -S_{23}\sin\alpha \\ \hline S_{11}\sin\alpha & S_{12}\sin\alpha & S_{13}\sin\alpha \\ -S_{21}\cos\alpha & -S_{22}\cos\alpha & -S_{23}\cos\alpha \\ \hline -S_{31} & -S_{32} & -S_{33} \\ +S_{11}R(1-\cos\alpha) & +S_{12}R(1-\cos\alpha) & +S_{13}R(1-\cos\alpha) \\ -S_{21}R\sin\alpha & -S_{22}R\sin\alpha & -S_{23}R\sin\alpha \end{array}\right]$$

.....(2-14a)

The other two submatrices in Eq.(2-7) can be computed as

$$[S_{BA}] = [S_{AB}]^T \qquad .....(2\text{-}14b)$$

and $$[S_{AA}] = [T_{AB}][S_{BB}][T_{AB}]^T \qquad .....(2\text{-}14c)$$

The latter, in the case of a circular arc with coordinates at A and B defined as in Figure 2.4a, reduces simply to

$$[S_{AA}] = \begin{bmatrix} S_{11} & -S_{12} & S_{13} \\ -S_{21} & S_{22} & -S_{23} \\ S_{31} & -S_{32} & S_{33} \end{bmatrix} \qquad .....(2\text{-}15)$$

Thus all the submatrices for $[S_m]$ in Eq.(2-7) are obtained.

b). <u>Rotation to global coordinates.</u> The local stiffness matrix, $[S_m]$, of an arc is used to obtain the global stiffness matrix, $[S_s]^i$, for member i between cylinder node points A and B as illustrated in Figure 2.5:

$$[S_s]^i = [R_i]^T [S_m][R_i] \qquad .....(2\text{-}16)$$

where $$[R_i] = \left[\begin{array}{ccc|ccc} \cos\theta_A & \sin\theta_A & 0 & & & \\ -\sin\theta_A & \cos\theta_A & 0 & & 0 & \\ 0 & 0 & 1 & & & \\ \hline & & & \cos\theta_B & \sin\theta_B & 0 \\ & 0 & & -\sin\theta_B & \cos\theta_B & 0 \\ & & & 0 & 0 & 1 \end{array}\right] \qquad .....(2\text{-}17)$$

The matrix $[S_s]^i$ can be partitioned corresponding to end A and B of member i as follows:

$$[S_s]^i = \begin{bmatrix} S_{AA}{}^i & S_{AB}{}^i \\ S_{BA}{}^i & S_{BB}{}^i \end{bmatrix} \qquad .....(2\text{-}18)$$

c). <u>Assembly of overall cylinder stiffness matrix, rotation included</u>

Once $[S_s]^i$ for all the cylinder nodes, i=1,2,...,nr, have been found, the overall cylinder stiffness matrix, $[S_{overall}]$, can be assembled by putting the submatrices $[S_{AA}{}^i]$, $[S_{AB}{}^i]$... etc in the appropriate joint locations in $[S_{overall}]$. For a node numbering system that increases consecutively around the cylinder as in Figure 2.3, $[S_{overall}]$ is assembled as:

$$[S_{overall}] = \begin{bmatrix} S_{AA}^{1} + S_{BB}^{nr} & S_{AB}^{1} & & & & S_{BA}^{nr} \\ S_{BA}^{1} & S_{BB}^{1} + S_{AA}^{2} & S_{AB}^{2} & & & \\ & S_{BA}^{2} & S_{BB}^{2} + S_{AA}^{3} & & & \\ & & & \ddots & & \\ & 0 & & & S_{AB}^{nr-1} & \\ S_{AB}^{nr} & & & & S_{BA}^{nr-1} & S_{BB}^{nr-1} + S_{AA}^{nr} \end{bmatrix}$$

member 1

member 2

member 3

.....(2-19)

d). Modified overall cylinder stiffness matrix (no rotational constraints).

$[S_{overall}]$ in Eq.(2-19) can be rearranged to separate translation and rotations. The rearranged matrix, $[S'_{overall}]$ is such that

$$\begin{Bmatrix} F \\ -- \\ F_R \end{Bmatrix} = [S'_{overall}] \begin{Bmatrix} U \\ -- \\ U_R \end{Bmatrix}$$

$$= \begin{bmatrix} S_{TT} & S_{TR} \\ S_{RT} & S_{RR} \end{bmatrix} \begin{Bmatrix} U \\ -- \\ U_R \end{Bmatrix} \qquad .....(2\text{-}20)$$

where {F} and {U} refer to translational forces and displacements, and $\{F_R\}$ and $\{U_R\}$ refer to moments and rotational displacements. The condition that the moments at all the nodes be zero is now imposed, i.e.,

$$\{F_R\} = \{0\} = [S_{RT}]\{U\} + [S_{RR}]\{U_R\} \qquad .....(2\text{-}21a)$$

from which

$$\{U_R\} = -\,[S_{RR}]^{-1}\,[S_{RT}]\{U\} \qquad .....(2\text{-}21b)$$

Also, from Eq.(2-20)

$$\{F\} = [S_{TT}]\{U\} + [S_{TR}]\{U_R\} \qquad .....(2\text{-}22a)$$

Substitution of Eq.(2-21b) in Eq.(2-22a) yields

$$\{F\} = ([S_{TT}] - [S_{TR}][S_{RR}]^{-1}\,[S_{RT}])\{U\}$$

$$= [S_R^*]\{U\} \qquad .....(2\text{-}22b)$$

Therefore, the final modified cylinder stiffness matrix, $[S_R^*]$, mentioned

in Eq.(2-5) is given as

$$[S_R^*] = [S_{TT}] - [S_{TR}][S_{RR}]^{-1}[S_{RT}] \qquad .....(2\text{-}23)$$

The elements of $[S_R^*]$ can then be put directly in the appropriate rows and columns in the stiffness matrix of the cylinder-soil composite.

2.4.2 Packing Soil

As mentioned previously and illustrated in Figure 2.1b and Figure 2.2, the term packing soil used in this study refers to an annular area of soil immediately around the cylinder. The thickness of this annulation is arbitrarily set at a small number relative to the dimensions of the cylinder-soil composite. The packing soil is modelled by radial shear and compression springs as opposed to the rest of the soil in the cylinder-soil composite which is modelled by two-dimensional finite elements. There is no particular advantage, computational or otherwise, from this aspect of modelling of the soil other than the fact that recognition is given to the following situation. Oftentimes in mining engineering practices, as pointed out in (13), a layer of soft, energy absorbing packing material is built around a tunnel to reduce the effects of disturbances transmitted from the surrounding rock medium. A spring would be appropriate to use as a model for such a material. However, in this investigation no such packing material is assumed and the term "packing soil" is used to designate the soil around the cylinder that is represented by springs rather than by finite elements.

The packing soil mass of area A1 (see Figure 2.2) will be lumped with the cylinder mass node m_i to which one end of the spring

is attached. The packing soil mass of area A2 will be lumped at the soil mass node (node J in Figure 2.2), to which the other end of the spring is attached. Node J will also include 1/4 of the mass from the soil finite elements JKLM and JMNO

In Figure 2.6 the shear spring constant, P1, and the compression spring constant, P2, are approximated by those of a column of soil whose width is equal to the average width, W_d, of the area the stiffness of which is represented by the spring. Therefore,

$$P1 = \frac{G_s \times W_d}{TH}$$

$$P2 = \frac{E_s \times W_d}{TH} \qquad \text{.....(2-24)}$$

in which E_s denotes the soil compressive modulus of elasticity in plain strain, G_s denotes the shear modulus of elasticity and TH is the thickness of the packing soil annulation.

The local stiffness matrix with the coordinates defined in Figure 2.6 is given by

$$[S_p]_{local} = \left[\begin{array}{cc|cc} P1 & 0 & -P1 & 0 \\ 0 & P2 & 0 & -P2 \\ \hline -P1 & 0 & P1 & 0 \\ 0 & -P2 & 0 & P2 \end{array}\right] \qquad \text{.....(2-25)}$$

The global stiffness matrix of member i of the packing soil is

$$[S_p]^i_{global} = [R^i]^T \, [S_p]_{local} [R^i] \qquad \text{.....(2-26)}$$

in which the rotation matrix $[R^i]$ is equal to

$$[R^i] = \left[\begin{array}{cc|cc} \cos\theta_i & \sin\theta_i & & \\ -\sin\theta_i & \cos\theta_i & & 0 \\ \hline & & \cos\theta_i & \sin\theta_i \\ & 0 & -\sin\theta_i & \cos\theta_i \end{array}\right] \qquad .....(2\text{-}27)$$

and the angle θ_i is defined in Figure 2.6

For each packing soil spring i , the elements of $[S_p]^i_{global}$ found from Eq.(2-26) can be put directly in the appropriate rows and columns in the stiffness matrix of the cylinder-soil composite.

2.4.3 Soil Finite Elements

2.4.3.1 General.-- Other than the cylinder of radius R and the packing soil of thickness TH, the rest of the cylinder-soil composite is idealized by two-dimensional finite elements. The finite elements pattern varies depending on many factors such as, for example, the number of lumped masses assumed for the cylinder. Most of the examples in this study use a twelve node model for the cylinder; the corresponding finite element mesh is shown in Figure 2.7. The triangular finite elements, such as (42,25,61) are the basic element shapes from which the stiffness is derived. Most of the studies , however, are done using a further approximation procedure referred to here as Method 1 that would delete the degrees of freedom associated with node 61 in Figure 2.7.

In formulating the problem, only the coordinates of the four corners of each quadrangle need be defined, e.g., the coordinates of nodes 42,25,26 and 41 for quadrangle number 25. Then the following steps will be used to obtain the soil finite element stiffness matrix.

a). For each quadrangle, an interior node is defined at the intersection of the two diagonals. An isolated typical quadrangle ABCD is shown in Figure 2.8a with I being the interior node. The coordinates of I are found by simple geometric consideration to be

$$X_I = \frac{\left(\frac{Y_C - Y_A}{X_C - X_A}\right) X_A - Y_A - \left(\frac{Y_B - Y_D}{X_B - X_D}\right) X_D + Y_D}{\left(\frac{Y_C - Y_A}{X_C - X_A}\right) - \left(\frac{Y_B - Y_D}{X_B - X_D}\right)} \qquad \text{.....(2-28)}$$

$$Y_I = Y_A + \left(\frac{Y_C - Y_A}{X_C - X_A}\right)\left(X_I - X_A\right)$$

b). After the coordinates of I are calculated, the stiffness of each triangular element ABI, BCI, CDI and DAI is derived according to the method of finite element. The principle underlying this method can be found in many literatures and will not be discussed here. The procedure used in this study followed that outlined in (14) for triangular element in plane strain and is summarized as follows.

For a typical triangular element "ijm" in Figure 2.9, the displacement functions are assumed to be

$$u = \alpha_1 + \alpha_2 x + \alpha_3 y$$

$$v = \alpha_4 + \alpha_5 x + \alpha_6 y$$

where u and v denote translations in the x and y directions, respectively, and $\alpha_1, \alpha_2, \ldots, \alpha_6$ are constants at each time instant that depend on the displacements of the three vertices i, j and m. The strain interpolation function matrix $[B]$ is then found to be

$$[B] = \frac{1}{2\,\Delta}\begin{bmatrix} b_i & 0 & b_j & 0 & b_m & 0 \\ 0 & d_i & 0 & d_j & 0 & d_m \\ d_i & b_i & d_j & b_j & d_m & b_m \end{bmatrix} \qquad .....(2\text{-}29)$$

where $b_i = y_j - y_m$, $d_i = x_m - x_j$,

$b_j = y_m - y_i$, $d_j = x_i - x_m$,

$b_m = y_i - y_j$, $d_m = x_j - x_i$,

$$2\Delta = \text{det.}\begin{vmatrix} 1 & x_i & y_i \\ 1 & x_j & y_j \\ 1 & x_m & y_m \end{vmatrix} = 2 \text{ (area of triangle ijm)}$$

and x_i, y_i, ... etc are the coordinates of the nodes as defined in Figure 2.9. Then the stiffness matrix, $[S_{triangle}]$, of the element ijm may be computed from the equation:

$$[S_{triangle}] = \int [B]^T [D][B]\ t'\ dx\ dy \qquad .....(2\text{-}30)$$

where t' is the thickness of the finite element. The matrix $[D]$ represents the stress strain relationship for the plane strain case and is given by:

$$[D] = \frac{E\ (1-\nu_s)}{(1+\nu_s)(1-2\nu_s)}\begin{bmatrix} 1 & \nu_s/(1-\nu_s) & 0 \\ \nu_s/(1-\nu_s) & 1 & 0 \\ 0 & 0 & (1-2\nu_s)/2(1-\nu_s) \end{bmatrix}$$

$$.....(2\text{-}31)$$

For constant t', Eq.(2-30) can be integrated to obtain

$$[S_{triangle}] = \frac{E}{4\Delta(1+\nu_s)(1-2\nu_s)} \times$$

$$\begin{bmatrix}
(1-\nu_s)b_i^2 + \frac{1-2\nu_s}{2}d_i^2 & \nu_s b_i d_i + \frac{1-2\nu_s}{2}b_i d_i & (1-\nu_s)b_i b_j + \frac{1-2\nu_s}{2}d_i d_j & \nu_s b_i d_j + \frac{1-2\nu_s}{2}b_j d_i & (1-\nu_s)b_i b_m + \frac{1-2\nu_s}{2}d_i d_m & \nu_s b_i d_m + \frac{1-2\nu_s}{2}b_m d_i \\
 & (1-\nu_s)d_i^2 + \frac{1-2\nu_s}{2}b_i^2 & \nu_s b_j d_i + \frac{1-2\nu_s}{2}b_i d_j & (1-\nu_s)d_i d_j + \frac{1-2\nu_s}{2}b_i b_j & \nu_s b_m d_i + \frac{1-2\nu_s}{2}b_i d_m & (1-\nu_s)d_i d_m + \frac{1-2\nu_s}{2}b_i b_m \\
 & & (1-\nu_s)b_j^2 + \frac{1-2\nu_s}{2}d_j^2 & \nu_s b_j d_j + \frac{1-2\nu_s}{2}b_j d_j & (1-\nu_s)b_j b_m + \frac{1-2\nu_s}{2}d_j d_m & \nu_s b_j d_m + \frac{1-2\nu_s}{2}b_m d_j \\
 & & & (1-\nu_s)d_j^2 + \frac{1-2\nu_s}{2}b_j^2 & \nu_s b_m d_j + \frac{1-2\nu_s}{2}b_j d_m & (1-\nu_s)d_j d_m + \frac{1-2\nu_s}{2}b_j b_m \\
 & \text{Symmetric} & & & (1-\nu_s)b_m^2 + \frac{1-2\nu_s}{2}d_m^2 & \nu_s b_m d_m + \frac{1-2\nu_s}{2}b_m d_m \\
 & & & & & (1-\nu_s)d_m^2 + \frac{1-2\nu_s}{2}b_m^2
\end{bmatrix}$$

.....(2-32)

c). After the stiffness for each of the triangles ABI, BCI, CDI and DAI in Figure 2.8 has been found by Eq.(2-32), the final stiffness matrix for the quadrangle area ABCD can be derived by either Method 1 or Method 2. These methods will be discussed in the next two sections.

2.4.3.2 Method 1.-- This is an approximate method (15) in which the degrees of freedom associated with node I (see Figure 2.8a) are eliminated from the dynamic analysis. Consider Figure 2.8b, a quadrangle stiffness matrix, $[S_{quad}]$, can be constructed by appropriate superposition of the four triangular stiffness matrices $[S_{triangle}]^i$, i = 1, 2, 3, 4, calculated from Eq.(2-32). This stiffness relates the quadrangle forces and displacements as follows:

$$\begin{Bmatrix} F_{ex} \\ F_{in} \end{Bmatrix} = [S_{quad}] \begin{Bmatrix} U_{ex} \\ U_{in} \end{Bmatrix}$$

$$= \begin{bmatrix} S_{q11} & S_{q12} \\ S_{q21} & S_{q22} \end{bmatrix} \begin{Bmatrix} U_{ex} \\ U_{in} \end{Bmatrix} \qquad \text{.....(2-33)}$$

where $\{F_{ex}\} = \{F_1, F_2, \ldots, F_8\}$ and $\{U_{ex}\} = \{U_1, U_2, \ldots, U_8\}$ refer to forces and displacements vectors at the exterior nodes A,B,C,d; and $\{F_{in}\} = \{F_9, F_{10}\}$ and $\{U_{in}\} = \{U_9, U_{10}\}$ refer to forces and displacements vectors at the interior node I.

Since the interior node I is connected to node A,B,C,D only and not to any other nodes, the equation of motion for node I will involve only $\{U_{ex}\}$ and $\{U_{in}\}$. Keeping in mind the absence of any external applied forces at I, this equation of motion can be written as:

$$[M_{in}]\{\ddot{U}_{in}\} + [S_{q21}]\{U_{ex}\} + [S_{q22}]\{U_{in}\} = \{0\}$$

or $$\{U_{in}\} = -[S_{q22}]^{-1} ([M_{in}]\{\ddot{U}_{in}\} + [S_{q21}]\{U_{ex}\}) \qquad .....(2\text{-}34)$$

where $[M_{in}]$ is the mass matrix for node I, and damping is ignored. From Eq.(2-33), the elastic forces at the external nodes caused by displacements within the quadrangle are

$$\{F_{ex}\} = [S_{q11}]\{U_{ex}\} + [S_{q12}]\{U_{in}\}$$

and, on substitution of Eq.(2-34),

$$\{F_{ex}\} = ([S_{q11}] - [S_{q12}][S_{q22}]^{-1} [S_{q21}])\{U_{ex}\}$$

$$- [S_{q12}][S_{q22}]^{-1} [M_{in}]\{\ddot{U}_{in}\} \qquad .....(2\text{-}35)$$

The second term on the right in Eq.(2-35) is the effect of the inertia force at the interior node I on the exterior nodes A,B,C,D. This effect can be approximately accounted for by lumping the interior node mass at the four exterior nodes. When this is done, Eq.(2-35) becomes

$$\{F_{ex}\} = [S_F^*]\{U_{ex}\} \qquad .....(2\text{-}36)$$

where $$[S_F^*] = [S_{q11}] - [S_{q12}][S_{q22}]^{-1} [S_{q21}] \qquad .....(2\text{-}37)$$

$[S_F^*]$ is the modified stiffness matrix for the quadrangle ABCD involving only the degrees of freedom associated with the exterior nodes A,B,C,D.

2.4.3.3 Method 2.-- No approximation of the inertia force of the interior node I is involved in this second method to represent the stiffness of the quadrangle ABCD (see Figure 2.8). Instead, a computer routine is written so that after the coordinates of node I

have been computed from Eq.(2-28), the node will be given a number designation and treated as a finite element node just as nodes A,B,C or D. For each triangle ABI, BCI, CDI and DAI in Figure 2.8b, a triangular finite element stiffness matrix is calculated from Eq.(2-32) and the elements of the resultant 6×6 stiffness matrix are put directly in the appropriate rows and columns in the stiffness matrix of the cylinder-soil composite.

2.4.3.4 Mass Matrix.-- For Method 1, 1/4 of the mass of the area ABCD in Figure 2.8a, for example, will be lumped at each of the nodes A,B,C and D. For Method 2, 1/5 of the mass of ABCD will be lumped at each of the nodes A,B,C,D and I.

2.5 Stiffness and Mass Matrices for the Cylinder-Soil Composite

2.5.1 Flexible Cylinder

The cylinder stiffness matrix, $[S_R^*]$, is given by Eq.(2-23) and the packing soil stiffness matrix, $[S_p]^i_{global}$, by Eq.(2-26) for each packing spring i, i=1,2,...,nr. The quadrangle finite element stiffness matrix for Method 1, $[S_F^*]$, is given by Eq.(2-37) for every soil quadrangle. Or, the triangular finite element stiffness matrix for Method 2, $[S_{triangle}]$, is given by Eq.(2-32) for every soil triangular finite element. The elements of all these stiffness matrices can be added directly to the appropriate joint stiffness in the stiffness matrix for the cylinder-soil composite shown in Figure 2.7. This assembly of the overall stiffness matrix is a routine procedure in matrix analysis of structures and will not be discussed here. The mass matrix, likewise, is simply a superposition of all the masses

within an area assigned to a joint.

2.5.2 Rigid Cylinder

As will be seen in the chapter on numerical results, the treatment of the cylinder as rigid results in a saving in computer time. However, the procedure is valid only when the cylinder is stiff enough so that its response can be approximated by that of a rigid cylinder. The rigid cylinder formulation can be achieved in two ways.

a). At each time integration, the equation of motion can be written for the cylinder as a whole, rather than for each cylinder node.The mass will then be the combined mass of all the cylinder nodes and the elastic forces in the x and y directions will be the combined elastic forces from each of the packing soil springs on the cylinder in the corresponding directions. This procedure is followed in this study when the equation of motion is solved numerically by direct integration and will be discussed in detail in the next chapter dealing with the equations of motion.

b). When the equation of motion is solved by modal analysis, the stiffness and mass matrices are formed incorporating the feature that the cylinder is infinitely rigid. The new stiffness matrix for the "rigid" cylinder-soil composite can be found as follows.

Suppose the stiffness matrix for the "non rigid" cylinder-soil composite is $[S]$, the matrix can be partitioned according to whether the nodes belong to the cylinder or to the soil:

$$\begin{Bmatrix} F \\ F_S \end{Bmatrix} = [S] \begin{Bmatrix} U \\ U_S \end{Bmatrix}$$

$$= \begin{bmatrix} S_{RR} & S_{RS} \\ S_{SR} & S_{SS} \end{bmatrix} \begin{Bmatrix} U \\ U_S \end{Bmatrix} \qquad .....(2\text{-}38)$$

where {F} and {U} refer to forces and displacements of the cylinder nodes, and $\{F_S\}$ and $\{U_S\}$ refer to forces and displacements of the soil nodes. Now for a cylinder with "nr" number of nodes, the 2×nr dimensional "non rigid" cylinder displacement vector ,{U}, can be related to the three dimensional rigid cylinder displacement vector,{U'}, as follows.

$$\{U\} = [A] \{U'\} \qquad .....(2\text{-}39)$$

or, expanding

$$\begin{Bmatrix} U_1 \\ U_2 \\ U_3 \\ U_4 \\ U_5 \\ U_6 \\ \vdots \\ U_{2\times nr} \end{Bmatrix} = \begin{bmatrix} 1 & 0 & -R\cos\theta_1 \\ 0 & 1 & -R\sin\theta_1 \\ 1 & 0 & -R\cos\theta_2 \\ 0 & 1 & -R\sin\theta_2 \\ 1 & 0 & -R\cos\theta_3 \\ 0 & 1 & -R\sin\theta_3 \\ \vdots & & \\ 0 & 1 & -R\sin\theta_{nr} \end{bmatrix} \begin{Bmatrix} U'_X \\ U'_Y \\ U'_Z \end{Bmatrix} \qquad .....(2\text{-}40)$$

The symbols are defined in Figures 2.10a and 2.10b.

Suppose that the 2×nr dimensional "non rigid" cylinder force vector, {F}, is related to the three dimensional rigid cylinder force

vector, $\{F'\}$, as

$$\{F\} = [B']\{F'\} \qquad .....(2\text{-}41)$$

For a virtual displacement of a rigid cylinder, the virtual work expressed in the non-rigid and the rigid cylinder coordinates must be the same:

$$\{U\}^T\{F\} = \{U'\}^T \{F'\} \qquad .....(2\text{-}42)$$

Substitution in Eq.(2-42) from Eq.(2-39) and Eq.(2-41) yields

$$\{U'\}^T [A]^T [B']\{F'\} = \{U'\}^T \{F'\}$$

or, $$\{U'\}^T ([A]^T [B'] - [I]) \{F'\} = 0 \qquad .....(2\text{-}43)$$

in which $[I]$ denotes the unit matrix. Since in a virtual displacement of a nonsingular system, neither $\{U'\}$ nor $\{F'\}$ can vanish, Eq.(2-43) implies

$$[A]^T [B'] = [I] \qquad .....(2\text{-}44)$$

We can make use of Eq.(2-44) to transform the coordinates from non-rigid to rigid cylinder. From Eq.(2-38),

$$\{F\} = [S_{RR}]\{U\} + [S_{RS}]\{U_S\} \qquad .....(2\text{-}45)$$

$$\{F_S\} = [S_{SR}]\{U\} + [S_{SS}]\{U_S\} \qquad .....(2\text{-}46)$$

Now, for rigid cylinder movement, we can substitute Eq.(2-39) and Eq.(2-41) in Eq.(2-45) and obtain

$$[B']\{F'\} = [S_{RR}][A]\{U'\} + [S_{RS}]\{U_S\}$$

Premultiplying by $[A]^T$, and using Eq.(2-44), we obtain

$$\{F'\} = [A]^T [S_{RR}][A]\{U'\} + [A]^T [S_{RS}]\{U_S\} \qquad .....(2\text{-}47)$$

Also, substituting Eq.(2-39) to Eq.(2-46), we get

$$\{F_S\} = [S_{SR}][A]\{U'\} + [S_{SS}]\{U_S\} \qquad .....(2\text{-}48)$$

Combine Eq.(2-47) and Eq.(2-48):

$$\begin{Bmatrix} F' \\ F_S \end{Bmatrix} = \left[\begin{array}{c|c} [A]^T [S_{RR}][A] & [A]^T [S_{RS}] \\ \hline [S_{SR}][A] & [S_{SS}] \end{array}\right] \begin{Bmatrix} U' \\ U_S \end{Bmatrix}$$

$$= [S'] \begin{Bmatrix} U' \\ U_S \end{Bmatrix} \qquad .....(2\text{-}49)$$

$[S']$ is then the stiffness for the rigid cylinder-soil composite.

The mass matrix for the rigid cylinder case differs from the non-rigid cylinder case in the fact that a 3×3 diagonal mass matrix replaces the original 2×nr by 2×nr non-rigid cylinder mass matrix. The first two diagonal entries, representing translational inertia in the x and y directions , are simply the sum of all the cylinder nodal masses. The third diagonal entry, representing rotational inertia, is equal to the sum of all the cylinder nodal masses multiplied by the square of the radius of the cylinder.

2.6 Damping Matrix

As mentioned in the section on basic assumptions and Eq.(2-2), the damping matrix, $[C]$, is assumed to be proportional to the stiffness

matrix , $[S]$, i.e.,

$$[C] = \mu[S]$$

In a direct integration procedure, the above expression is used as is. In modal analysis, each modal damping ratio, λ_n, will be related to μ by the equation

$$\lambda_n = \frac{\omega_n \mu}{2} \qquad \text{.....(2-50)}$$

where ω_n is the circular frequency of the nth mode.

The drawback to this assumption of proportional damping is apparent, i.e., only one damping parameter can be arbitrarily specified; this can either be the damping factor μ or one of the modal damping ratios λ_n. The rest of the damping parameters then become fixed relative to this parameter by Eq.(2-50). Obviously, the same equation also imposes the condition that the damping be more effective in the higher modes than in the lower modes. The decision to use proportional damping rests on the following considerations:

a). The problem becomes much more simplified.

b). The actual loss mechanisms in most structures are highly complicated such that other alternatives (for example, assigning an individual damping ratio to each mode) would also involve a high degree of uncertainty.

c). Most importantly, the damping terms in problems involving earthquake excitations are not expected to have an overly large effect on the responses.

CHAPTER III

METHOD OF ANALYSIS

3.1 General

The models have been developed and their structural properties determined. The next step is to derive the equations of motion.

An eigenvalue analysis to obtain the mode shapes and frequencies of the cylinder-soil composite will be discussed in the first section.

The main body of the analysis can be separated into two parts in line with the two part representation of the problem as shown in Figure 2.1b. The motions of the free field soil column will first be determined. Then the parts of these motions that correspond to the boundary of the cylinder-soil composite will be used as excitation inputs for the cylinder-soil composite.

3.2 The Eigenproblem

The homogenous equation of motion for the cylinder-soil composite vibrating in one of the harmonic modes is

$$[S]\{X_i\} = \omega_i^2 \, [M_I]\{X_i\} \qquad .....(3\text{-}1)$$

where $[S]$ is the stiffness matrix and $[M_I]$ is the diagonal mass matrix (assuming that the boundary points do not move), both of which are

discussed in Section 2.5, and $\{X_i\}$ and ω_i are the shape and circular frequency of the ith mode. Eq.(3-1) can be reduced to the standard form:

$$[K]\{\bar{X}_i\} = \omega_i^2\{\bar{X}_i\} \qquad .....(3\text{-}2)$$

by the substitution

$$[K] = [M_I]^{-\frac{1}{2}}[S][M_I]^{-\frac{1}{2}}$$

$$\{\bar{X}_i\} = [M_I]^{\frac{1}{2}}\{X_i\} \qquad .....(3\text{-}3)$$

Because of the diagonal form of $[M_I]$, computation of $[K]$ and $\{\bar{X}_i\}$ from Eq.(3-3) becomes very simple.

There are various mathematical and iterative schemes to solve the eigenproblem of Eq.(3-2). The computer routine used in this study is a library program available at Michigan State University based on Jacobi's Method, the discussion of which is beyond the scope of this study.

Once $\{\bar{X}_i\}$ is found, the mode shape $\{X_i\}$ can be computed from the relation in Eq.(3-3). For consistency, all mode shapes in this study are normalized with respect to mass, i.e.,

$$\{X_i\}^T [M_I]\{X_i\} = 1 \qquad .....(3\text{-}4)$$

3.3 Equations of Motion for Free Field Soil

From the notations for the free field soil column in Figure 2.1b, the equation of motion for a typical mass i, i=1,2,...n,

in the vertical direction can be written as:

$$m_i(\ddot{v}_i + \ddot{v}_g) = (v_{i+1} - v_i)K_{i+1} + (\dot{v}_{i+1} - \dot{v}_i)C_{i+1}$$

$$- (v_i - v_{i-1})K_i - (\dot{v}_i - \dot{v}_{i-1})C_i \qquad .....(3\text{-}6)$$

with $\quad v_0 = \dot{v}_0 = K_{n+1} = C_{n+1} = 0$;

and in the horizontal direction as:

$$m_i(\ddot{u}_i + \ddot{u}_g) = (u_{i+1} - u_i)k_{i+1} + (\dot{u}_{i+1} - \dot{u}_i)c_{i+1}$$

$$- (u_i - u_{i-1})k_i - (\dot{u}_i - \dot{u}_{i-1})c_i \qquad .....(3\text{-}7)$$

with $\quad u_0 = \dot{u}_0 = k_{n+1} = c_{n+1} = 0$.

In the above equations, v_i and u_i denote the displacements of mass i in the vertical and horizontal directions with respect to the bedrock motion, and $\ddot{v}_g$ and $\ddot{u}_g$ are the bedrock vertical and horizontal accelerations.

3.4 Interpolation from Free Field to Cylinder-Soil

With the assumption that the feedback between the free field soil and the cylinder-soil composite is negligible, the motions of the side and the bottom boundaries of the cylinder-soil composite will be equated to those of the free field soil at the same level. If the mass points of the two do not fall on the same level, the motions of the boundaries will be obtained from a straight line interpolation from the motions of the free field soil mass points.

Consider Figure 3.1. The displacement and velocity components,

u_i, v_i and $\dot{u}_i, \dot{v}_i$, $i=8,9,10$, are the motions of the three topmost masses of the free field soil column that will be prescribed at the boundaries of the cylinder-soil composite. The horizontal displacements, $U_{B3}, U_{B11}, U_{B5}, U_{B13}, U_{B7}, U_{B15}, U_{B9}, U_{B1}, U_{B17}$, of the nine boundary masses can be found by a straight line interpolation from the three horizontal displacements u_8, u_9, u_{10} as on the right of Figure 3.1. The same procedure is followed when dealing with velocities. This interpolation can be written in terms of coordinate transformation as

$$\begin{aligned} \{U_B\} &= [T]\{u_F\} \\ \{\dot{U}_B\} &= [T]\{\dot{u}_F\} \end{aligned} \qquad \text{.....(3-9)}$$

where $\{U_B\} = \{U_{B1}, U_{B2}, \ldots, U_{B18}\}$ and $\{u_F\} = \{u_8, v_8, u_9, v_9, u_{10}, v_{10}\}$ (see Figure 3.1) and, for the case of Figure 3.1 with the dimensions as shown, the transformation matrix is

$$[T] = \begin{bmatrix} 1/3 & & & 2/3 & & & & & & & & \\ & 1/3 & & & 2/3 & & & & & & & \\ & & & & & & 1 & & & & & \\ & & & & & & & & & 1 & & \\ & & & 2/5 & & & & 3/5 & & & & \\ & & & & & 2/5 & & & & 3/5 & & \\ & & & 14/15 & & & & 1/15 & & & & \\ & & & & & 14/15 & & & & 1/15 & & \\ 1/3 & & & 2/3 & & & & & & & & \\ & 1/3 & & & 2/3 & & & & & & & \\ & & & & & & 1 & & & & & \\ & & & & & & & & & 1 & & \\ & & & 2/5 & & & & 3/5 & & & & \\ & & & & & 2/5 & & & & 3/5 & & \\ & & & 14/15 & & & & 1/15 & & & & \\ & & & & & 14/15 & & & & 1/15 & & \\ 1/3 & & & 2/3 & & & & & & & & \\ & 1/3 & & & 2/3 & & & & & & & \end{bmatrix} \qquad \text{.....(3-10)}$$

[T] will have to be constructed individually for each different case of boundary dimensions locating the mass points.

3.5 Equation of Motion for Cylinder-Soil Composite

3.5.1 For Direct Integration

3.5.1.1 Flexible Cylinder.-- Consider Figure 2.7. Let $\{U_B\}$ and $\{\dot{U}_B\}$ denote the displacements and velocities (relative to the bedrock) of the boundary nodes, i.e., nodes 40, 41, 42, 43, 44, 45, 46, 47, 48; and $\{U_I\}$, $\{\dot{U}_I\}$ and $\{\ddot{U}_I\}$ denote the displacements, velocities and accelerations (relative to the bedrock) of all the interior nodes not located at the boundary, i.e., nodes 1, 2, 3, 4, 5, ..., 39; and let $\{\ddot{x}_g\} = \{\ddot{u}_g, \ddot{v}_g, \ddot{u}_g, \ddot{v}_g, \ldots, \ddot{v}_g\}$ be the bedrock acceleration vector with the horizontal and vertical accelerations alternately placed. The dimension of this vector is 2ni where ni is the number of interior nodes.

The stiffness matrix, [S], of the cylinder-soil composite can be rearranged and partitioned as

$$[S] = \begin{bmatrix} S_{II} & S_{IB} \\ S_{BI} & S_{BB} \end{bmatrix} \qquad \ldots\ldots(3\text{-}11)$$

to separate the stiffness related to the interior nodes and those related to the boundary nodes. This can be done with the stiffness calculated from either Method 1 or Method 2 in Section 2.4.3.2 and Section 2.4.3.3, respectively.

The equation of motion expressing the equilibrium of the dynamic forces may be generally written as

$$\{F_I\} + \{F_S\} + \{F_D\} = \{P\} \qquad .....(3\text{-}12a)$$

in which the terms on the left side represent the inertia force, elastic force and damping force vectors, respectively, and the right side is the applied load vector. For the case of the interior nodes of the cylinder-soil composite, the inertia force vector can be expressed as:

$$\{F_I\} = [M_I](\{\ddot{U}_I\} + \{\ddot{x}_g\})$$

the elastic force vector as:

$$\{F_S\} = [S_{II}]\{U_I\} + [S_{IB}]\{U_B\}$$

the damping force vector as:

$$\{F_D\} = \mu[S_{II}]\{\dot{U}_I\} + \mu[S_{IB}]\{\dot{U}_B\}$$

and, due to the fact that there is no applied force, the applied force vector as:

$$\{P\} = \{0\}$$

where

$$[M_I] = \begin{bmatrix} M_1 & & & & & \\ & M_1 & & & 0 & \\ & & M_2 & & & \\ & & & M_2 & & \\ & 0 & & & \ddots & \\ & & & & & M_{ni} \end{bmatrix}_{2ni\times 2ni}$$

represents the mass of the interior nodes in the horizontal and vertical directions, μ is the damping constant as defined in Eq.(2-2) and Eq.(2-50), and the rest of the variables have been defined earlier.

Thus the equation of motion for the interior nodes of the cylinder-soil composite becomes

$$[M_I](\{\ddot{U}_I\} + \{\ddot{x}_g\}) + [S_{II}]\{U_I\} + [S_{IB}]\{U_B\}$$

$$+ \mu[S_{II}]\{\dot{U}_I\} + \mu[S_{IB}]\{\dot{U}_B\} = 0 \qquad .....(3\text{-}12b)$$

At each time instant, $\{U_B\}$ and $\{\dot{U}_B\}$ can be interpolated from the free field soil motions as in Eq.(3-9) and used as inputs in Eq.(3-12b) along with the bedrock acceleration input $\{\ddot{x}_g\}$. Eq.(3-12b) can then be integrated to obtain the motions $\{U_I\}$, $\{\dot{U}_I\}$ and $\{\ddot{U}_I\}$.

3.5.1.2 Rigid Cylinder.-- For the case of the rigid cylinder-soil composite, the equations of motion for the soil nodes are exactly the same as Eq.(3-12b). For the cylinder nodes, however, the number of variables may be reduced as shown below.

a). The force on node i of the cylinder from the packing soil spring can be computed as (see Figure 3.2):

$$\begin{Bmatrix} F_{xi} \\ F_{yi} \end{Bmatrix} = [S_{in}] \begin{Bmatrix} u_{n1} - u_{i1} \\ u_{n2} - u_{i2} \end{Bmatrix} \qquad .....(3\text{-}13)$$

where F_{xi}, F_{yi} represent the forces in the x and y directions on the cylinder node i, and U_{n1}, U_{n2}, U_{i1}, U_{i2} represent the displacements in the x and y directions of the packing soil node n and the cylinder node i. $[S_{in}]$ is the appropriate stiffness involving

node i and n.

b). Once Eq.(3-13) is applied for all the cylinder nodes, the total forces on the rigid cylinder can be computed as

$$F_{x\ total} = \sum_{i=1}^{nr} F_{xi}$$

$$F_{y\ total} = \sum_{i=1}^{nr} F_{yi} \qquad .....(3\text{-}14)$$

c). The equations of motion for the rigid cylinder can then be written as:

$$M_{rigid}\ (\ddot{U}_{x\ rigid} + \ddot{u}_g\ ) = F_{x\ total}$$

$$M_{rigid}\ (\ddot{U}_{y\ rigid} + \ddot{v}_g\ ) = F_{y\ total} \qquad .....(3\text{-}15)$$

where M_{rigid} represents the total mass of all the cylinder nodes and $\ddot{U}_{x\ rigid}$, $\ddot{U}_{y\ rigid}$ are the accelerations (relative to those of the bedrock) of the rigid cylinder in the x and y directions.

3.5.2 <u>For Modal Analysis.</u>

For the modal analysis method, the equations of motion for all the interior nodes remain the same as Eq.(3-12b). Next we express the motions in terms of the modal amplitudes.

$$\{U_I\} = [\Phi]\ A$$

$$\{\dot{U}_I\} = [\Phi]\ \dot{A} \qquad .....(3\text{-}16)$$

$$\{\ddot{U}_I\} = [\Phi]\ \ddot{A}$$

where $[\Phi] = [\{X_1\}\{X_2\}...\{X_{2ni}\}]$ is a square matrix containing mode

shape columns obtained as in Section 3.2 , and {A} is the modal amplitudes.

Substituting Eq.(3-16) into Eq.(3-12b), premultiplying by $[\Phi]^T$ and using the orthogonality conditions:

$$[\Phi]^T[M_I][\Phi] = [I]$$

$$[\Phi]^T[S_{II}][\Phi] = [\omega_i^2]_D \qquad .....(3\text{-}17)$$

and $$[\Phi]^T[C_{II}][\Phi] = [2\lambda_i\omega_i]_D$$

we obtained the decoupled equation of motion for each mode i :

$$\ddot{A}_i + \omega_i^2 A_i + 2\lambda_i\omega_i\dot{A}_i = -\{X_i\}^T[S_{IB}]\{U_B\} - \mu\{X_i\}^T[S_{IB}]\{\dot{U}_B\}$$

$$- \{X_i\}^T[M_I]\begin{Bmatrix}1\\0\\1\\0\\\vdots\\0\end{Bmatrix}\ddot{u}_g - \{X_i\}^T[M_I]\begin{Bmatrix}0\\1\\0\\1\\\vdots\\1\end{Bmatrix}\ddot{v}_g \qquad .....(3\text{-}18)$$

Note that the last orthogonality condition in Eq.(3-17) involving damping follows directly from the proportionality of the damping matrix to the stiffness matrix and implies the relation indicated in Eq.(2-50) between the modal damping ratio λ_i and the damping constant μ.

For the rigid cylinder case, the number of degrees of freedom is reduced accordingly and the equation of motion for mode i becomes:

$$\ddot{A}_i' + \omega_i'^2 A_i' + 2\lambda_i'\omega_i'\dot{A}_i' = -\{X_i'\}^T[S_{IB}']\{U_B\} - \mu\{X_i'\}^T[S_{IB}']\{\dot{U}_B\}$$

$$- \{X_i'\}^T[M_I']\begin{Bmatrix} 1 \\ 0 \\ 0 \\ \hline 1 \\ 0 \\ 1 \\ 0 \\ \vdots \\ 0 \end{Bmatrix}\ddot{u}_g - \{X_i'\}^T[M_I']\begin{Bmatrix} 0 \\ 1 \\ 0 \\ \hline 0 \\ 1 \\ 0 \\ 1 \\ \vdots \\ 1 \end{Bmatrix}\ddot{v}_g \qquad .....(3\text{-}19a)$$

The superscript " ' " signifies that, e.g., the mode shape $\{X_i'\}$ and the stiffness matrix $[S_{IB}']$ all derive from the modified stiffness matrix $[S']$ in Eq.(2-49) for the rigid cylinder. The modified mass matrix for the rigid cylinder, $[M_I']$, is as discussed at the end of Section 2.5.2.

Eq.(3-18) and Eq.(3-19a) can also be written in terms of $\{u_F\}$ and $\{\dot{u}_F\}$, the displacement and velocity inputs from the free field soil. For example, by substituting (see Eq.(3-9) and Eq.(3-10))

$$[T]\{u_F\} = \{U_B\}$$

in Eq.(3-19a), we obtain

$$\ddot{A}_i' + \omega_i'^2 A_i' + 2\lambda_i'\omega_i' \dot{A}_i' = -\{d_i\}^T\{u_F\} - \mu\{d_i\}^T\{\dot{u}_F\}$$

$$- c_i^x \ddot{u}_g - c_i^y \ddot{v}_g \qquad .....(3\text{-}19b)$$

The mode participation factors and vector for the various inputs on the right hand side of Eq.(3-19b) are defined as follows:

$$\{d_i\} = \{X_i'\}^T[S_{IB}'][T] \qquad .....(3\text{-}20a)$$

is the mode participation vector for the displacement inputs from the free field soil.

$$c_i^x = \{X_i'\}^T [M_I'] \begin{Bmatrix} 1 \\ 0 \\ 0 \\ \hline 1 \\ 0 \\ \vdots \\ 0 \end{Bmatrix} \qquad \text{.....(3-20b)}$$

is the mode participation factor for the horizontal bedrock acceleration.

$$c_i^y = \{X_i'\}^T [M_I'] \begin{Bmatrix} 0 \\ 1 \\ 0 \\ \hline 0 \\ 1 \\ \vdots \\ 1 \end{Bmatrix} \qquad \text{.....(3-20c)}$$

is the mode participation factor for the vertical bedrock acceleration.

For the example in Figure 3.1, the right hand side of Eq.(3-19b) for mode i can be expanded corresponding to the 14 inputs:

$$\begin{aligned} \ddot{A}_i' + \omega_i'^2 A_i' + 2\lambda_i'\omega_i' \dot{A}_i' = & -(d_{i1}u_8 + d_{i2}v_8 + d_{i3}u_9 \ldots + d_{i6}v_{10}) \\ & -(\mu d_{i1}\dot{u}_8 + \mu d_{i2}\dot{v}_8 + \mu d_{i3}\dot{u}_9 \ldots + \mu d_{i6}\dot{v}_{10}) \\ & - c_i^x \ddot{u}_g - c_i^y \ddot{v}_g \qquad \text{.....(3-20d)} \end{aligned}$$

where $d_{i1}, d_{i2}, \ldots, d_{i6}$ are the mode participation factors forming the elements of $\{d_i\}$.

Eq.(3-20d) is a linear differential equation which can be integrated directly to obtain the modal amplitude, A_i' . Alternatively, A_i' can be found as the sum of the contributions from the forcing functions associated with each of the 14 inputs, i.e.,

$$A_i' = \sum_{j=1}^{14} (\text{mode part. fact.})_{ij} \, B_{ij} \qquad .....(3\text{-}20e)$$

In the above equation, $(\text{mode part. fact.})_{ij}$ signifies one of the mode participation factors: $d_{i1}, d_{i2}, \ldots, d_{i6}, \mu d_{i1}, \mu d_{i2}, \ldots, \mu d_{i6}, c_i^x, c_i^y$; and B_{ij} is the solution obtained from the equation of motion;

$$\ddot{B}_{ij} + \omega_i'^2 \, B_{ij} + 2\lambda_i'\omega_i' \, \dot{B}_{ij} = (\text{input})_j \qquad .....(3\text{-}20f)$$

where $(\text{input})_j$ signifies one of the 14 inputs: $u_8, v_8, u_9, \ldots, v_{10}$, $\dot{u}_8, \dot{v}_8, \dot{u}_9, \ldots, \dot{v}_{10}, \ddot{u}_g$, and $\ddot{v}_g$. It should be noted here that the free field motions which are prescribed to the boundary of the cylinder-soil composite are inputs only in so far as the cylinder-soil composite is analyzed independently from the rest of the soil. These motions are the result of the bedrock accelerations being transmitted up the free field soil column. The only real inputs to the problem as a whole are, of course, the bedrock accelerations.

3.6 Moment Calculation

3.6.1 General

The final results of interest in this study are the internal moments that occur in the cylinder wall. For the flexible cylinder case, obtaining the moments is a straight forward procedure once the displacements of the cylinder nodes are determined, because the stiffness matrix that would give the resulting moments has already been obtained earlier. For the rigid cylinder case, the forces (including the D'Alembert forces) on the rigid cylinder nodes are first found and then the moments are computed as though the cylinder is flexible, i.e., with a finite E_rI_r. The final expression, however, is independent of E_rI_r; therefore, it is valid for $E_rI_r \rightarrow \infty$. The problem is somewhat similar to that of finding the moments in a rigid beam fixed at both ends.

When the solution is obtained by modal analysis, it is instructive to know the moments in the cylinder wall caused by each mode and the term "modal moment" is used to represent the moment magnitude and distribution in the cylinder wall corresponding to each of the normalized mode shapes found as in Section 3.2.

Each of these three topics will be discussed in detail.

3.6.2 Flexible Cylinder

When the cylinder is treated as flexible, the procedure to obtain cylinder moments is as follows:

a). At each time instant, the numerical integration will have been carried out and the displacements of all the node points will have been determined including the global cylinder node displacements,

$\{U\}$. Then the rotations, $\{U_R\}$, of the cylinder nodes can be obtained by applying Eq.(2-21b).

b). For each cylinder arc i of Figure 2.5, the local displacement vector can be obtained by using the rotation matrix, $[R_i]$, in Eq.(2-17):

$$\{U_m\} = [R_i] \begin{Bmatrix} U_A \\ U_B \end{Bmatrix} \qquad .....(3\text{-}21)$$

$\{U_m\}$ represents the local displacement vectors at node A and B including rotation (see Figure 2-5). $\{U_A\}$ and $\{U_B\}$ are the global displacement vectors obtain in the preceding step as appropriate elements of $\{U\}$ and $\{U_R\}$.

c). The force vector $\{F_m\}$ will be obtained by application of Eq.(2-6), $\{U_m\}$ having been known. The third and sixth rows of $\{F_m\}$ will then be the internal moment in the cylinder wall at the two nodes A and B.

Step b). and c). will be repeated for all cylinder arcs until the moments are found at all the cylinder nodes.

3.6.3 Rigid Cylinder

The problem of finding the moments in this case is different in nature from the case when the cylinder is treated as flexible; i.e., instead of the cylinder nodes' displacements being obtained explicitly, here the packing soil forces acting on the cylinder nodes are determined, the D'Alembert forces are added and then the analysis can be treated as a static problem. The moment computation becomes a routine solution of a statically indeterminate

structure (to the third degree in this case). The procedure is outlined step by step as follows.

a). The moment acting on the rigid cylinder can be found by summing the moments around the center of the cylinder caused by all the packing soil forces on the cylinder nodes (see Figure 3.3a):

$$M = \sum_{i=1}^{nr} (-F_{xi} \times d_{yi}) + (F_{yi} \times d_{xi}) \qquad .....(3\text{-}22)$$

M is the scalar moment and F_{xi}, F_{yi} are found from Eq.(3-13).

b). M above will be equilibrated by the D'Alembert moment which is equal to the sum of the "tangential D'Alembert" forces about the center of the cylinder. If the tangential D'Alembert force at node i is designated by f_i (see Figure 3.3b), then

$$f_i = -\frac{M}{nr \times R} \qquad .....(3\text{-}23)$$

Note that the magnitude of f_i is the same for all the cylinder nodes due to the fact that all the nodes have the same rotational acceleration equal to the rotational acceleration of the rigid cylinder.

c). The tangential D'Alembert force f_i will be rotated into the x and y global coordinates (see Figure 3.3b):

$$\begin{aligned} F'_{xi} &= \cos\theta_i \, f_i \\ F'_{yi} &= \sin\theta_i \, f_i \end{aligned} \qquad .....(3\text{-}24)$$

d). The final static forces, F''_{xi} and F''_{yi}, for node i will be the sum of the spring forces from the packing soil, the translational D'Alembert forces and the tangential D'Alembert forces:

$$F''_{xi} = F_{xi} - M_i \ddot{U}_{x\ rigid} + F'_{xi}$$

$$F''_{yi} = F_{yi} - M_i \ddot{U}_{y\ rigid} + F'_{yi} \qquad .....(3\text{-}25)$$

where M_i is the mass of node i and $\ddot{U}_{x\ rigid}$, $\ddot{U}_{y\ rigid}$ are the accelerations of the rigid cylinder as given by Eq.(3-15). The forces F''_{xi} , F''_{yi} for i=1,2,...,nr will now become for the cylinder a statically equilibrated system of forces.

The remaining step is a routine procedure for analysing a statically indeterminate structure.

e). A cut is made at the left horizontal end (Figure 3.4a) to release the structure into a statically determinate one. The released structure is assumed fixed at the upper end of the cut.

f). For each node i, a flexibility matrix, $[FLEX]_i$, for the section between the fixed end of the released structure and node i is found. Also, a transformation matrix, $[T]_i$, that will transform the translation and rotation at node i to the free end at the cut is found (see Figure 3.4b).

The expression for the flexibility matrix in local coordinates is the same as the right hand side of Eq.(2-8):

$$[FLEX_{local}]_i = \text{right hand side of Eq.(2-8)} \qquad .....(3\text{-}26)$$

the only difference being that α here signifies the subtending angle between node i and the fixed end, rather than being the subtending angle of a typical cylinder arc as in Eq.(2-8).

Then the global flexibility matrix is

$$[FLEX]_i = [R_i]^T \, [FLEX_{local}]_i \, [R_i] \qquad .....(3\text{-}27)$$

in which the rotation matrix $[R_i]$ is given as

$$[R_i] = \begin{bmatrix} \cos\theta_i & \sin\theta_i & 0 \\ -\sin\theta_i & \cos\theta_i & 0 \\ 0 & 0 & 1 \end{bmatrix} \qquad .....(3\text{-}28)$$

and θ_i is defined as in Figure 3.4b.

The transformation matrix is given as

$$[T]_i = \begin{bmatrix} 1 & 0 & -Y_F & -Y_I \\ 0 & 1 & X_F & -X_I \\ 0 & 0 & & 1 \end{bmatrix} \qquad .....(3\text{-}29)$$

where (X_I, Y_I) and (X_F, Y_F) are the coordinates of node i and the free end respectively.

g). The total displacements at the free end caused by the applied cylinder nodal forces around the released structure are (see Figure 3.4a)

$$\begin{Bmatrix} D_1 \\ D_2 \\ D_3 \end{Bmatrix} = \sum_{i=1}^{nr-1} [T]_i \, [FLEX]_i \begin{Bmatrix} F''_{xi} \\ F''_{yi} \end{Bmatrix} \qquad .....(3\text{-}30)$$

f). The actual internal forces at the cut, $\{F_{int}\}$, would be the forces that restore compatibility at the cut, therefore

$$\{F_{int}\} = -[FLEX]_{nr}\begin{Bmatrix} D_1 \\ D_2 \\ D_3 \end{Bmatrix} \qquad .....(3\text{-}31)$$

where $[FLEX]_{nr}$ is the flexibility of the whole arc (360°) between the fixed end and the free end.

g). Once $\{F_{int}\}$ are known, the internal forces, including the moments, at the other cylinder nodes can be found by simple statics.

It should be noted that even though the procedure above involved the flexibility matrix , and thus the flexural rigidity, $E_r I_r$, of the cylinder, this term cancels out in the final computation of the internal forces, Eq.(3-31)

3.6.4 Modal Moment

In the usual method of normal modes, the displacement vector can be obtained by superposition of the mode shapes weighed by the modal amplitudes, as in the first of Eq.(3-16). In this study, however, the results of interest are the internal moment in the cylinder wall which could be obtained likewise by superposition of the "modal moment" , $\{M_0\}_i$, weighed by the modal amplitudes. The modal moment can be found as follows:

a). If the cylinder is treated as flexible, the mode shapes, $\{X_i\}$, obtained for each mode i will yield the displacements of the cylinder nodes which can be treated in the same way as the cylinder node displacements, $\{U\}$, in Section 3.6.2. The procedure to obtain the modal moment the proceeds in exactly the same way as the procedure to obtain the moments at the cylinder nodes in Section 3.6.2.

b). If the cylinder is treated as rigid, the mode shape , $\{X_i'\}$, for each mode i yields the displacements of the rigid cylinder and the

surrounding packing soil which can be treated the same way as the displacements U_{n1}, U_{i1}, ... etc in Eq.(3-13). Eq.(3-13) will give the forces F_{xi}, F_{yi} from the packing soil on the cylinder nodes. The procedure to obtain the modal moment is then the same as in Section 3.6.3.

CHAPTER IV

NUMERICAL PROCEDURE AND COMPUTER PROGRAM

4.1 General

The equations of motion for the different models have been developed in the preceding chapter. The next step in the analysis is to numerically solve the differential equations from one time station to the next, step-by-step. For completeness the equations of motion to be solved are listed below.

a). Free field soil column- Eq.(3-6), Eq.(3-7)

b). Cylinder-soil composite:

direct integration method- Eq.(3-12b) for flexible cylinder
- Eq.(3-15) and Eq.(3-12b) for rigid cylinder

modal analysis method- Eq.(3-18) for flexible cylinder
- Either Eq.(3-19a), Eq.(3.19b) or Eq.(3-20d) for rigid cylinder

4.2 Numerical Integration Procedure

Each of the above equations is a second order differential equation of the initial value type which can be solved numerically by the Newmark's β-integration procedure (17). In particular, the $\beta = 0$ method is chosen in this study. This method has the advantage

of being non-iterative if the acceleration does not explicitly depend on the velocity. Even though this is not the case here, damping terms being included in the equations of motion, we can still approximate the velocity at each time step by the velocity in the previous time step and then the $\beta = 0$ method when applied will again be non-iterative. This approximation is justified by the fact that damping terms usually have relatively small influences in problems of this type, and the fact that velocity varies one order slower than acceleration. The approximation has been applied to many problems in the past with good results.

If the displacement, velocity and acceleration of component i (which can either be the ith mass or the ith mode as the case may be) are denoted by u_i, $\dot{u}_i$, and $\ddot{u}_i$ then the $\beta = 0$ method prescribes the displacement and velocity at time $t+\Delta t$ by the relations

$$u_i(t+\Delta t) = u_i(t) + \Delta t\ \dot{u}_i(t) + \frac{1}{2}\Delta t^2\ \ddot{u}_i(t) \qquad .....(4\text{-}1)$$

$$\dot{u}_i(t+\Delta t) = \dot{u}_i(t) + \frac{1}{2}\Delta t[\ \ddot{u}_i(t) + \ddot{u}_i(t+\Delta t)\ ] \qquad .....(4\text{-}2)$$

where Δt denotes the time increment.

4.3 Step-by-Step Numerical Solution

The general procedure involved in extending the solution from the "previous" time t to the "present" time $t+\Delta t$ is briefly explained below. It is necessary at the outset that the state of the cylinder and the soil be known at time t. In this problem the state can be completely defined by the displacement, the velocity and the

acceleration.

a). The "present" displacement $u_i(t+\Delta t)$ is found from Eq.(4-1) in terms of the variables of the previous time step.

b). The "present" acceleration $\ddot{u}_i(t+\Delta t)$ is obtained from the appropriate equation of motion among those listed in Section 4.1. The acceleration in all cases is actually in terms of the present displacement, velocity and the bedrock input accelerations. As mentioned earlier, the present velocity will be approximated by the previous velocity.

c). The present velocity $\dot{u}_i(t+\Delta t)$ can then be found from Eq.(4-2).

These three steps complete the solution for all the variables at time $t+\Delta t$. The same process can be repeated to advance in the time domain for the next time step and so on.

It should be noted that due to the assumption of no feedback between the free field soil column and the cylinder-soil composite, the responses of the free field within the entire period of interest can be obtained completely independent of the cylinder-soil composite. These can of course be used later as inputs for the numerical solution of the responses of the cylinder-soil composite.

4.4 Stability of the Numerical Solution

Newmark (17) has shown that the stability of the $\beta = 0$ integration method requires that the time increment, Δt, be less than $1/\pi$ times the smallest natural period of the system. Strictly speaking, this implies that an eigenvalue analysis should be made for each problem to determine the proper time increment before any

numerical integration can proceed. However, in many instances the extra work involved in the frequency analysis can be avoided by applying some simple rule of thumb for a rough estimate of the smallest period and then a "safe" fraction of that period, say 1/10, be taken as the time increment.

For the free field soil column, the smallest period can be approximated by the period of the smallest one degree of freedom lumped mass with all other lumped mass fixed. For the free field soil shown in Figure 2.1b, supposing m_i to be the smallest mass, the time increment can be taken as

$$\Delta t = \min.\left[\frac{1}{10}\,\frac{2\pi}{\sqrt{\dfrac{K_i + K_{i+1}}{m_i}}}\;;\;\frac{1}{10}\,\frac{2\pi}{\sqrt{\dfrac{k_i + k_{i+1}}{m_i}}}\right]$$

$$= \min.\left[\frac{1}{10}\text{ the vertical period of } m_i\;;\;\frac{1}{10}\text{ the horizontal period of } m_i\right] \quad .....(4\text{-}3)$$

For the rigid cylinder-soil composite, Δt can similarly be taken as

$$t = \frac{1}{10}\,\frac{2\pi}{\sqrt{\dfrac{K_c}{M_{rigid}}}} \quad .....(4\text{-}4)$$

where K_c is the total resisting spring force from the packing soil against a unit movement of the rigid cylinder, all other (soil) nodes being fixed, and M_{rigid} is the total mass of the rigid cylinder. This approximation of the smallest period for the rigid cylinder-soil

composite was found to be reasonable for all the cases encountered in this study.

However, no easy rule of thumb was found for the case when the cylinder is treated as flexible. Here the frequency analysis will have to be resorted to. Another not necessarily less tedius alternative sometime followed in this study is to try various values of Δt and that value is used when it yields stable results in the sense that the responses computed are not sensitive to small changes in the Δt used.

4.5 Computer Programs

There are several packages of programs developed for this study: they are shown in Figure 4.1 each symbolized by a rectangle. Each package, containing a main program and (usually) a number of subprograms, does a certain portion of the analysis and its results may be used as one of the inputs for another package. In Figure 4.1 each package is headed by the name as was actually used in the main program in the computer code, and a summarization of its main function is described within the rectangle. Then the outputs are summarized immediately below the rectangle. The arrow pointing down might branch off to many other packages where the outputs of this particular package will be used as inputs. Most of the information between the packages were transmitted in binary mode (i.e., using unformatted READ and WRITE) and, in between the packages, were stored on disks or tapes. For a floating point number, this would

preserve a 14 digit (48 bit coefficient) accuracy.

The programs were checked separately on the two main parts. Firstly, the stiffness matrices were checked by statics. Static loads were applied to the cylinder and displacements of the cylinder nodes were compared with known solutions. In addition, static loads were applied at the top (free) surface nodes of the cylinder-soil composite and checks were made on the equilibrium between the loads and the boundary reactions and also on the displacement distributions. Secondly, the dynamics part of the programs was validated by comparisons between the responses obtained from the modal analysis and from direct integration.

The following is a brief discussion for each of the packages. The computer codes themselves are given in Appendix A.

1). NSTIFF. This package reads in the geometric and material properties for the cylinder-soil composite and computes the stiffness and mass matrices, treating the cylinder as flexible, in the manner described in Sections 2.4 and 2.5.

The only inputs required are the five material parameters E_s, ν_s, m_s, E_r, and m_r described in the bottom right corner of Figure 4.2 and the five geometric parameters R, THICK, TH, B and H, also shown in Figure 4.2. The program will then automatically assume the node and element number (in accordance with the rules which are given below) and compute the nodes' coordinates to give a problem definition (for a standard twelve node cylinder) similar to that in Figure 2.7. To facilitate computer coding, the following rules on geometry and the numbering system are observed.

a). Given a set of the five geometric parameters mentioned earlier, the coordinates of all nodes will then be fixed in terms of these parameters in the manner shown in Figure 4.2. The origin will be at the center of the cylinder.

b). The node number will start with the node at the left horizontal perimeter of the cylinder and will increase consecutively in a clockwise fashion and in a widening circle of soil nodes. The last interior nodes will be the nodes at the top ground surface. The boundary nodes will be numbered in the following order: bottom nodes left to right, left side boundary nodes top to bottom, right side boundary nodes top to bottom (see Figure 2.7).If the stiffness of the soil finite elements are computed by Method 2, the extra interior nodes within the quadrangles will be numbered next after the boundary nodes, again in a clockwise widening circle manner.

c). The element number will start with the left horizontal packing soil spring and again will increase in a clockwise widening circle manner.

The cylinder, packing soil and soil finite element stiffnesses and masses are calculated in accordance with Sections 2.4.1, 2.4.2 and 2.4.3. Each of the non-zero upper triangular cylinder-soil composite stiffnesses will be stored row by row as a one-dimensional array. The diagonal elements of the mass matrix, the only ones that are non-zero, are also stored in a one-dimensional array.

2). MSOLVE. This package reads in the geometric and material properties and the resultant stiffness and mass matrices of the

flexible cylinder-soil composite obtained from package NSTIFF, reads in the free field soil column properties, the damping factor μ, the integration time increment and the input and output control parameters. Finally, it reads in, all at one time, the horizontal and vertical bedrock earthquake accelerations for the entire period of interest.

Then making use of the numerical integration procedure outlined in Section 4.2, the step-by-step solution will begin as follows:

a). The responses of the free field soil column will be obtained according to the equation of motion in Section 3.3.

b). The boundary displacements and velocities of the cylinder-soil composite will be interpolated from the result of a). in the manner described in Section 3.4.

c). The responses of the flexible cylinder-soil composite will be obtained according to the equation of motion in Section 3.5.1.1. The direct integration method is used.

d). The internal moments at the cylinder nodes will be obtained in the manner described in Section 3.6.2.

Step a). to d). will be repeated up to the time desired.

3). RIG20. This package does the same thing as MSOLVE except that here the cylinder is treated as rigid. All the steps in the solution are similar to those of MSOLVE except the following:

c). The responses of the rigid cylinder-soil composite will be obtained with the rigid cylinder equation of motion as described in Section 3.5.1.2.

d). The internal moments at the rigid cylinder nodes are found in

the manner described in Section 3.6.3.

4). WACC. In modal analysis, the responses of the free field are found for the entire period of interest by this package. These responses will be read later on at each time increment as inputs for the cylinder-soil composite.

As before, the equation of motion for the free field soil column in Section 3.3 will be integrated numerically up to the time desired.

5). FQTA1. This package reads in the stiffness and mass matrices of the cylinder-soil composite, deletes the degrees of freedom associated with the boundary nodes and then performs the eigenvalue analysis as described in Section 3.2 to obtain the frequencies and mode shapes.

6). EIG1. This package reads in the mode shapes of the flexible cylinder-soil composite from package FQTA1 and calculates the modal moments in the manner described in Section 3.6.4.

7). SRIGFQ1. This package reads in the stiffness and mass matrices of the flexible cylinder-soil composite from NSTIFF, then the operation described in Section 2.5.2 is performed on these matrices to obtain the stiffness and mass matrices for the case of a rigid cylinder-soil composite.

8). SRIGFQ2. This package reads in the stiffness and mass matrices of a rigid cylinder-soil composite from package SRIGFQ1, deletes the degrees of freedom associated with the boundary nodes and performs the eigenvalue analysis described in Section 3.2 to obtain the frequencies and mode shapes.

9). EIGRIG. This package reads in the mode shapes of the rigid cylinder-soil composite from package SRIGFQ2 and calculates the modal moments in the manner described in Section 3.6.4.

10). PA. This package reads in the stiffness matrix of the cylinder-soil composite (including the boundary degrees of freedom) from SRIGFQ1, the mode shapes from SRIGFQ2, and then calculates the mode participation factors c_i^x, c_i^y, and $\{d_i\}$ according to Eqs.(3-20a), (3-20b) and (3-20c) in Section 3.5.2.

11). TNORM4. This package reads in the mode participation factors c_i^x, c_i^y and $\{d_i\}$ from package PA and multiplies them at each time step by either the appropriate free field displacements, $\{u_F\}$, the appropriate free field velocities, $\{\dot{u}_F\}$, or the bedrock accelerations, $\ddot{u}_g$ and $\ddot{v}_g$ (see Eq.(3-19b)) read in from WACC. For each mode all the results of the multiplications above are added to form the right hand side of Eq.(3-19b). With the excitation input on the right hand side found and with the frequencies read in from SRIGFQ2, the equation of motion, Eq.(3-19b), is then numerically solved to determine the modal amplitude, A_i.

12). DINORM4. This package reads from TNORM4 the modal amplitude, A_i, for all the modes at each time step; from EIGRIG2 the modal moments for each mode; and from SRIGFQ2 the mode shape for each mode. The sum over all the modes of each modal amplitude multiplied by the corresponding mode shape give the displacements for all the nodes. The sum over all the modes of each modal amplitude multiplied by the corresponding modal moment gives the internal moments for the cylinder nodes.

CHAPTER V

NUMERICAL RESULTS

5.1 General

This chapter presents the results that were obtained by applying the method of analysis and computer programs developed previously to a number of numerical problems. Inferences can be made from these results to gain insights into the behavior of the models as well as of the physical problems of engineering interest they represent.

A summary of all the parameters that enter the problem is given in the following.

a). For the eigenproblem of the cylinder-soil composite, the parameters are the four geometric parameters - B, H, THICK, R - and the five material parameters - E_r, m_r, E_s, ν_s, m_s - as noted in Figure 4.2.

If the cylinder is assumed to be rigid, the result will be independent of the cylinder elasticity modulus, E_r. In such case any nominal value for E_r may be used for computational purposes.

b). For the free field soil column, the parameters are the geometric parameters l_i , i=1,2,...,n for "n" number of lumped mass (see Figure 2.1b) and the material parameters E_s, G_s, m_s and μ , all of which have been defined in Section 2.3.

c). The damping matrix for the cylinder-soil composite is defined by the damping proportionality constant μ as given in Eq.(2-2).

Also, note should be given to the following.

a). The number of cylinder nodes is twelve in all the examples used unless otherwise stated. This is considered to be the maximum number of cylinder nodes that is practical considering the limited computational resources.

b). The packing soil annular thickness, TH, is .5 ft. unless otherwise stated.

5.2 Influences of Modelling Parameters for the Cylinder-Soil Composite

5.2.1 General

Parameters such as the boundary distance, the packing soil annulation thickness and the number of cylinder nodes do not have any meaning in the real physical problem, but rather exist only in the particular numerical model used. The effects of these parameters on the natural frequencies and modal moments will be investigated. This will be done following the discussion in the next section on the frequencies and mode shapes of a representative problem.

5.2.2 Frequencies and Mode Shapes

An eigenvalue analysis is made of a cylinder-soil composite with the following parameters:

$B = 12$ ft. , $H = 4$ ft. , THICK = 3/8 in. , $R = 2$ ft. ,

$E_r = 4.589\times10^9$ psf. , $m_r = 15.155$ lb.-sec.^{2}/ft.^{4} ,

$E_s = 1.85\times10^5$ psf. , $\nu_s = .4$, $m_s = 3.725$ lb.-sec.^{2}/ft.^{4}

With the cylinder treated as rigid, the frequencies are listed in Table 5.1, a few of the mode shapes are plotted in Figure 5.1 and a few typical modal moments are listed in Table 5.2. With the cylinder treated as flexible, a few of the mode shapes are plotted in Figure 5.2.

The following observations are made.

a). Unlike the case of a shear beam in which the fundamental frequency is much smaller than the higher frequencies, the frequencies of the cylinder-soil composite increase quite gradually as shown in Table 5.1. This would tend to lessen the dominance of the lowest few modes in the response as is the case of the shear beam.

b). The first five modes of the rigid cylinder case (Figure 5.1) have very similar configurations to the corresponding ones of the flexible cylinder case (Figure 5.2). They would most likely converge to the same frequency and mode shape, mode by mode, as the flexible cylinder is made incresingly stiffer. The sixth modes for the two cases obviously have different mode shapes and can not be said to correspond to each other.

5.2.3 Variation of Boundary Distance

One of the basic assumptions in this investigation is that the motions of the bottom and side boundaries of the cylinder-soil composite are the same as those of the free field soil column at the same level. Intuitively, the appropriateness of this assumption should increase as the boundaries are set further away from the cylinder. In other words, the frequencies and mode shapes of

the cylinder-soil composite should converge toward certain values and shapes as the boundary distance is increased .

To verify the above, frequencies analyses were made of rigid cylinder-soil composites with varying boundary distance, B. The dimensionless frequency term, $f_i/\sqrt{E_s/(m_s H^2)}$, are plotted in Figure 5.3a and Figure 5.3b for the first 15 modes as a function of the dimensionless boundary distance term, B/R. In these figures f_i is the frequency of mode i in cps. It should also be noted that, as the cylinder are assumed to be rigid, the parameters m_s/m_r and THICK/R will enter only in that portion of the mass matrix that involves the cylinder masses.

As expected, both Figures 5.3a and 5.3b suggest that the frequencies do tend to become constant as B/R is increased. The mode shapes, not shown here, also have the same trend. In most of the examples in this study the value of B/R used is about 7. It can be seen from Figure 5.3a that at that point, even though some of the frequencies still indicate a dependence on the parameter B/R, the rate of change is small and thus it will be assumed that these frequencies are close to their asymptotes at B/R = ∞.

5.2.4 Variation of Packing Soil Annulation Thickness.

Eigenvalues analyses were made of four cases of rigid cylinder-soil composites with varying packing soil annulation thickness, TH. For the cases 1, 2, 3 and 4 the values of TH will be .25, .5, 1.0 and 1.5 ft. respectively. Other parameters are as follows:

$B = 12$ ft. , $H = 4$ ft. , THICK = 3/8 in. , $R = 2$ ft. ,

$m_r = 15.155$ lb.-sec.^{2}/ft.^{4} , $E_s = 1.85\times10^5$ psf. ,

$\nu_s = .4$, $m_s = 3.725$ lb.-sec.^{2}/ft.^{4}

The frequencies and modal moments for the first four modes and for mode 20 are listed in Table 5.3. It is seen that the frequencies and modal moments for case 1 and case 2 are very close together for the first four modes, while those of case 3 and case 4 have somewhat larger discrepancies. However, for the higher modes such as mode 20 in Table 5.3, the modal moments for the four cases have a totally different configurations.

5.2.5 Variation of Number of Cylinder Nodes

Eigenvalue analyses were made of four cases of rigid cylinder-soil composite in which the number of cylinder nodes are 8, 12, 16 and 20 for the cases 1, 2, 3 and 4 respectively. Note that each case would involve a different finite element mesh pattern for the soil. The other parameters are as follows:

$B = 56$ ft. , $H = 20$ ft. , THICK = .41 ft. , $R = 9$ ft. ,

$m_r = 15.155$ lb.-sec.^{2}/ft.^{4} , $E_s = 1.85\times10^5$ psf. ,

$\nu_s = .4$, $m_s = 3.725$ lb.-sec.^{2}/ft.^{4}

Since each of the four cases involves a substantially different number of degrees of freedom, the comparison of any other than the lowest frequencies is considered to be inappropriate.

Figure 5.4 shows the lowest frequencies and the corresponding modal moments for the four cases. They are seen to be in reasonably close agreement.

5.3 Responses from Direct Integration and Modal Analysis

Responses were obtained, using both direct integration and modal analysis, for a problem defined in Figure 5.5 and summarized in the following:

a). The rigid cylinder-soil composite has the following parameters:

$B = 12$ ft. , $H = 4$ ft. , THICK = 3/8 in. , $R = 2$ ft. ,

$E_r = 4.589\times10^9$ psf. , $m_r = 15.155$ lb.-sec.^{2}/ft.^{4} ,

$E_s = 1.85\times10^5$ psf. , $\nu_s = .4$, $m_s = 3.725$ lb.-sec.^{2}/ft.^{4}

This is the same cylinder-soil composite as discussed in Section 5.2.2 whose frequencies and mode shapes are given in Table 5.1 and Figure 5.1.

b). The depth of the soil layer down to bedrock is 150 ft. which will be divided into ten equal sublayers. Thus for the free field soil column, $l_i = 15$ ft. for i=1,2,...,10. The soil properties are uniform throughout the ten sublayers and are the same as those of the cylinder-soil composite, i.e., $E_s = 1.85\times10^5$ psf., $G_s = 6.607\times10^4$ psf. (corresponding to $\nu_s = .4$) and $m_s = 3.725$ lb.-sec.^{2}/ft.^{4}.

c). The damping proportionality constant for the cylinder-soil composite is assumed to be $\mu = .00136$ which, by Eq.(2-50), corresponds to the following modal damping ratios:

$\lambda_1 = .02078$, $\lambda_2 = .02485$, $\lambda_3 = .02660$, $\lambda_4 = .04084$,

$\lambda_{20} = .09583$, $\lambda_{57} = .25934$

for mode 1, 2, 3, 4, 20 and mode 57 (the last mode) respectively. These damping ratios seem reasonable values for the physical systems

under consideration.

If the dashpot damping constant and the spring constant of the free field soil are assumed to be related by the same proportionality $\mu = .00136$, the shear damping coefficient of the soil would be equal to 140.17 psf.-sec.

The bedrock motions will be those of 1940 El Centro earthquake in the N-S and the vertical directions.

For the earthquake up to 20 secs. the maximum moments for each of the cylinder nodes (from direct integration) are listed in Table 5.4. The maximum moment for all nodes is 1668.142 ft.-lb. occuring at node 11 at 8.748 secs.

The moments at node 1, 2, 3 and 4 from both direct integration and modal analysis are plotted up to 9 secs. of earthquake in Figures 5.6a, 5.6b, 5.6c and 5.6d. It is noted that at all the four nodes, the responses calculated from the two methods are almost identical except for a few small discrepancies that are most likely due to round off errors. This constitutes a check on the reliability of the dynamic part of the computer programs.

5.4 Method 1 and Method 2

The soil finite element stiffness is calculated either by a procedure involving reduced degrees of freedom, referred to here as Method 1 and discussed in Section 2.4.3.2 or by using the triangular finite element stiffness, referred to as Method 2 and discussed in Section 2.4.3.3. The degree of approximation introduced by Method 1

has been discussed in (15) but in the framework of a different physical problem. For the example in Section 5.3, the moments at node 1 of the cylinder when the stiffness is calculated by Method 1 and Method 2 are shown in Figure 5.7. The magnitude of differences shown is typical of all the other nodes. It will be noted that the difference in the maximum moments between the two methods is about 8 % in Figure 5.7 which is small considering the approximate nature of the stiffness calculation. The Method 1 case requires 94 secs. of CP time for the solution up to 2 secs. of earthquake while the Method 2 case requires 415 secs. of CP time.

5.5 Effects of Stiffness of Cylinder (Relative to Soil)

5.5.1 General

Results are given in the following sections to show the effects of the cylinder stiffness on the behavior of the cylinder-soil composite. Specifically, these results are presented in such a way as to emphasize the relationship between the stiffness of the cylinder and the convergence of its behavior to that of a rigid one. The rigid cylinder case, even though a limitting case for the flexible cylinder, involves a different treatment and solution method and usually requires a smaller computer time to solve. The information in these sections could be helpful for the determination of whether a cylinder is stiff enough to be treated as rigid.

In connection with the above, the stiffness of the cylinder is meaningful only when it is considered relative to that of the soil. In this study, the relative cylinder-soil stiffness is expressed as

$$\alpha = \frac{E_r I_r}{E_s (1-\nu_s^2) R^3 H} \qquad \text{.....(5-1)}$$

To obtain a feel for the range of values of α in actual physical situations, it may be noted that a 36 in. diameter steel pipe with a thickness of 0.7 in. (I_r = .343 in.^{4}) having $E_r = 30\times10^6$ psi., buried under a cover depth (H) equal to 36 in. in a soil having $E_s = 1.85\times10^5$ psf. would correspond to α = .032; an R.C. concrete pipe 36 in. in diameter conforming to ASTM Spec. for Class III, wall A culverts (19) with I_r of the transformed section equal to approximately 96.33 in.^{4} and buried under the same conditions would correspond to α = .079.

5.5.2 Effects on Frequencies

Curves of the ratio, $(f_{flexible}/f_{rigid})_i$, of the ith frequency for the flexible cylinder case to that for the rigid cylinder case are plotted against the relative cylinder-soil rigidity, α , in Figure 5.8a and Figure 5.8b for i=1,2,...,5. These figures show that, with increase in cylinder stiffness, the frequencies, as expected, approach those of the rigid cylinder. The comparison is done only for the first five modes due to considerations as explained in b). of Section 5.2.2.

Figure 5.8a which is for H/R = 2 indicates that a cylinder must have $\alpha \geqslant .15$ for the frequencies of the first five modes to converge to within 5 % of those of the rigid cylinder. Figure 5.8b which is for H/R = 6 (other constants being the same as those for Figure 5.8a) indicates that for the same 5 % convergence the

cylinder must have $\alpha \geqslant .004$. This seems to suggest that a more deeply buried cylinder would behave more like a rigid one.

5.5.3 Effects on Response of a Simplified Problem

A very simplified problem is devised as shown in Figure 5.9a in which the cylinder is loaded by the indicated symmetrical sinusoidal displacements of the outer boundary of the packing soil. The procedures for obtaining the stiffness and mass matrices, the equations of motion and the moment computations for both rigid and flexible cylinder are the same as those discussed earlier for the cylinder-soil composite except that, of course, here the finite element soil is out of the picture and the emphasis is on the responses of the cylinder itself.

The example considered here has the following properties (see Figure 5.9a):

T = Period of boundary displacement = $\frac{2\pi}{p}$ = .1224 secs.,

a = .004 ft. , R = 1 ft. , THICK = 1/4 in. , TH = .5 ft. ,

m_r = 15.155 lb.-sec.^{2}/ft.^{4} , $E_s = 3\times10^5$ psf. , ν_s = .25 ,

m_s = 3.725 lb.-sec.^{2}/ft.^{4}

Three values for E_r are considered; they are 47.0×10^7 psf., 45.9×10^8 psf., and ∞ (rigid cylinder) referred to as case 1, 2 and 3 respectively.

The moments that occur at node 1, 2 and 3 for the three cases of cylinder rigidity are shown in Figure 5.10. The spring forces on the cylinder nodes (see Figure 5.9b) at .0324 secs., which is approximately the time when the maximum moments occur at all the nodes, are shown in Table 5.5. From these results it is noted that the pattern

of the forces from the surrounding soil on the cylinder changes as the rigidity of the cylinder varies. The maximum force and the maximum moment become bigger with increase in cylinder rigidity. The above behavior is observed when the period of the exciting load (.1224 secs. in this case) is one order of magnitude larger than the largest period of the flexible cylinder and packing soil system (.0153 secs. for case 1). This is expected to roughly resemble the interaction within a typical cylinder-soil composite where the modulus of elasticity of the soil surrounding the cylinder is much smaller than the modulus of elasticity of the cylinder material.

5.5.4 Effects on Response

5.5.4.1 Problems with Prescribed Motion on the Top Boundary.-- A number of problems were solved in which the top nodes' boundary (node 37, 38 and 39, for example, in Figure 2.7) are prescribed to have the same motions as the top side boundary nodes (node 41 and 45). Hence, the top boundary cannot be regarded as a free surface. Nevertheless, the responses obtained from these problems should still be useful in giving us a feel in so far as the quantitative relationship between the relative cylinder-soil stiffness and the convergence of the response to that of a rigid cylinder case is concerned.

A cylinder-soil composite with eight cylinder nodes is used with the following parameters:

$B = 4$ ft. , $H = 2$ ft. , THICK = 1/4 in. , $R = 1$ ft. ,

$m_r = 15.155$ lb.-sec.^{2}/ft.^{4} , $E_s = 3.0\times10^5$ psf. ,

$\nu_s = .25$, $m_s = 3.725$ lb.-sec.^{2}/ft.^{4}

The cylinder stiffness varies for three cases in which $E_r = \infty$ (rigid cylinder), $E_r = 45.9\times10^9$ psf. ($\alpha = .074$) and $E_r = 45.9\times10^8$ psf. ($\alpha = .0074$) referred to as case 1, 2 and 3 respectively. The soil layer depth is D = 100 ft. which is divided into 10 equal layers and all the parameters are the same as those for the cylinder-soil composite. The bedrock motions are the 1940 El Centro earthquake in the N-S and the vertical directions starting at 1.5 secs.

Moments at nodes 1, 2 and 3 are shown in Figure 5.11. It is seen that the moment for case 3 ($\alpha = .0074$) and those for the rigid cylinder case have a maximum discrepancy of about 60 % at 1.6 secs., whereas the moment for case 2 ($\alpha = .074$) and that for the rigid cylinder case have a discrepancy of only about 15 % at the same time.

5.5.4.2 Responses of Rigid and Flexible Cylinder.-- The example in Section 5.3 is used here to demonstrate the difference between a rigid cylinder and a flexible cylinder solutions for this particular case in which the cylinder stiffness is $\alpha = .0044$. Moments at nodes 1, 2 and 4 for both solutions are shown in Figures 5.12a, 5.12b and 5.12c. It is seen that in this case in which the cylinder is apparently very flexible, the assumption that the cylinder is rigid will give moments which are higher by as much as eighteen times (i.e., at node 4 at .9 secs.).

The rigid cylinder case having 57 degrees of freedom requires a CP time of about 94 secs. and the flexible cylinder case having 78 degrees of freedom requires about 1168 secs. of CP time. The much

larger computer time required for the flexible cylinder case is due to the fact that, beside the increase in degrees of freedom, the smallest period for the flexible cylinder case is .0004 secs. necessitating an integration time increment of .0001 secs while the smallest period for the rigid cylinder case is .01648 secs. allowing a time increment of .002 secs.

5.6 Contributions of the Modes

It is of interest to consider the relative importance of the various normal modes in the response of the system. The response of the example in Section 5.3 and Figure 5.5 will be used. The following additional information for that example is pertinent. First it is noted that the bedrock accelerations (1940 El Centro earthquake) have significant frequency components ranging from .003 cps. to about 30 cps. The free field soil column has frequencies ranging from .210 cps. to 4.668 cps. Finally the cylinder-soil composite (which has both the bedrock accelerations and the free field soil motions as inputs) has frequencies ranging from 4.865 cps. to 60.690 cps., as shown in Table 1. From the above, we would not expect any large modal responses of the cylinder-soil composite in modes having frequencies higher than, say, 40 cps.

The response up to 9 secs of earthquake, discussed previously in Section 5.3, has been given in Figures 5.6a, 5.6b, 5.6c and 5.6d, from which it is seen that three "peak" moments occur at approximately 6.0, 7.0 and 8.8 secs. The maximum moments at node 11 at these times

are 1517.81, 1368.72, and 1492.82 ft.-lb. respectively. The contributions to these three moments broken down by the modes are shown in Table 5.6. The modal amplitudes for the time 6.0, 7.0 and 8.8 secs. are shown in Table 5.7, and the free field soil displacements inputs at these times are shown in Figure 5.13. The following observations are made.

a). From Table 5.6 it is seen that the bigger moment contributions are from the lower half of the modes. The most important mode is mode 4. Other modes whose contributions are also significant are mode 1, 2, 3, 6, 7, 8, 9, 16, 18, and 19.

b). The moment contributions from the modes at 6.0 secs. and 8.8 secs. are of different nature even though the values of the moments (sum of all modes) for the two cases are of the same order of magnitude. At 8.8 secs. (see Table 5.6), the maximum contribution from the modes is at most of the same order of magnitude as the final sum (e.g., the maximum contribution from mode 4 of 2153.09 ft.-lb. as compared to the sum of 1492.82 ft.-lb.). The moment from any of the last four modes, for example, constitutes at most 2.9 % of the final sum and thus can be neglected without appreciable error. At 6.0 secs. however, the moment contributions from some of the modes can be as much as 40 times the final sum (e.g., the contribution from mode 4 of 47685.30 ft.-lb. as compared to the sum of 1517.81 ft.-lb.). This case of getting a relatively small number as the difference of large numbers necessitates a high degree of computational accuracy. The moment from one of the last five modes, for example, is as much as 41 %

of the final sum and thus can not be neglected. This apparent significance of the higher modes is unusual and is analyzed further below.

It will be shown in the next section that the response of the cylinder-soil composite is predominantly governed by the displacement inputs at the boundary (as against the boundary velocities and the bedrock accelerations). It is then noticed from Figure 5.13 that even though the relative distortions among the free field masses (i.e., the distortion of the boundary) are about the same at both 6.0 and 8.8 secs., the values of the displacements as measured relative to the instantaneous bedrock displacements all have much higher values at 6.0 secs. than at 8.8 secs. The large magnitudes of the moment contributions from the various modes at 6.0 secs. are the results of these large inputs of free field displacements. Although the contributions of the higher modes may be small in comparison with those of the lower modes, they are not small in comparison with the final sum. That sum, i.e., the final value of the moment is relatively small due to the fact that the boundary distortions are actually much smaller than the individual displacements. The preceding observations seem to point to the desirability of separating the boundary displacements input into two parts; (1) a uniform displacement (same for all boundary points), and (2) deviations from the uniform displacement. With such an approach the moment contributions from the modes would probably have smaller numerical values and the contributions of the higher modes would then become negligible as compared to the magnitude of the final sum.

It may also be noted from Figure 5.13 that at 7.0 secs.

the relative distortions of the free field masses have the same order of magnitude as those at 6.0 and 8.8 secs. The displacements as measured from the reference (bedrock) are approximately half way between those at 6.0 and 8.8 secs. As expected, the apparent importance of the higher modes is also seen to fall roughly half way between those at 6.0 and 8.8 secs.

5.7 Relative Importance of the Various Input Motions

The example of Section 5.3 and Figure 5.5 will again be used to examine the contributions of the various inputs to the response of the cylinder-soil composite. In this case the inputs consist of the free field displacements inputs u_8, v_8, u_9, v_9, u_{10}, v_{10}; the free field velocities inputs $\dot{u}_8$, $\dot{v}_8$, $\dot{u}_9$, $\dot{v}_9$, $\dot{u}_{10}$, $\dot{v}_{10}$; and the bedrock accelerations inputs $\ddot{u}_g$ and $\ddot{v}_g$ as shown on the left side of Figure 5.5.

Consider Eq.(3-20f). For a certain mode i, the maximum response caused by an input, $(\text{input})_j$, alone with no multiplication by the mode participation factor (in other words, the mode participation factor is set equal to one unit) will be represented by the maximum value of B_{ij}, $(B_{ij})_{max}$, over the entire time period considered, i.e., 20 secs. $(B_{ij})_{max}$ when multiplied by the appropriate mode participation factor, $(\text{mode part. fact.})_{ij}$, as in Eq.(3-20e) will give the maximum contribution from the forcing function associated with $(\text{input})_j$ to the amplitude of mode i, A_i'.

Table 5.8 shows $(B_{ij})_{max}$ caused by the inputs $\ddot{u}_g$, $\ddot{v}_g$, u_{10},

v_{10}, u_9, v_9, $\dot{u}_{10}$, $\dot{v}_{10}$, $\dot{u}_9$, and $\dot{v}_9$ for the more important modes, i.e., mode 1, 2, 3, 4, 6, 7, 8, 9, 16, 18 and 19. The corresponding mode participation factors are listed in Table 5.9. Finally, the maximum contributions to the modal amplitudes obtained by multiplication of the appropriate corresponding elements in Table 5.8 and 5.9 as indicated in Eq.(3-20e) are listed in Table 5.10.

In Table 5.8 it is noticed that the maximum responses due to each of the inputs (with the mode participation factor equal to one unit) decrease as the mode becomes higher. This is reasonable, considering the fact that (see the beginning of Section 5.6) the frequency components of both the bedrock accelerations inputs and the free field displacements inputs are lower than the middle frequencies range of the cylinder soil composite.

It should be emphasized that $(B_{ij})_{max}$ in Table 5.8 and the maximum contributions to the modal amplitudes in Table 5.10 are the maximum values over the 20 secs. period of earthquake. These maximum values in general do not occur at the same time for different inputs.

Table 5.10 shows that the actual maximum contributions to the modal amplitudes from each of the inputs do not necessarily decrease as the mode becomes higher. This is, of course, due to the influence of the mode participation factors.

It is also noted in Table 5.10 that the free field displacements inputs have far greater maximum contribution than the other inputs. For example, for mode 4 the maximum contribution, 8.5477 ft.$^{1/2}$-lb.$^{1/2}$-sec., from the displacement input u_9 is about 240 times greater than that from the bedrock accelerations and about 310 times

that from the free field velocities.

To have a feel for the magnitude of contributions from various inputs at any one instant in time, the "peak" response time at 6.0 and 8.8 secs. will be used for illustrative purposes. At 6.0 secs. it is seen from Table 5.7 that the three highest modal amplitudes are 27.5570, 6.8248 and 5.0661 $ft.^{1/2}$-$lb.^{1/2}$-sec. for mode 2, 4 and 9 respectively. From Table 5.10 the maximum contributions for all times to mode 2, 4 and 9 from the bedrock accelerations inputs are .71527, .03541 and .00988 $ft.^{1/2}$-$lb.^{1/2}$-sec., respectively; and from the free field velocities inputs are .08398, .02767 and .01649 $ft.^{1/2}$-$lb.^{1/2}$-sec., respectively. It is seen that the major portion of the modal amplitudes come from the free field displacements. At 8.8 secs. the three highest modal amplitudes are 2.037, .3628 and .3081 $ft.^{1/2}$-$lb.^{1/2}$-sec. for mode 1, 8 and 4. The maximum contributions for all times to these modes from the bedrock accelerations inputs are .38415, .01482 and .03541 $ft.^{1/2}$-$lb.^{1/2}$-sec.; and from the free field velocities inputs are .02966, .00345 and .02767 $ft.^{1/2}$-$lb.^{1/2}$-sec. It is, therefore, apparent that the free field displacements have a dominating influence on the response.

5.8 Effects of Damping

Figure 5.14 shows the effects on the response at node 1 of the example presented in Section 5.3 if the damping (velocity) term is deleted from the equation of motion. It is seen that the damping in this example has negligible effects on the response for the short

period of 2.0 secs. considered. The maximum difference between the damped and undamped case is about 2 %. The magnitude of the difference is typical of all other cylinder nodes. It should be kept in mind, however, that the above relates only a single type of damping (i.e., proportional viscous damping) and a single value denoting the amount of damping as specified by the damping constant, μ.

CHAPTER VI

SUMMARY AND CONCLUDING REMARKS

6.1 Summary

A numerical model has been developed for the plane strain formulation of the dynamic response of a buried cylinder subjected to earthquake motions transferred from the bedrock. The model consists of:

a). The free field soil - a series of lumped masses, springs and dashpots extending from the bedrock to the top surface represents a typical column of soil at a relatively large distance in the horizontal direction away from the cylinder.

b). The cylinder-soil composite - a rectangular region of two-dimensional finite elements represents the soil surrounding a circular region of radial springs (packing soil), which in turn circumscribes the cylinder. Two models were used for the cylinder. One was lumped mass and continuous flexibility and the other lumped mass but with infinite rigidity. A viscous type of damping is assumed.

The earthquake (bedrock) motion excites the free field soil column, whose resultant motions are used as inputs to the boundary of the cylinder-soil composite. The feedback between the two parts is assumed to be negligible.

The equations of motion of the model were solved by both

direct integration and modal analysis. In both cases, the Newmark's β numerical integration procedure is applied. Computer programs in FORTRAN were written to carry out the numerical solutions. The stiffness matrices were checked by statics, and the dynamics part of the program were checked by comparison of results between modal analysis and direct integration. The programs developed were utilized in a series of response analysis and parametric studies. Inferences were made from the results in order to gain more complete understanding of the behavior of the problem and the relative importance of the various parameters. The major results are summarized as follows:

a). Concerning the modelling parameters, it was found that the frequencies and mode shapes of the cylinder-soil composite tend to become constant as the boundary distance is increased, that the packing soil annulation thickness significantly affects the higher modes, and that the values of the first mode of different cylinder-soil composites with the number of nodes of the cylinder ranging from eight to twenty are in close agreement with one another.

b). The responses of models with the stiffness of the finite element representing the soil calculated by Method 1 and Method 2 do not differ significantly.

c). Curves are given which show the quantitative relationships between the cylinder stiffness and the convergence of the first five frequencies to those of the rigid cylinder case. It was found that with an increase in the cylinder stiffness the maximum internal

moments in the cylinder wall increase and converge to the values calculated for the rigid cylinder case. The rigid cylinder case is found to require much less computer time to solve.

d). The free field soil displacements have a much greater influence on the cylinder response than either the free field velocity inputs or the bedrock acceleration inputs.

e). A number of modes in the lower half of the frequency spectrum have significant influence on the response. It also appears likely that if the boundary displacements of the cylinder-soil composite are separated into a uniform part and deviations from the uniform part, the role of the higher modes may be drastically diminished.

6.2 Concluding Remarks

A model and method of analysis have been developed to study the problem of a cylinder embedded in a semi-infinite soil layer subjected to bedrock earthquake excitation. Parametric studies and analyses of the responses yielded data and information that have provided much insight into the behavior of the system and the relative importance of the parameters.

The studies involving numerical data in this investigation must be considered exploratory in nature. This is due largely to resource limitations. It appears that a number of pertinent topics deserve further consideration. They include: the effects of the various modelling parameters on the response and their bearings on the degree of approximation; the potential advantage that may

accrue from considering the boundary displacements of the cylinder-soil composite as made up of a uniform part plus a deviatory part; a sufficient number of response studies which would provide a clearer picture, and possibly some criteria, as to the stiffness range of the cylinder which can be approximated by an infinitely rigid one.

Even though the method of analysis in this study utilizes well known principles of mechanics and the problem formulation employs reasonable numerical values and assumptions, the final validation of this study, strictly speaking, must come from experimental data. Such experiments are difficult to perform, to say the least. Once the analytical method in the linear range has been validated, the next logical extension to this study would be the incorporation of non-linearity in the soil and the cylinder material.

Table 5.1.--Frequencies

Mode	Frequency, cps.
1	4.865
2	5.816
3	6.225
4	9.560
5	11.320
6	12.117
7	12.362
8	12.829
9	13.263
10	13.751
11	15.179
12	15.591
13	15.894
14	16.357
15	16.543
16	17.386
17	17.427
18	19.113
19	21.443
20	22.429
21	23.397
22	25.193
23	25.988
24	26.605
25	26.920
26	28.947
27	29.193
28	30.642
29	30.878

Mode	Frequency, cps.
30	33.628
31	33.708
32	34.486
33	35.093
34	35.159
35	35.437
36	36.164
37	36.804
38	39.558
39	39.717
40	42.173
41	42.175
42	42.489
43	42.596
44	42.763
45	46.126
46	48.814
47	48.998
48	49.405
49	49.625
50	50.303
51	50.404
52	51.066
53	51.332
54	52.464
55	54.097
56	56.603
57	60.690

Table 5.2.--Modal Moments

Mode	Modal Moments , ft.-lb.											
	Node 1	Node 2	Node 3	Node 4	Node 5	Node 6	Node 7	Node 8	Node 9	Node 10	Node 11	Node 12
1	-1198.34	-479.95	685.92	1188.65	685.67	-480.45	-1197.43	-658.30	683.03	1348.03	682.78	-658.86
2	299.40	-1140.06	-1428.15	-.24	1427.84	1140.23	-299.51	-1123.46	-832.80	.00	832.81	1123.44
3	224.74	-1079.02	-1363.44	-.16	1363.20	1079.02	-224.87	-1080.39	-837.17	.06	837.26	1080.39
4	-175.40	7066.64	7229.34	.34	-7228.70	-7066.14	175.43	7004.14	6986.61	-.23	-6987.02	-7004.37
5	-2706.20	-1838.96	1145.57	2989.03	1145.80	-1838.61	-2707.04	-938.79	1370.39	2420.64	1370.63	-938.24
6	-7854.75	-5710.66	3595.15	9784.39	3595.53	-5709.91	-7853.00	-3070.79	3658.98	6739.04	3658.34	-3072.12
7	1381.87	607.11	-471.30	.79	472.04	-606.97	-1381.87	359.56	1987.27	.02	-1987.30	-359.67
8	-6708.23	-1037.57	3748.98	4327.36	3749.21	-1037.16	-6707.94	-4595.29	3583.98	8021.73	3583.81	-4595.57
9	2881.29	1783.40	-872.02	-.06	871.91	-1783.44	-2881.26	2011.88	4860.03	.08	-4859.86	-2011.76
18	-1736.67	6751.47	10093.28	.47	-10092.39	-6750.75	1736.71	6911.19	6170.33	-.21	-6170.71	-6911.40
19	829.52	2794.92	3421.57	.00	-3421.55	-2794.87	-829.41	3282.16	4797.25	.10	-4797.05	-3281.98
36	-188.40	-516.54	-529.99	-.03	529.84	516.32	188.65	-551.19	-591.45	-.10	591.33	551.29
37	231.76	-10198.13	-11328.61	-.45	11327.61	10196.96	-232.26	-10137.41	-10022.72	-.28	10022.16	10136.91
56	-239.25	-6551.80	-8959.21	-5.48	8948.95	8543.77	236.69	-3584.99	-3368.91	3.05	3373.87	3586.78
57	-11154.32	-7712.01	7448.08	17639.29	7450.78	-7707.40	-11150.72	-3876.97	5596.39	9714.54	5594.42	-3880.29

Table 5.3.--Effects of Varying Packing Soil Annulation Thickness

	Case	Frequency, CPS.	Modal Moments, ft.-lb.											
			Node 1	Node 2	Node 3	Node 4	Node 5	Node 6	Node 7	Node 8	Node 9	Node 10	Node 11	Node 12
Mode 1	1	5.12	-1317.0	-495.1	735.2	1269.0	734.7	-495.9	-1316.0	-743.7	738.2	1474.8	737.8	-744.4
	2	5.03	-1266.1	-489.2	714.5	1237.3	714.0	-490.1	-1265.0	-703.7	714.9	1419.0	714.5	-704.5
	3	4.90	-1203.1	-483.1	693.6	1197.9	693.1	-483.9	-1201.9	-651.9	689.4	1352.0	689.0	-652.6
	4	4.78	-1169.9	-485.4	689.3	1180.4	689.0	-486.2	-1169.0	-619.2	679.6	1318.4	679.3	-619.6
Mode 2	1	6.00	232.9	-1175.3	-1341.3	.0	1341.3	1175.3	-233.5	-1139.7	-883.6	.1	883.8	1139.5
	2	5.94	253.3	-1176.0	-1382.0	.0	1382.1	1176.0	-253.9	-1146.4	-883.1	.1	883.3	1146.3
	3	5.82	301.2	-1187.6	-1478.3	.0	1478.3	1187.7	-301.7	-1169.7	-881.0	.0	881.1	1169.5
	4	5.72	356.7	-1211.5	-1601.6	.0	1601.5	1211.6	-357.0	-1207.5	-886.0	.0	886.0	1207.4
Mode 3	1	6.91	-206.5	1376.0	1560.6	.0	-1560.6	-1376.0	206.8	1347.1	1105.6	.0	-1105.6	-1347.0
	2	6.69	-213.4	1295.8	1519.2	.0	-1519.2	-1295.8	213.6	1277.3	1041.8	.0	-1041.8	-1277.2
	3	6.30	-226.6	1132.8	1431.1	.0	-1431.1	-1132.9	226.8	1133.1	899.9	.0	-899.9	-1133.0
	4	5.98	-233.2	962.2	1330.1	.0	-1330.1	-962.2	233.5	980.7	749.8	.0	-749.8	-980.6
Mode 4	1	10.45	-287.7	7341.1	7507.9	.0	-7507.7	-7341.0	287.5	7283.9	7166.2	.1	-7166.0	-7283.9
	2	10.21	-238.5	7565.7	7728.0	.0	-7727.9	-7565.6	238.4	7489.9	7451.2	.1	-7451.0	-7489.9
	3	9.73	-158.5	7432.0	7603.6	.0	-7603.5	-7431.8	158.5	7337.9	7428.4	.0	-7428.2	-7337.8
	4	9.28	-115.1	6942.6	7168.9	.0	-7168.8	-6942.4	115.1	6848.2	7024.2	.0	-7024.1	-6848.2
Mode 20	1	24.78	1179.4	10056.8	9337.6	.1	-9337.3	-10056.8	-1179.3	9877.3	11754.3	.1	-11754.0	-9877.1
	2	23.59	9215.6	4060.3	-6255.2	-7487.2	-6254.7	4061.0	9215.1	5442.1	-4749.5	-11332.7	-4749.2	5442.6
	3	22.49	-3984.3	-1594.8	3433.4	1977.3	3433.0	-1595.5	-3983.7	-2957.5	1957.9	5928.0	1957.6	-2958.0
	4	21.57	-281.4	798.3	1120.2	-2190.3	1119.9	797.9	-280.9	-1551.1	-111.9	2428.6	-112.1	-1551.5

Table 5.4.--Maximum Moments

Node	Maximum Moment, ft.-lb.	Time, secs.
1	364.76	3.948
2	1624.27	8.748
3	1442.40	8.748
4	258.27	5.348
5	1464.08	8.748
6	1598.30	8.748
7	249.90	5.298
8	1614.88	8.748
9	1647.30	8.748
10	254.56	5.348
11	1668.14	8.748
12	1586.57	8.748

Table 5.5.--Forces on Cylinder Nodes for the Simplified Problem

Time = .0324 secs.

Case 1 $E_r = 47.0 \times 10^7$ psf.

Case 2 $E_r = 45.9 \times 10^8$ psf.

Case 3 E_r = infinite

	Forces , ft.-lb.					
	Node 1		Node 2		Node 3	
	$F_x(1)$	$F_y(1)$	$F_x(2)$	$F_y(2)$	$F_x(3)$	$F_y(3)$
Case 1	-602.9	0.	-268.3	486.8	0.	460.5
Case 2	-1105.6	0.	-614.1	900.3	0.	1006.4
Case 3	0.	0.	-574.8	1149.7	0.	2351.7

Table 5.6.--Moment Contributions from the Modes

Contributions from various modes to the moment at node 11

Time, sec.	Moment Sum of All Modes, ft.-lb.	Moment contribution, ft.-lb.							
		Mode 1	Mode 2	Mode 3	Mode 4	Mode 5	Mode 6	Mode 7	Mode 8
6.0	1517.81	-643.43	22949.98	3546.82	-47685.30	-22.17	291.60	-4556.19	599.52
7.0	1368.72	2695.66	5459.50	732.70	-10100.25	67.76	-1087.41	-1004.29	-2453.95
8.8	1492.82	1391.46	-73.05	-189.63	2153.09	39.94	-604.60	142.90	-1300.42

Time, sec.	Moment contribution, ft.-lb.								
	Mode 9	Mode 10	Mode 11	Mode 12	Mode 13	Mode 14	Mode 15	Mode 16	Mode 17
6.0	24620.54	38.32	-213.55	-54.15	-6.04	-75.72	9.19	-102.69	949.74
7.0	5926.37	-181.70	-43.40	248.94	26.79	300.49	1.93	386.44	248.67
8.8	24.38	-90.55	12.99	124.32	14.16	161.72	-.44	213.52	33.23

Table 5.6 (cont'd)

Time, sec.	Moment contribution, ft.-lb.								
	Mode 18	Mode 19	Mode 20	Mode 21	Mode 22	Mode 23	Mode 24	Mode 25	Mode 26
6.0	3979.15	-4451.45	-27.36	77.12	29.68	-114.59	-2.41	-269.12	249.75
7.0	778.76	-1332.22	108.94	8.48	-140.59	-14.79	11.59	-51.23	56.28
8.8	-283.42	-424.41	58.01	-16.40	-68.51	19.69	5.40	20.75	-6.32

Time, sec.	Moment contribution, ft.-lb.								
	Mode 27	Mode 28	Mode 29	Mode 30	Mode 31	Mode 32	Mode 33	Mode 34	Mode 35
6.0	5.19	12.06	1469.89	-165.09	-3.36	-116.02	510.54	6.10	.43
7.0	-12.50	-45.53	351.20	-44.75	12.17	-30.96	143.86	-28.54	7.34
8.8	-7.65	-24.64	1.09	-8.14	6.87	-4.97	34.18	-14.19	1.43

Table 5.6 (cont'd)

Time, sec.	Moment contribution, ft.-lb.								
	Mode 36	Mode 37	Mode 38	Mode 39	Mode 40	Mode 41	Mode 42	Mode 43	Mode 44
6.0	6.47	2921.14	.01	-256.74	.16	-56.16	-2.90	35.39	-2.11
7.0	2.23	777.71	-.04	-71.66	-.66	-13.61	10.46	9.83	8.52
8.8	1.09	122.89	-.02	-16.09	-.31	-.22	5.77	2.17	4.51

Time, sec.	Moment contribution, ft.-lb.								
	Mode 45	Mode 46	Mode 47	Mode 48	Mode 49	Mode 50	Mode 51	Mode 52	Mode 53
6.0	-12.34	-406.55	.03	-800.51	-16.21	95.09	4.48	21.40	2.19
7.0	52.50	-82.91	.01	-203.23	60.16	22.01	-19.01	7.26	-13.71
8.8	27.29	23.71	.00	-18.59	33.04	-.83	-9.68	3.26	-6.05

Table 5.6 (cont'd)

Time, sec.	Moment contribution, ft.-lb.			
	Mode 54	Mode 55	Mode 56	Mode 57
6.0	-611.68	-13.43	-229.36	2.45
7.0	-174.08	61.63	-56.76	-9.72
8.8	-43.92	30.94	-2.73	-5.22

Table 5.7.--Modal Amplitudes

Time, sec.	Modal Amplitudes, $ft.^{1/2}$-$lb.^{1/2}$-sec.									
	Mode 1	Mode 2	Mode 3	Mode 4	Mode 5	Mode 6	Mode 7	Mode 8	Mode 9	Mode 10
6.0	-.9423	27.5570	4.2361	6.8248	-.0161	.0797	2.2926	.1672	-5.0661	-.0235
7.0	3.9480	6.5554	.8751	1.4455	.0494	-.2972	.5053	-.6847	-1.2194	.1116
8.8	2.0379	-.0877	-.2264	-.3081	.0291	-.1652	-.0719	-.3628	-.0050	.0556

Time, sec.	Modal Amplitudes, $ft.^{1/2}$-$lb.^{1/2}$-sec.									
	Mode 11	Mode 12	Mode 13	Mode 14	Mode 15	Mode 16	Mode 17	Mode 18	Mode 19	Mode 20
6.0	.0977	.0550	.0063	-.0287	-.5695	-.0348	.4426	-.6448	.9279	-.0135
7.0	.0198	-.2531	-.0281	.1141	-.1196	.1311	.1159	-.1262	.2777	.0537
8.8	-.0059	-.1264	-.0149	.0614	.0275	.0724	.0154	.0459	.0884	.0286

Table 5.7 (cont'd)

Time, sec.	Modal Amplitudes, $ft.^{1/2}$-$lb.^{1/2}$-sec.									
	Mode 21	Mode 22	Mode 23	Mode 24	Mode 25	Mode 26	Mode 27	Mode 28	Mode 29	Mode 30
6.0	.0827	-.0118	-.1544	-.0010	-.0721	-.2368	.0024	-.0194	-.5443	-.1820
7.0	.0091	.0561	-.0199	.0051	-.0137	-.0533	-.0060	.0732	-.1300	-.0493
8.8	-.0175	.0273	.0265	.0023	.0055	.0059	-.0036	.0396	-.0004	-.0089

Time, sec.	Modal Amplitudes, $ft.^{1/2}$-$lb.^{1/2}$-sec.									
	Mode 31	Mode 32	Mode 33	Mode 34	Mode 35	Mode 36	Mode 37	Mode 38	Mode 39	Mode 40
6.0	.0031	-.4289	.1920	-.0027	-.0001	.0109	.2914	-.0000	.0393	-.0000
7.0	-.0112	-.1144	.0541	.0128	-.0020	.0037	.0775	.0003	.0109	.0001
8.8	-.0063	-.0183	.0128	.0063	-.0004	.0018	.0122	.0001	.0024	.0000

Table 5.7 (cont'd)

Time, sec.	Modal Amplitudes, $ft.^{1/2}$-$lb.^{1/2}$-sec.									
	Mode 41	Mode 42	Mode 43	Mode 44	Mode 45	Mode 46	Mode 47	Mode 48	Mode 49	Mode 50
6.0	-.0059	-.0002	.0060	-.0004	-.0011	-.0159	.0000	.0235	-.0010	-.0115
7.0	-.0014	.0009	.0016	.0017	.0050	-.0032	.0000	.0059	.0040	-.0026
8.8	-.0000	.0005	.0003	.0009	.0026	.0009	.0000	.0005	.0022	.0001

Time, sec.	Modal Amplitudes, $ft.^{1/2}$-$lb.^{1/2}$-sec.									
	Mode 51	Mode 52	Mode 53	Mode 54	Mode 55	Mode 56	Mode 57			
6.0	-.0003	-.0038	.0003	-.0293	.0013	-.0679	.0004			
7.0	.0015	-.0013	-.0022	-.0083	-.0060	-.0168	-.0017			
8.8	.0008	-.0005	-.0010	-.0021	-.0030	-.0008	-.0009			

Table 5.8.--Maximum Response

Input	Maximum Response, $(B_{ij})_{max}$											
	Mode 1	Mode 2	Mode 3	Mode 4	Mode 6	Mode 7	Mode 8	Mode 9	Mode 16	Mode 18	Mode 19	
$\ddot{u}_g$	.04580	.o2862	.02376	.00549	.00274	.00255	.00236	.00216	.00090	.00075	.00062	units in ft.
$\ddot{v}_g$	.01474	.01243	.01197	.01121	.00350	.00342	.00322	.00262	.00093	.00099	.00071	
u_{10}	.00167	.00116	.00102	.00043	.00027	.00026	.00024	.00022	.00013	.00011	.00009	units in ft.-sec.^{2}
v_{10}	.00052	.00036	.00032	.00013	.00008	.00008	.00007	.00007	.00004	.00003	.00003	
u_9	.00164	.00114	.00100	.00042	.00026	.00025	.00023	.00022	.00013	.00010	.00008	
v_9	.00051	.00036	.00031	.00013	.00008	.00008	.00007	.00007	.00004	.00003	.00003	
$\dot{u}_{10}$	.00466	.00361	.00321	.00115	.00070	.00068	.00063	.00059	.00034	.00028	.00022	units in ft.-sec.
$\dot{v}_{10}$	.00138	.00101	.00093	.00035	.00022	.00021	.00019	.00018	.00010	.00008	.00007	
$\dot{u}_9$	.00427	.00318	.00284	.00100	.00062	.00059	.00055	.00051	.00030	.00024	.00019	
$\dot{v}_9$	.00130	.00093	.00086	.00033	.00020	.00019	.00018	.00017	.00010	.00008	.00006	

Table 5.9.--Mode Participation Factor

Input	Mode Participation Factor											
	Mode 1	Mode 2	Mode 3	Mode 4	Mode 6	Mode 7	Mode 8	Mode 9	Mode 16	Mode 18	Mode 19	
$\ddot{u}_g$	.004893	24.9922	4.03619	6.45143	.000125	2.13845	0.	4.57712	0.	.625040	.758230	units in $lb.^{1/2}$-sec./$ft.^{1/2}$
$\ddot{v}_g$	26.0623	.001117	.000372	.000050	2.07499	0.	4.60529	0.	.911122	0.	0.	
u_{10}	.727440	17106.4	520.458	3291.85	.147649	3577.45	.018169	20551.8	.016479	765.343	23763.6	units in $lb.^{1/2}/ft.^{1/2}$-sec.
v_{10}	714.191	.037212	.014919	.009393	10798.3	.319870	13356.1	.015758	8886.11	.005728	.002161	
u_9	.772440	16414.8	5591.79	20351.8	.362770	9557.83	.006735	11058.6	.001762	9934.52	9965.60	
v_9	16780.1	.747657	.248680	.045832	178.727	.016260	9462.43	.001593	832.683	.007001	.002105	
$\dot{u}_{10}$	.000989	23.2647	.707823	4.47691	.000200	4.68534	.000024	27.9504	.000022	1.04086	32.3185	units in $lb.^{1/2}/ft.^{1/2}$
$\dot{v}_{10}$	.971299	.000050	.000020	.000012	14.6858	.000435	18.1643	.000021	12.0851	.000007	0.	
$\dot{u}_9$	.001050	22.3242	7.60483	27.6784	.000493	12.9986	0.	15.0397	0.	13.5109	13.5532	
$\dot{v}_9$	.02966	.001016	.000338	.000062	.243069	.000022	12.8689	0.	1.13244	.000009	0.	

Table 5.10.--Maximum Contribution to the Modal Amplitudes

Function corresponding to	Maximum Contribution to the Modal Amplitudes										
	Mode 1	Mode 2	Mode 3	Mode 4	Mode 6	Mode 7	Mode 8	Mode 9	Mode 16	Mode 18	Mode 19
$\ddot{u}_g$	.00022	.71527	.09589	.03541	0.	.00545	0.	.00988	0.	.00046	.00047
$\ddot{v}_g$	.38415	.00001	0.	0.	.00726	0.	.01482	0.	.00084	0.	0.
u_{10}	.00121	19.843	.53086	1.4154	.00003	.93013	0.	4.5214	0.	.08418	2.1387
v_{10}	.37137	.00001	0.	0.	.86387	.00002	.93492	0.	.35544	0.	0.
u_9	.00126	18.712	5.5917	8.5477	.00009	2.3894	0.	2.4329	0.	.99345	.79724
v_9	8.5578	.00026	.00007	0.	.01429	0.	.66237	0.	.03330	0.	0.
$\dot{u}_{10}$	0.	.08398	.00227	.00514	0.	.00330	0.	.01649	0.	.00029	.00711
$\dot{v}_{10}$	.00134	0.	0.	0.	.00323	0.	.00345	0.	.00120	0.	0.
$\dot{u}_9$	0.	.07099	.02159	.02767	0.	.00766	0.	.00767	0.	.00324	.00257
$\dot{v}_9$	.02966	0.	0.	0.	.00004	0.	.00231	0.	.00011	0.	0.

units in $ft.^{1/2}$-$lb.^{1/2}$-sec.

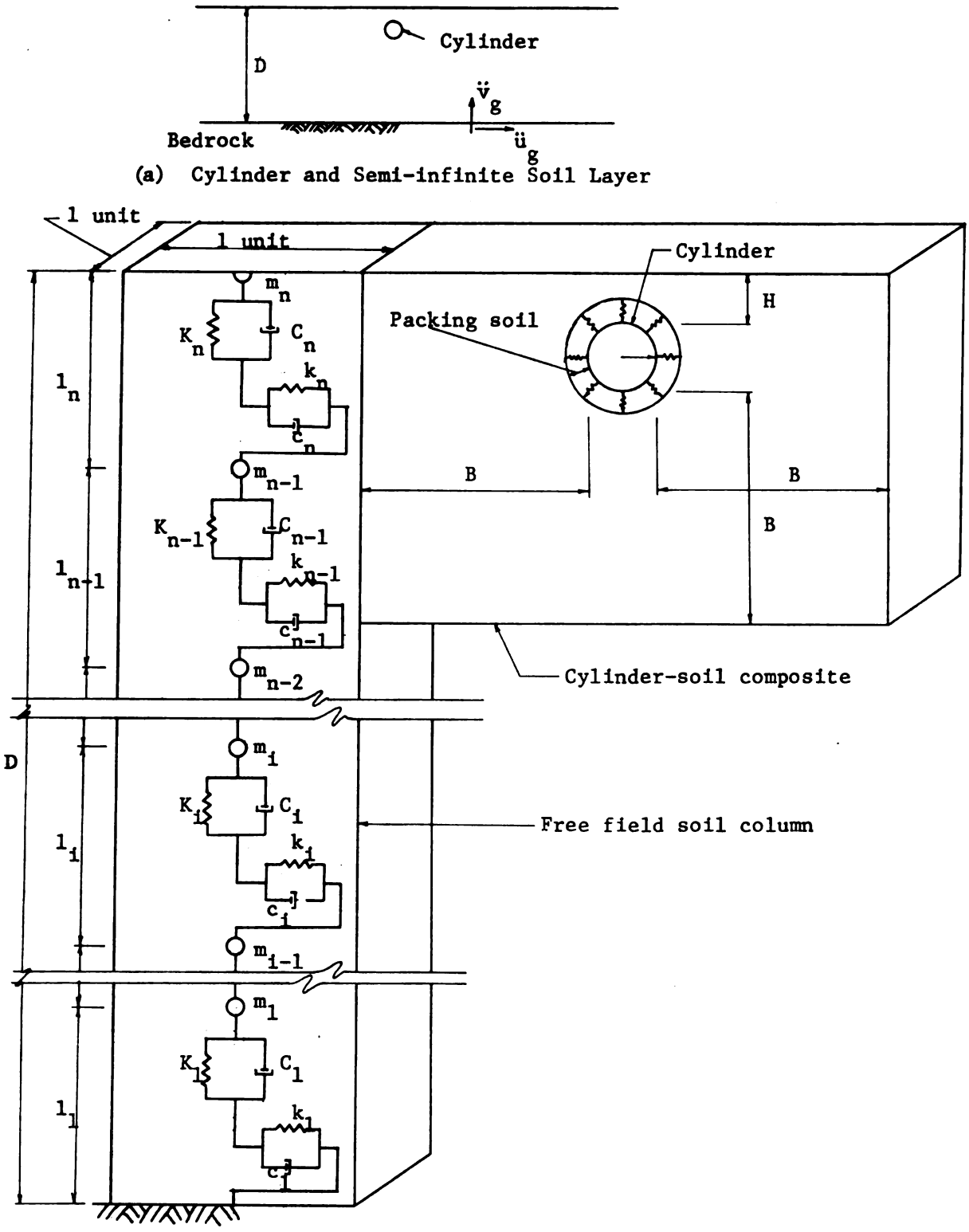

Figure 2.1 Idealization of Cylinder and Semi-infinite Soil Layer

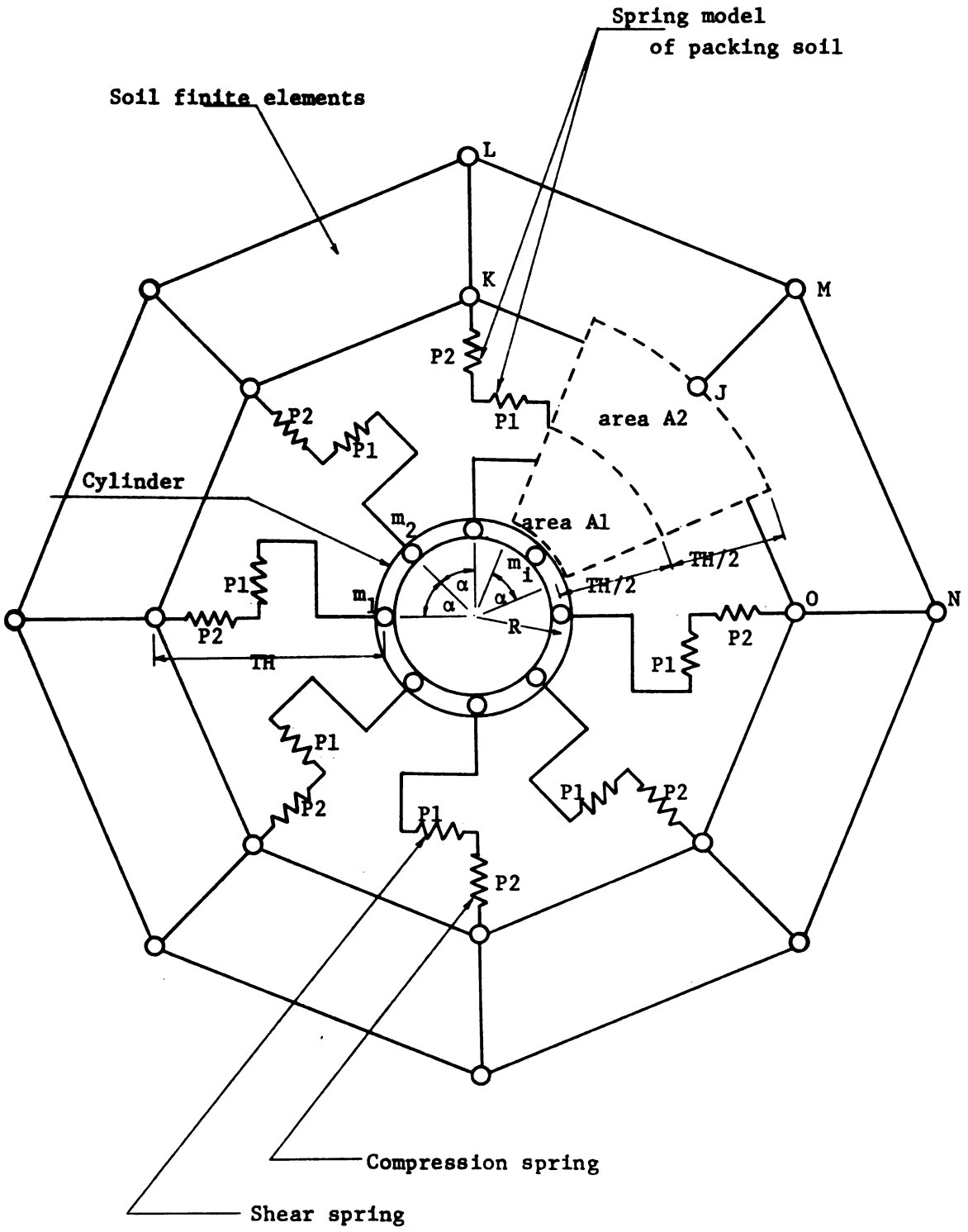

Figure 2.2 Idealization of Cylinder and Packing Soil

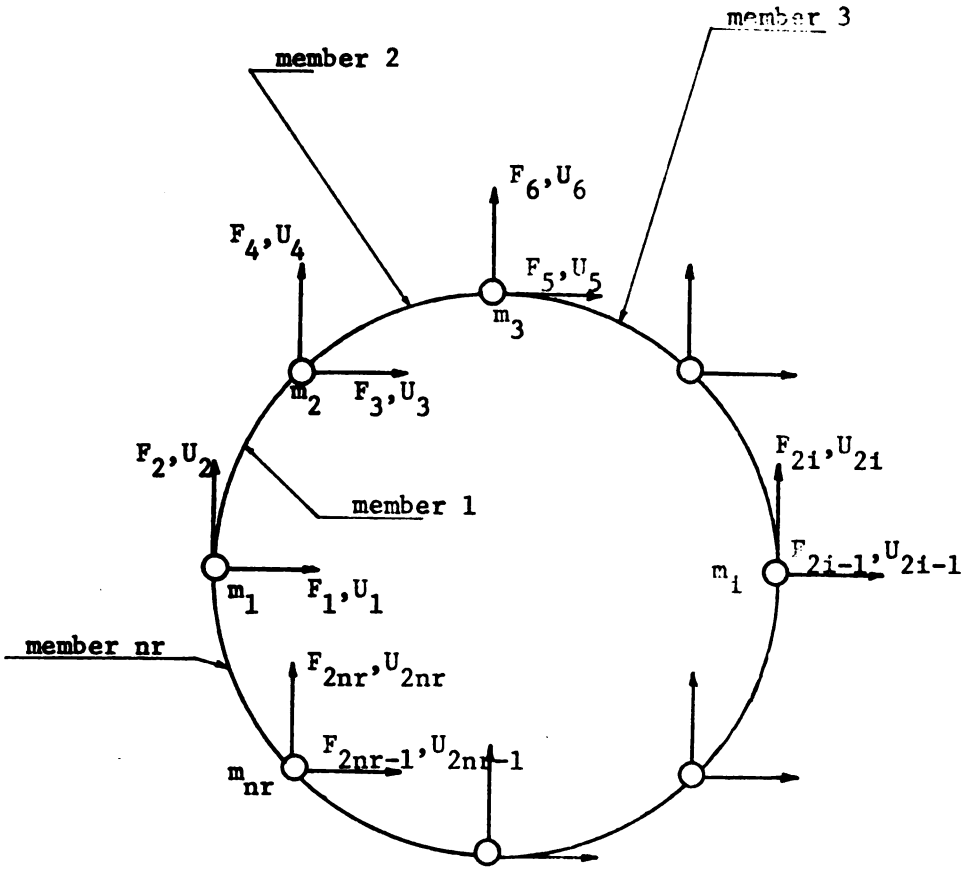

Total number of cylinder
lumped mass = nr

Figure 2.3 Degrees of Freedom of Cylinder in Global Coordinates

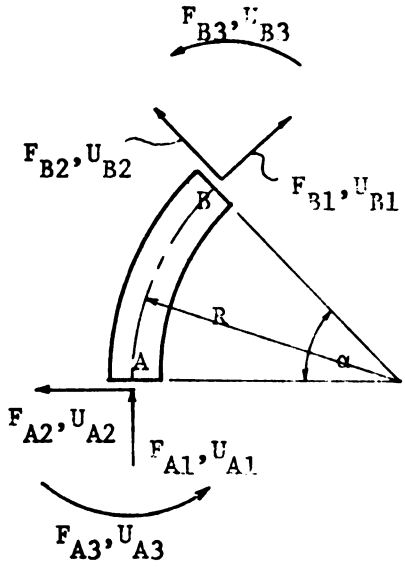

(a) Coordinates for Stiffness Matrix $[S_m]$

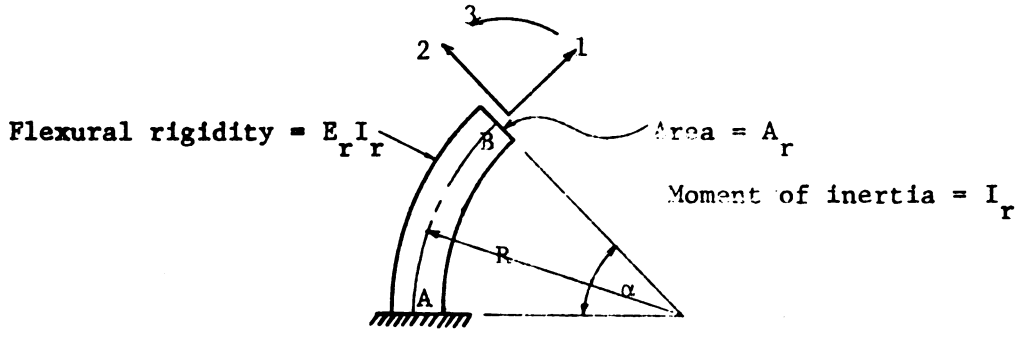

(b) Coordinates for Flexibility Matrix $[F_{BB}]$

Figure 2.4 A Typical Arc

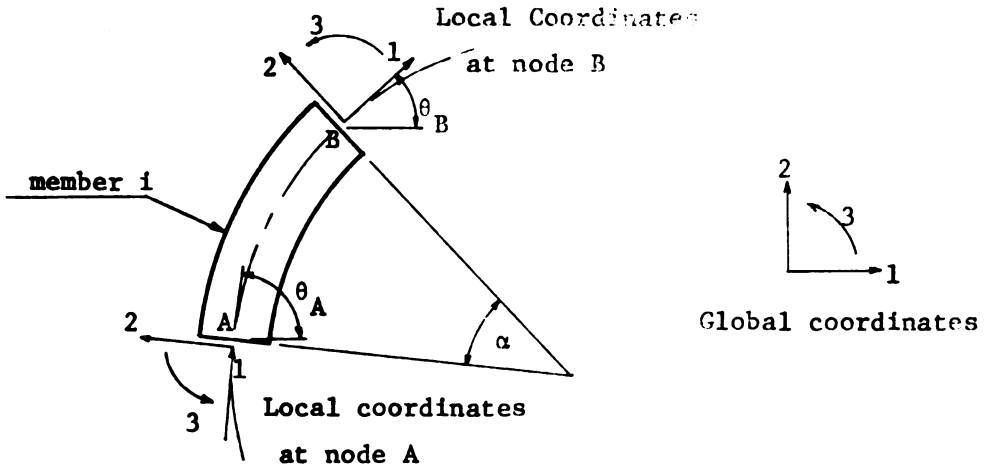

Figure 2.5 Local and Global Coordinates of an Arc

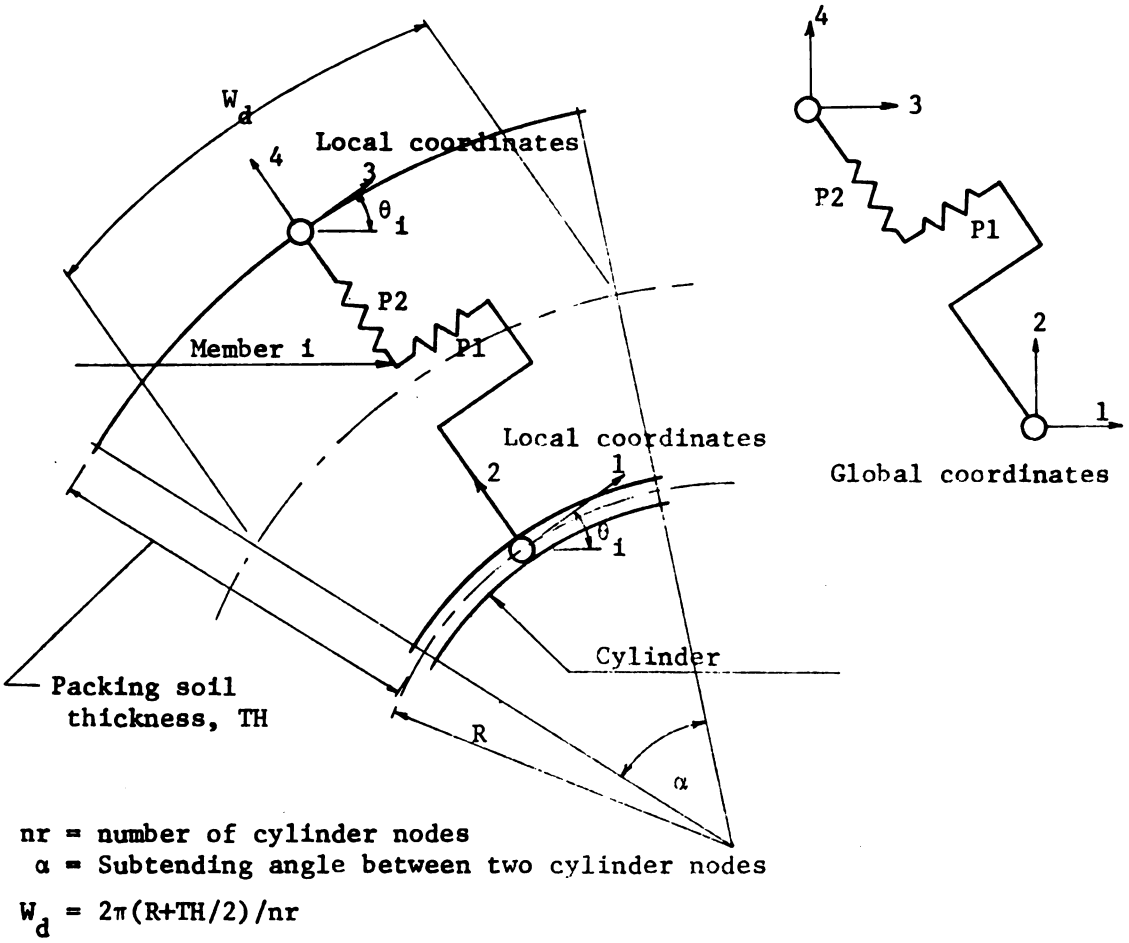

Figure 2.6 Local and Global Coordinates of Packing Soil

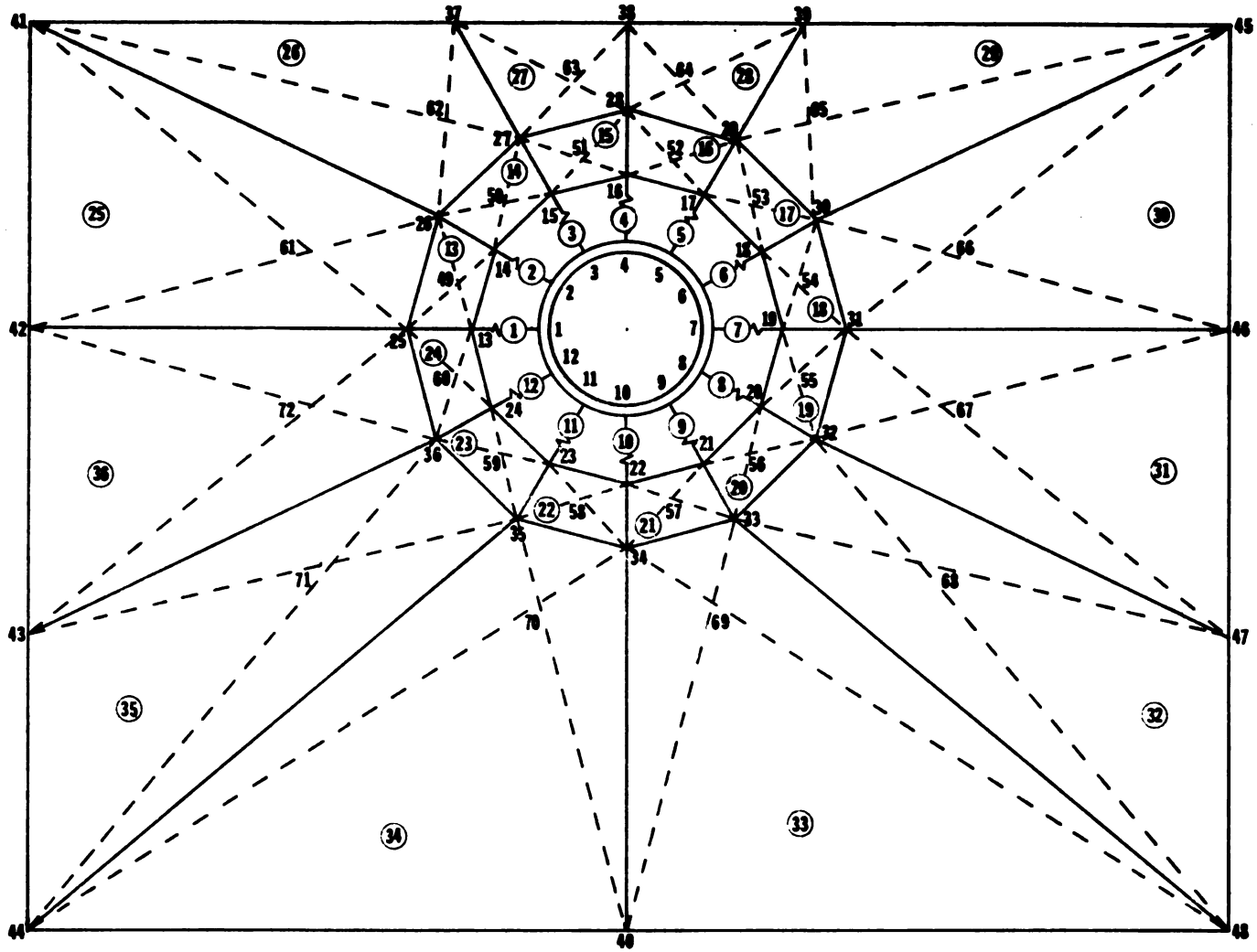

Figure 2.7 Nodes and Elements Numbering System

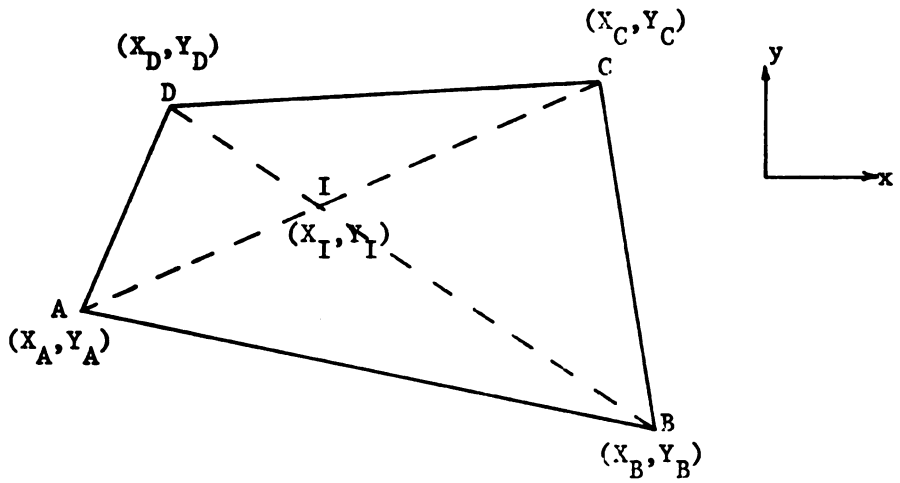

(a)

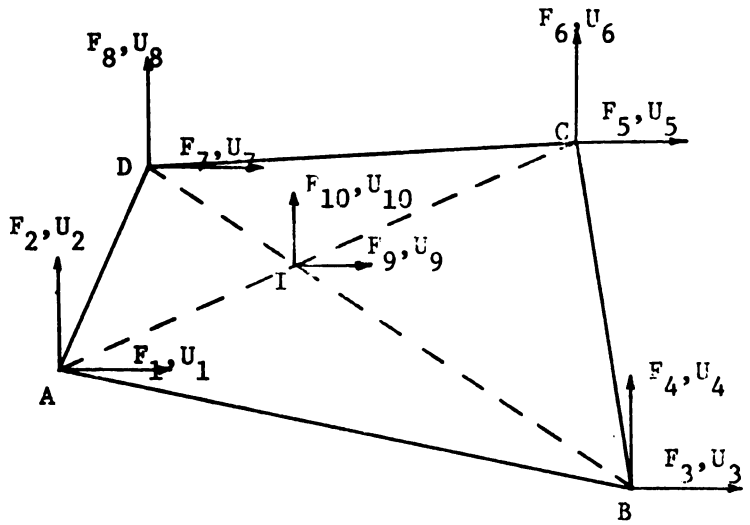

(b)

Figure 2.8 A Finite Element Quadrangle

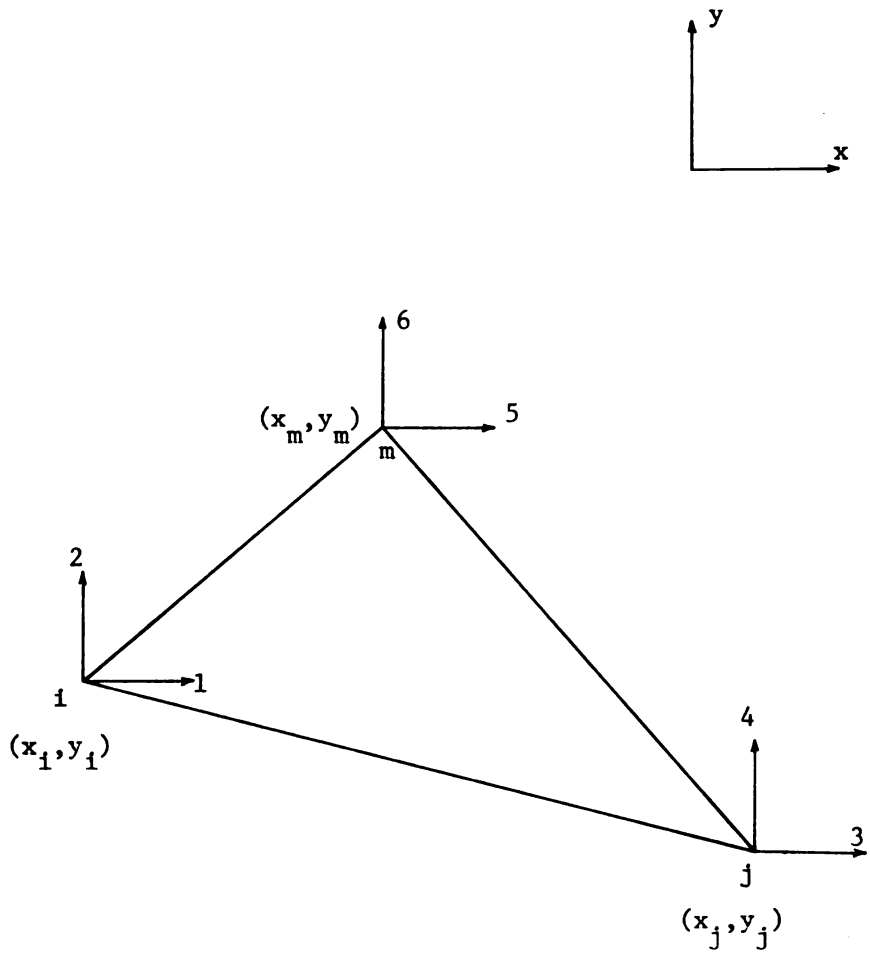

Figure 2.9 A Triangular Finite Element

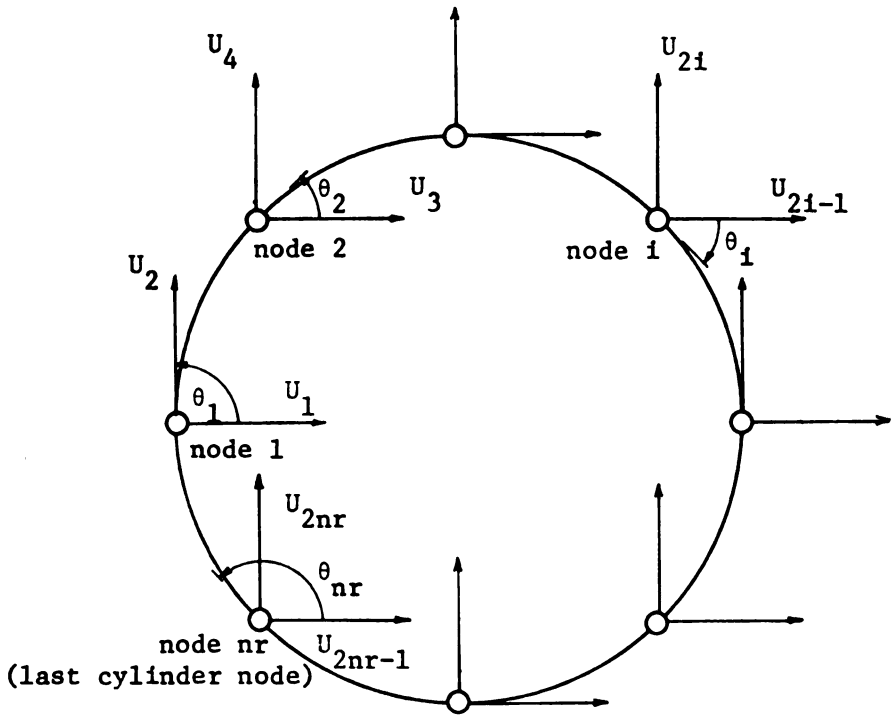

(a) Flexible Cylinder Degrees of Freedom

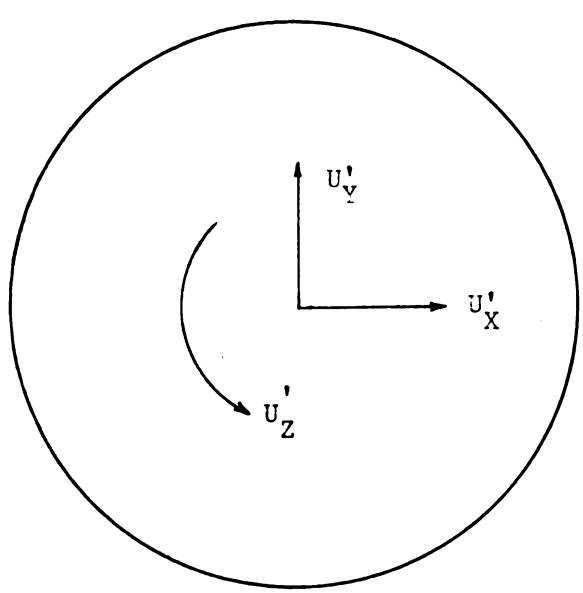

(b) Rigid Cylinder Degrees of Freedom

Figure 2.10 Flexible and Rigid Cylinder

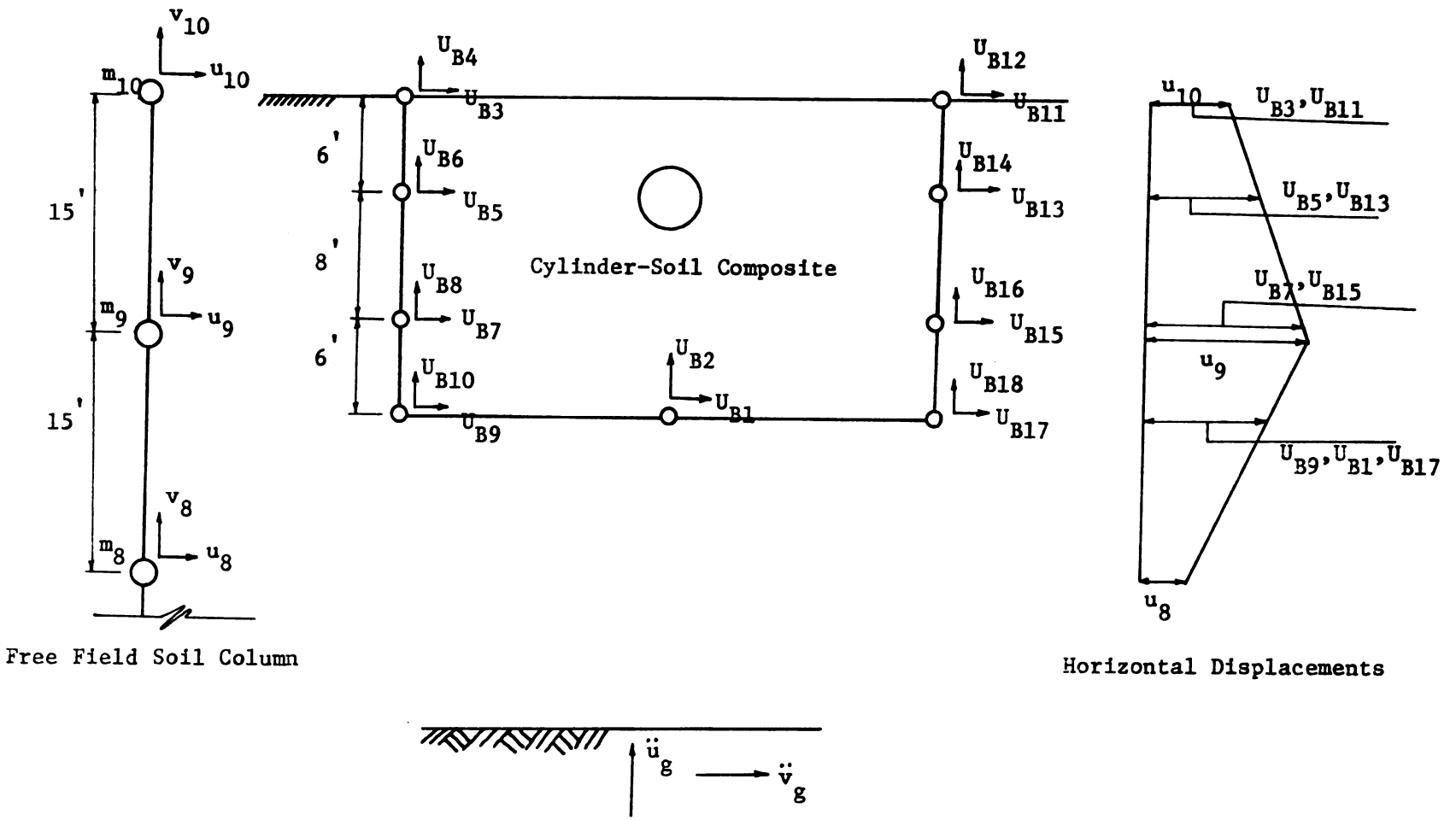

Figure 3.1 Interpolation from Free Field to Cylinder-Soil

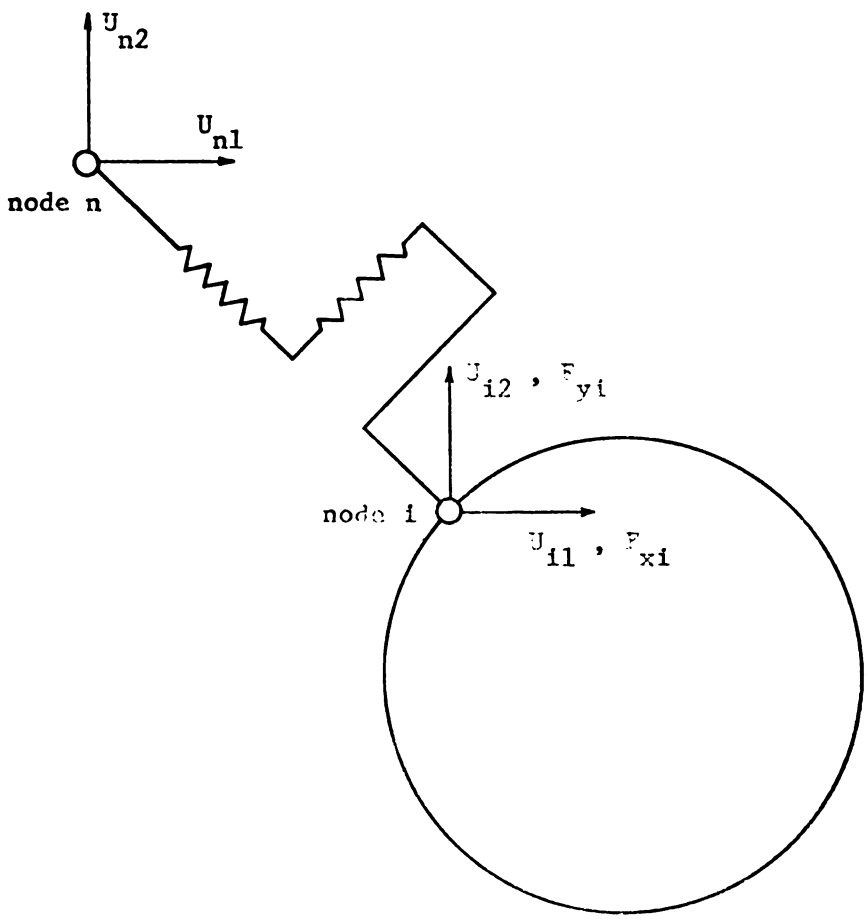

Figure 3.2 Force on a Typical Cylinder Node

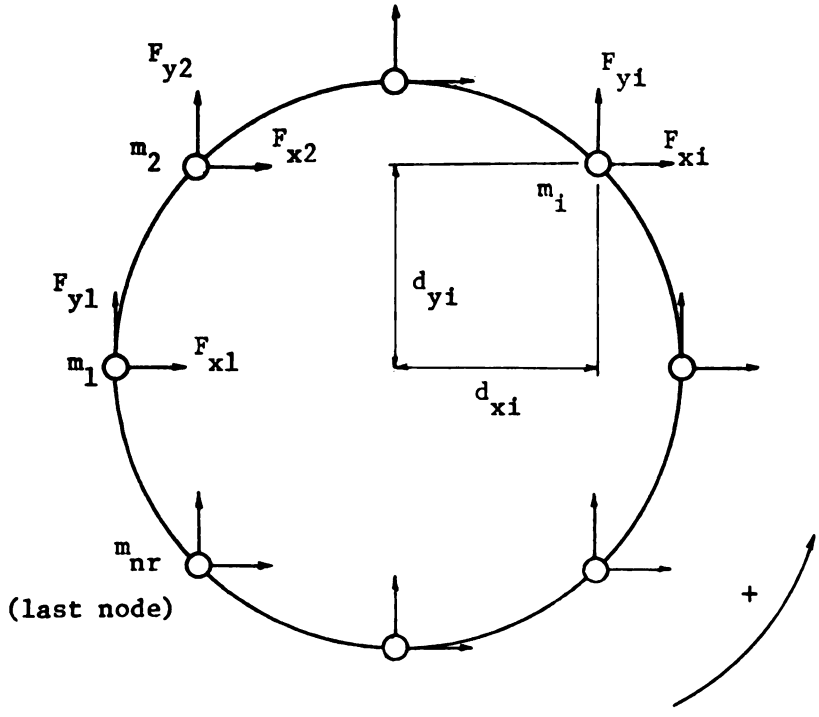

(a) Node Forces on Rigid Cylinder

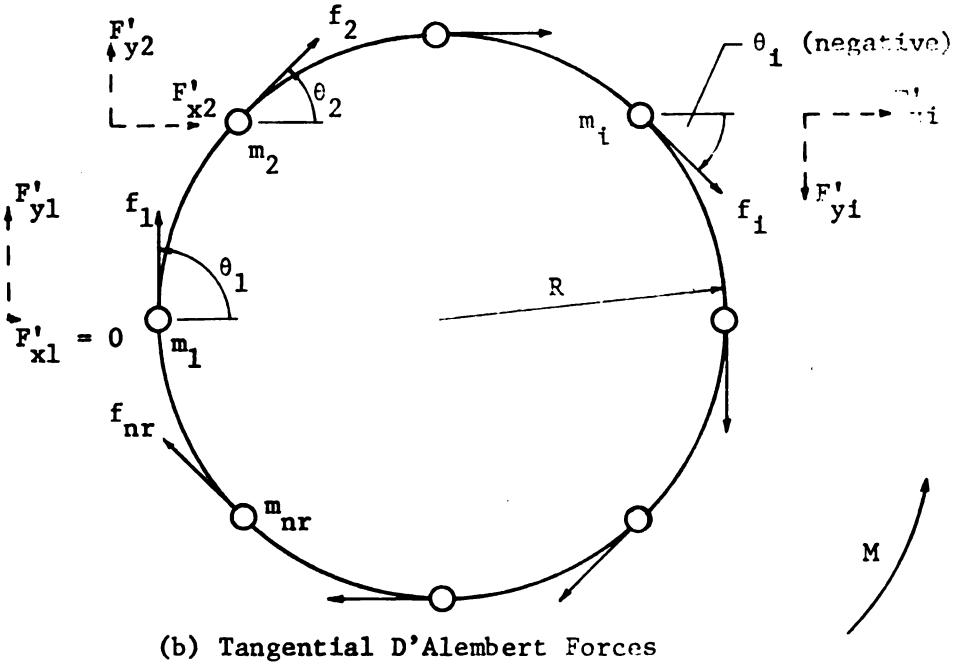

(b) Tangential D'Alembert Forces

Figure 3.3 Forces on a Rigid Cylinder

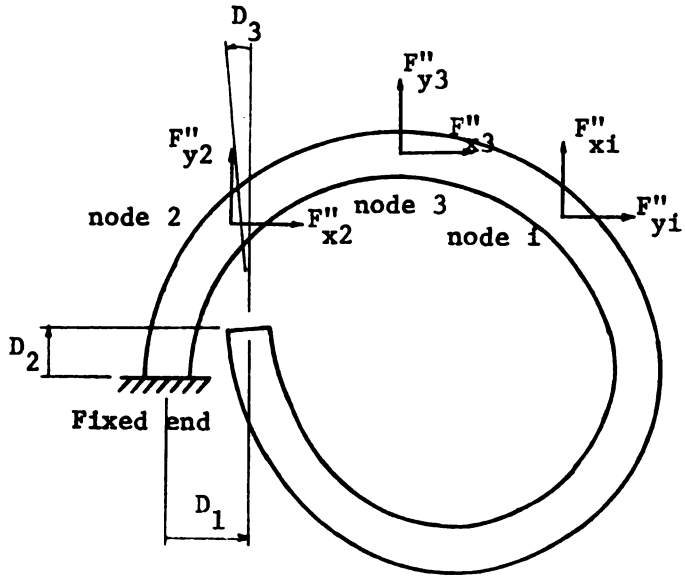

(a) Released Structure

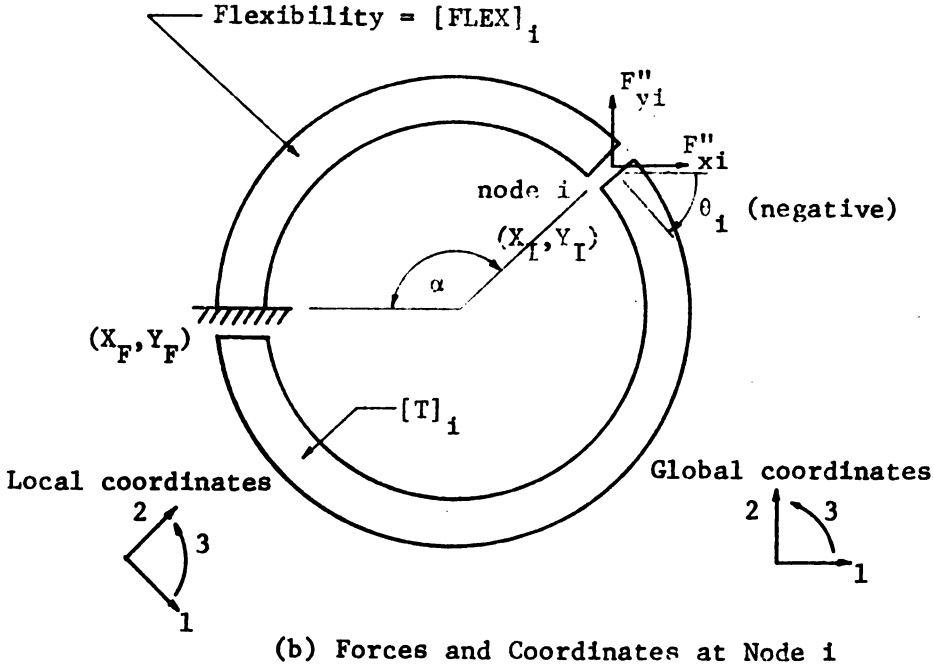

(b) Forces and Coordinates at Node i

Figure 3.4 Released Structure

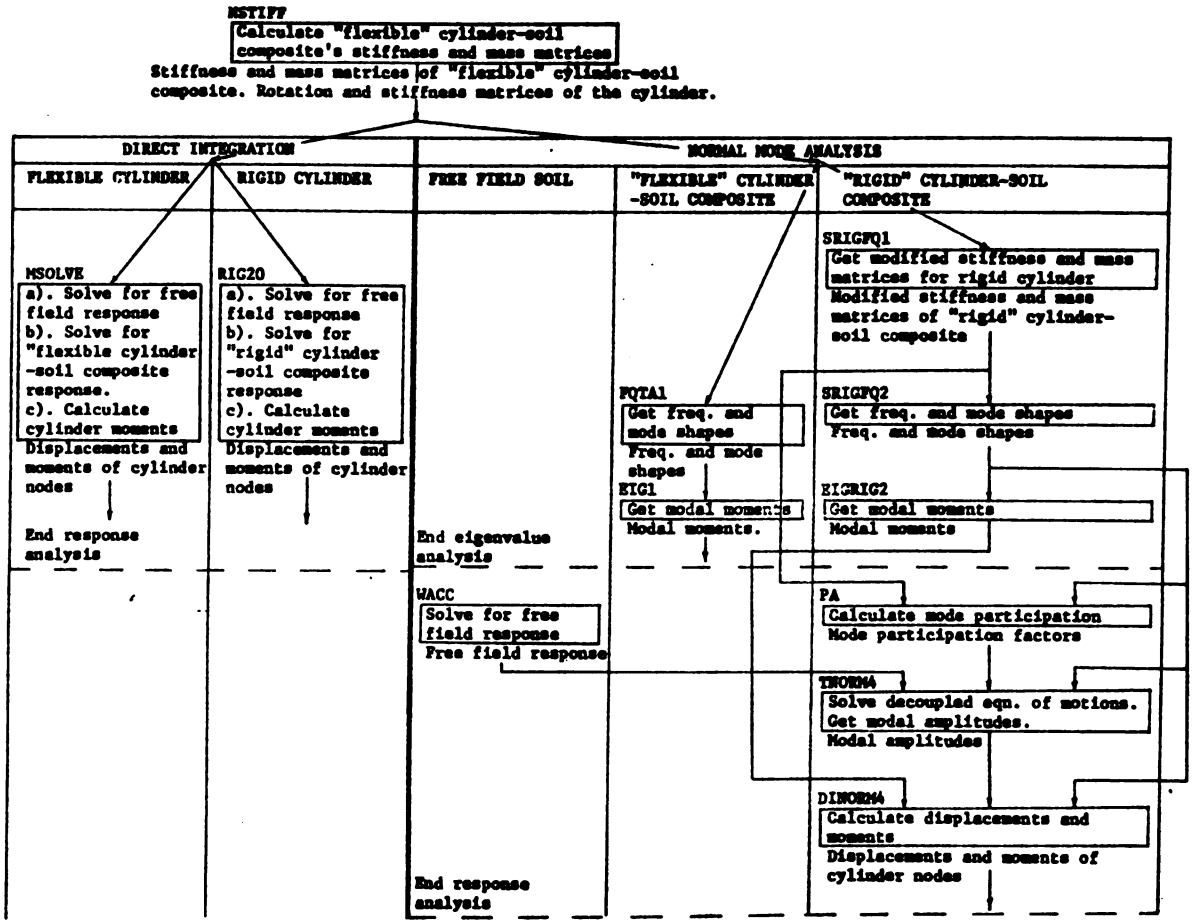

Figure 4.1 Computer Program Packages

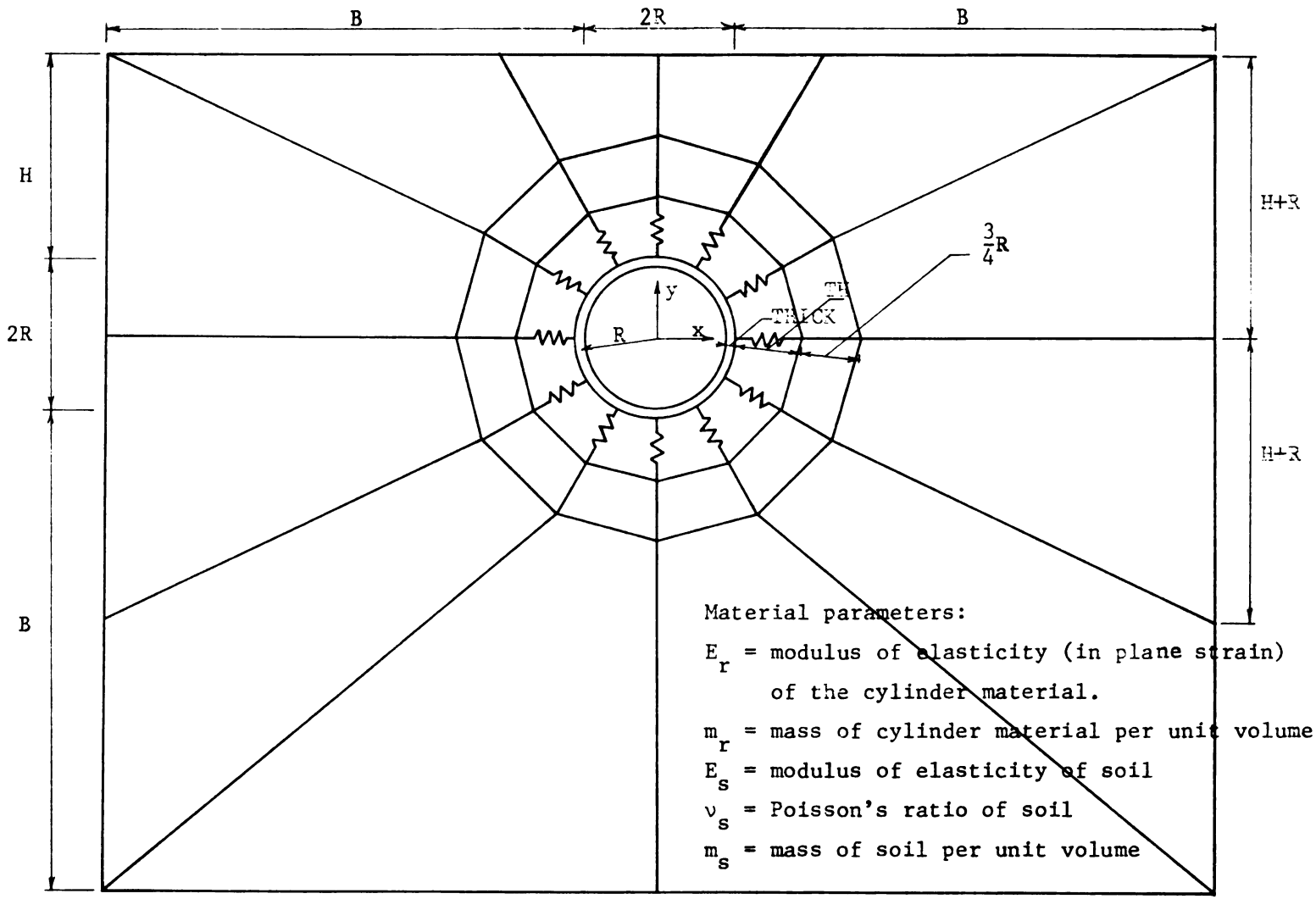

Figure 4.2 Geometric and Material Parameters

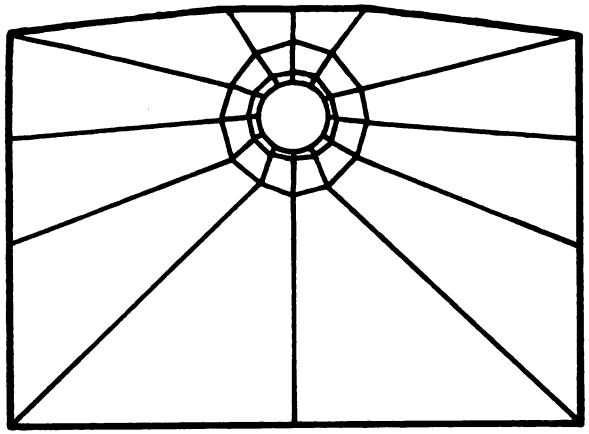

Mode 1 T = .2055 secs.

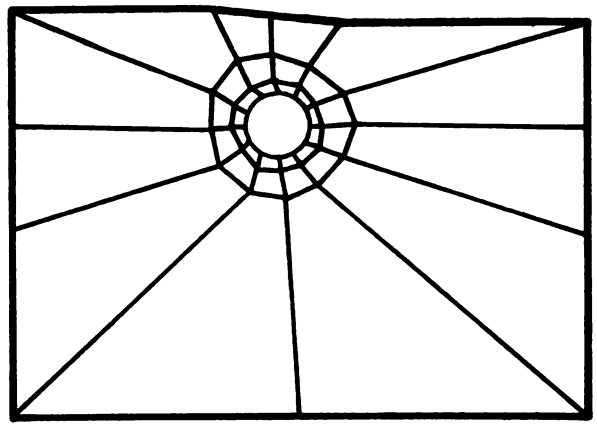

Mode 2 T = .1719 secs.

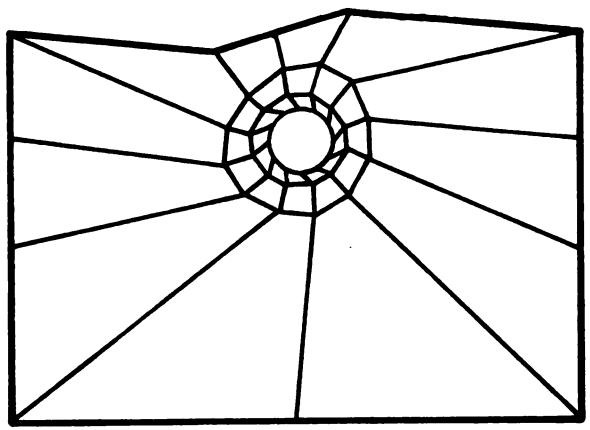

Mode 3 T = .1606 secs.

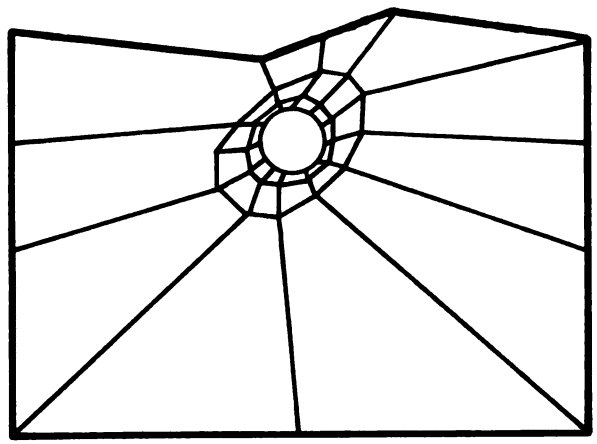

Mode 4 T = .1045 secs.

Figure 5.1 Mode Shapes for Rigid Cylinder Case

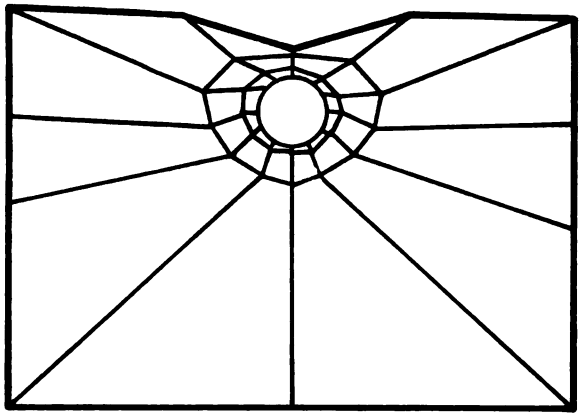

Mode 5 T = .0883 secs.

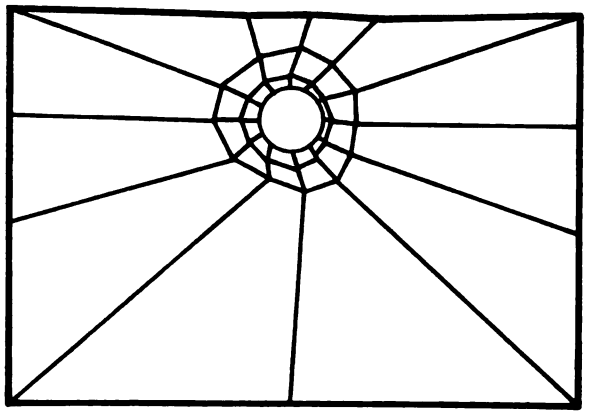

Mode 6 T = .0825 secs.

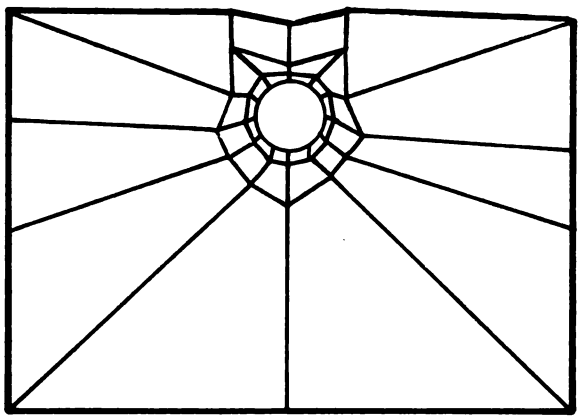

Mode 20 T = .0445 secs.

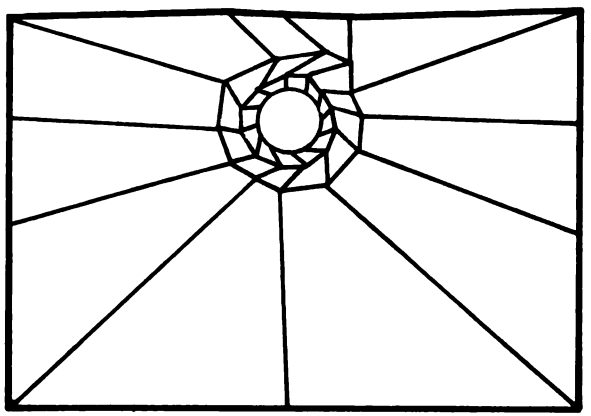

Mode 21 T = .0427 secs.

Figure 5.1 (cont'd)

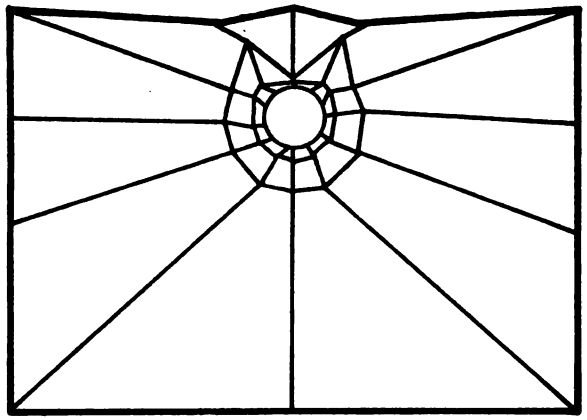

Mode 22 T = .0396 secs.

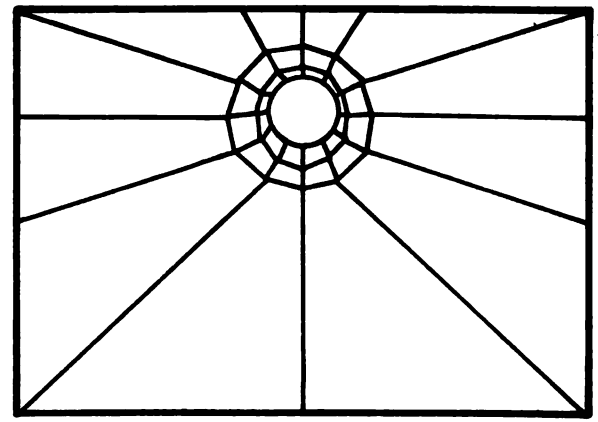

Mode 55 T = .0184 secs.

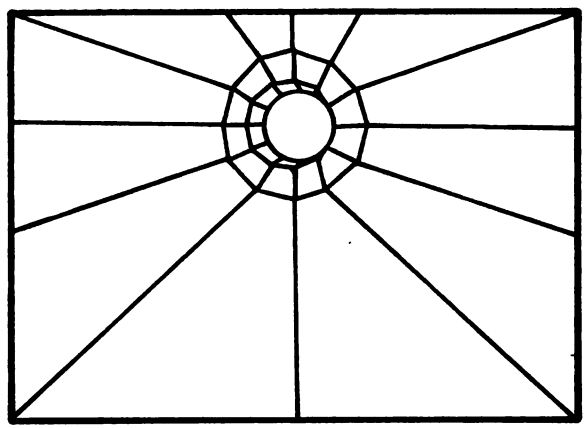

Mode 56 T = .0176 secs.

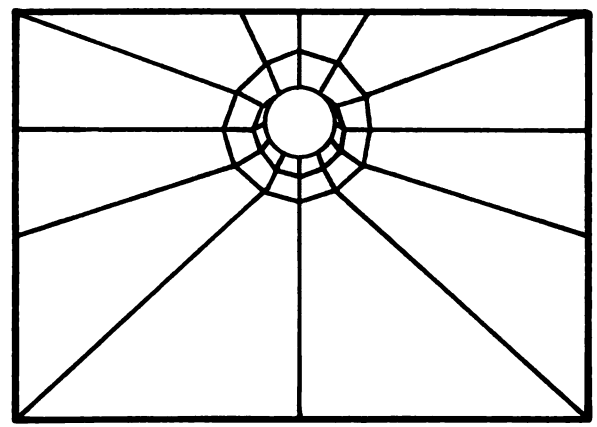

Mode 57 T = .0164 secs.
(last mode)

Figure 5.1 (cont'd)

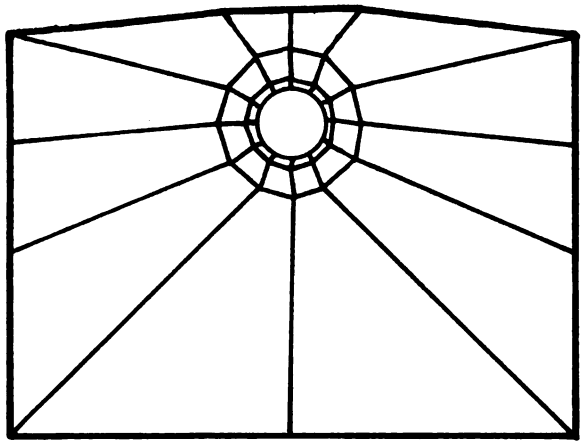

Mode 1 T = .2076 secs.

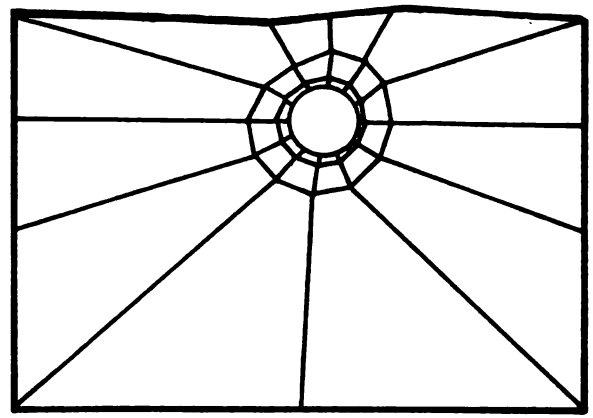

Mode 2 T = .1737 secs.

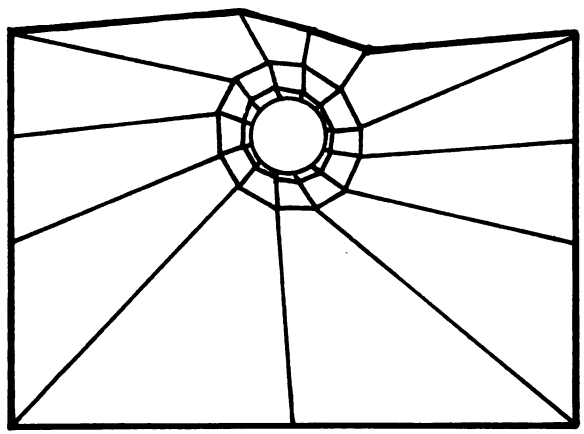

Mode 3 T = .1617 secs.

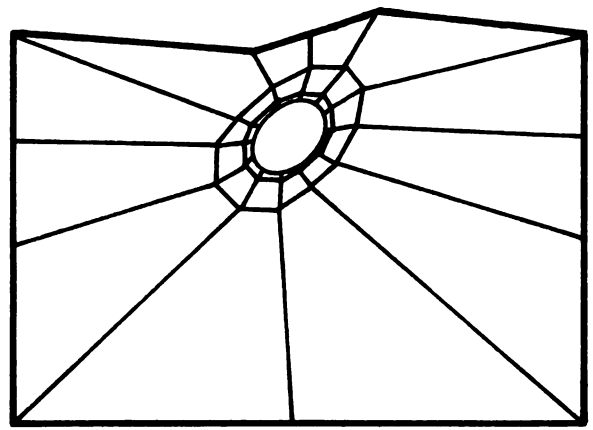

Mode 4 T = .1159 secs.

Figure 5.2 Mode Shapes for Flexible Cylinder Case

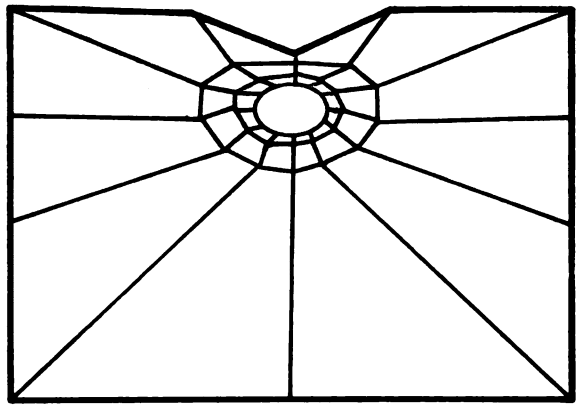

Mode 5 T = .0923 secs.

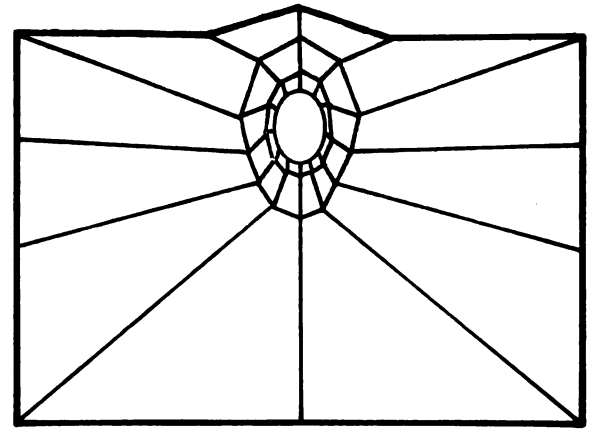

Mode 6 T = .0870 secs.

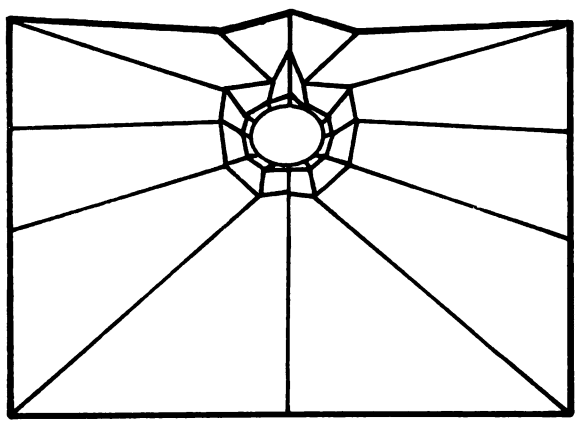

Mode 20 T = .0448 secs.

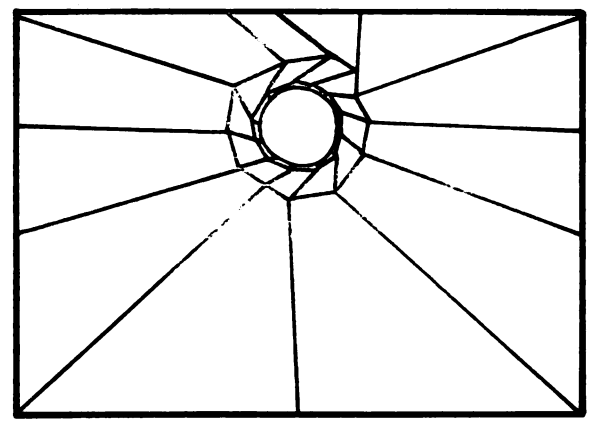

Mode 21 T = .0429 secs.

Figure 5.2 (cont'd)

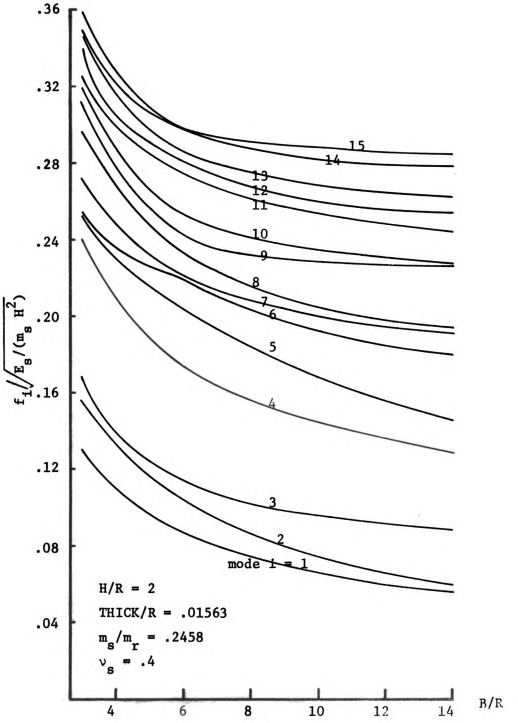

(a)

Figure 5.3 Influences of Boundary Distance

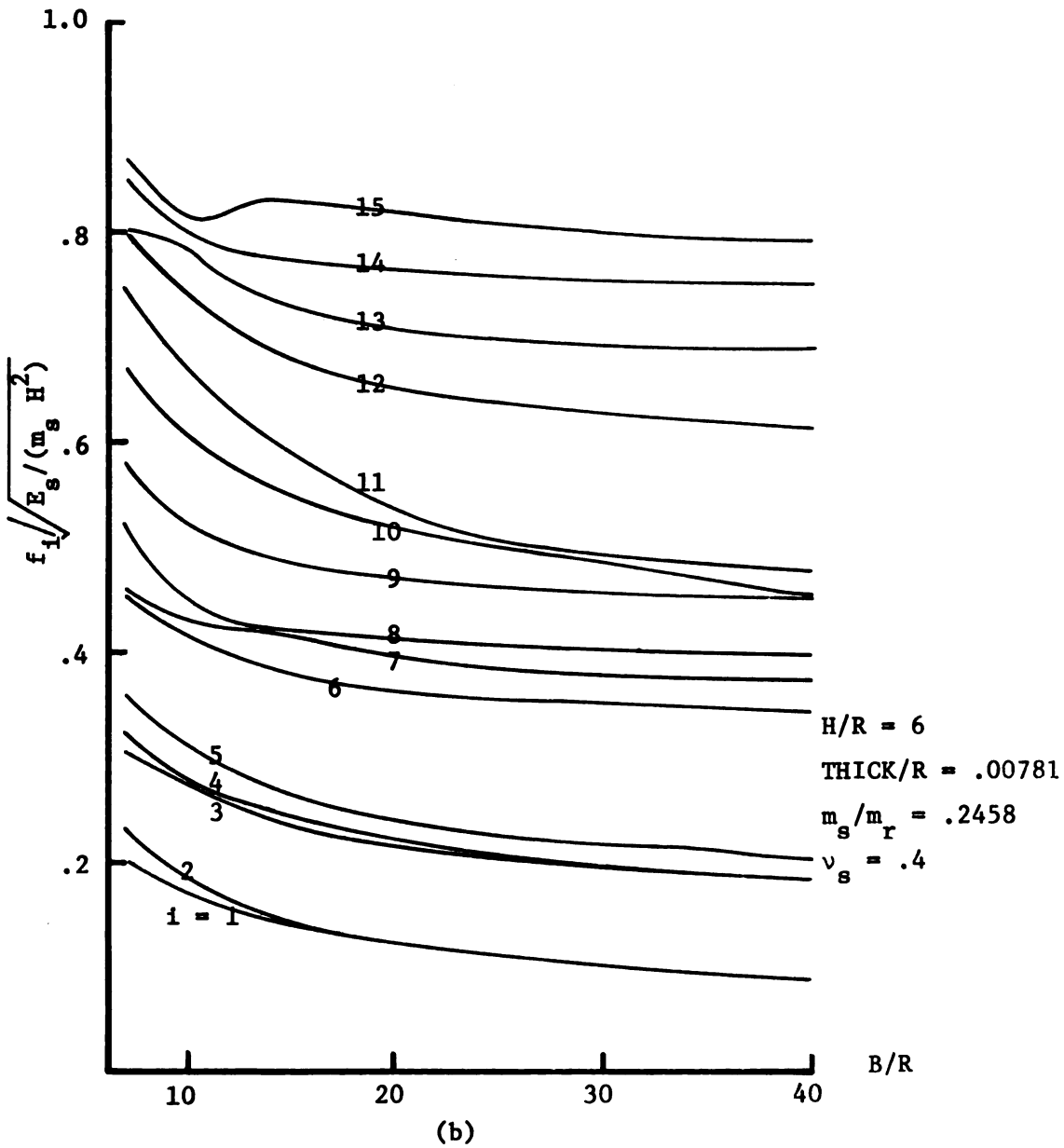

(b)

Figure 5.3 (cont'd)

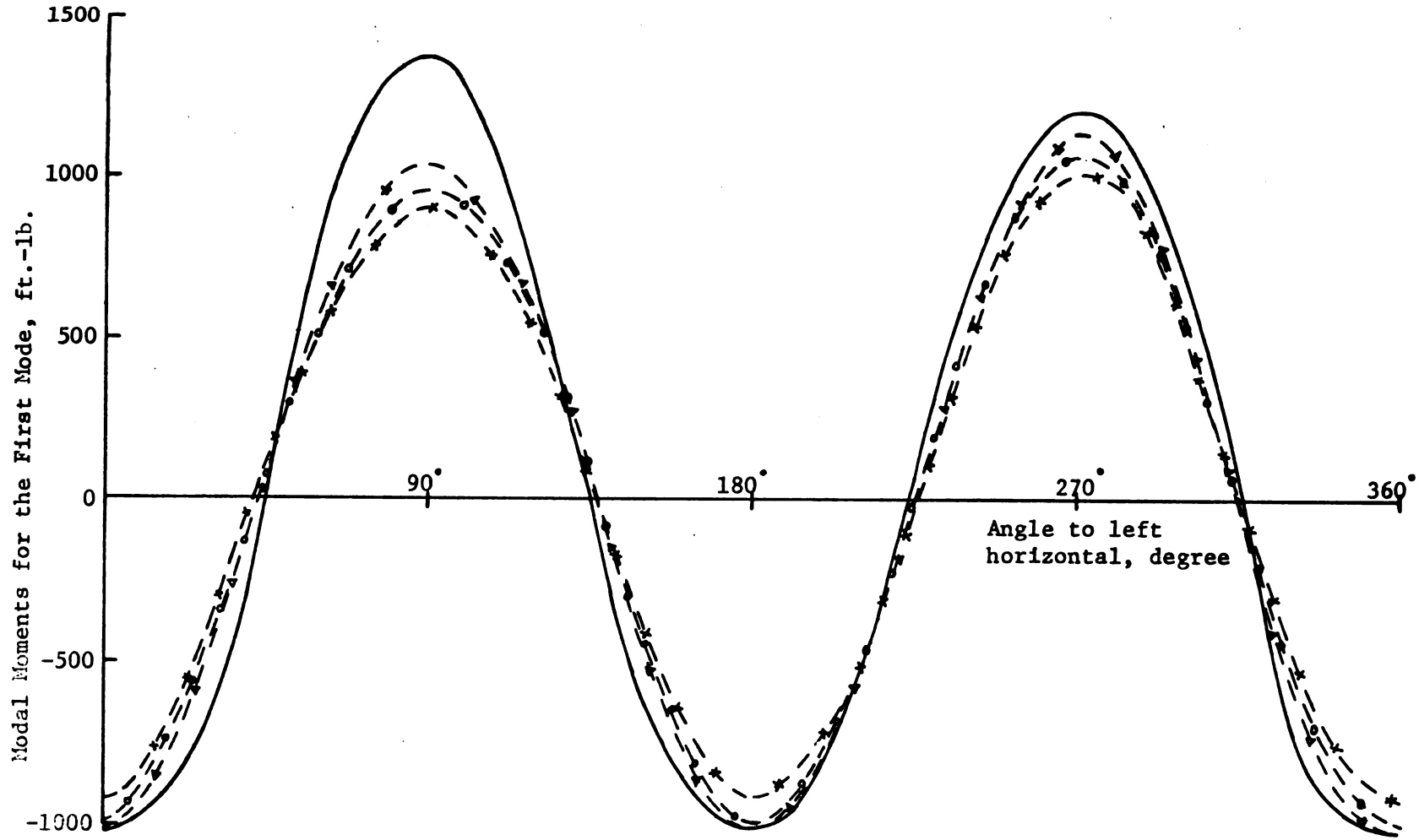

——————— case 1 , 8 nodes , fundamental frequency = 1.00489 radian/sec.
–▲– – –▲– case 2 , 12 nodes , ,, ,, = 1.00395 ,,
–✱– – –✱– case 3 , 16 nodes , ,, ,, = 1.00875 ,,
–●– – –●– case 4 , 20 nodes , ,, ,, = 1.00417 ,,

Figure 5.4 Influence of Number of Cylinder Nodes

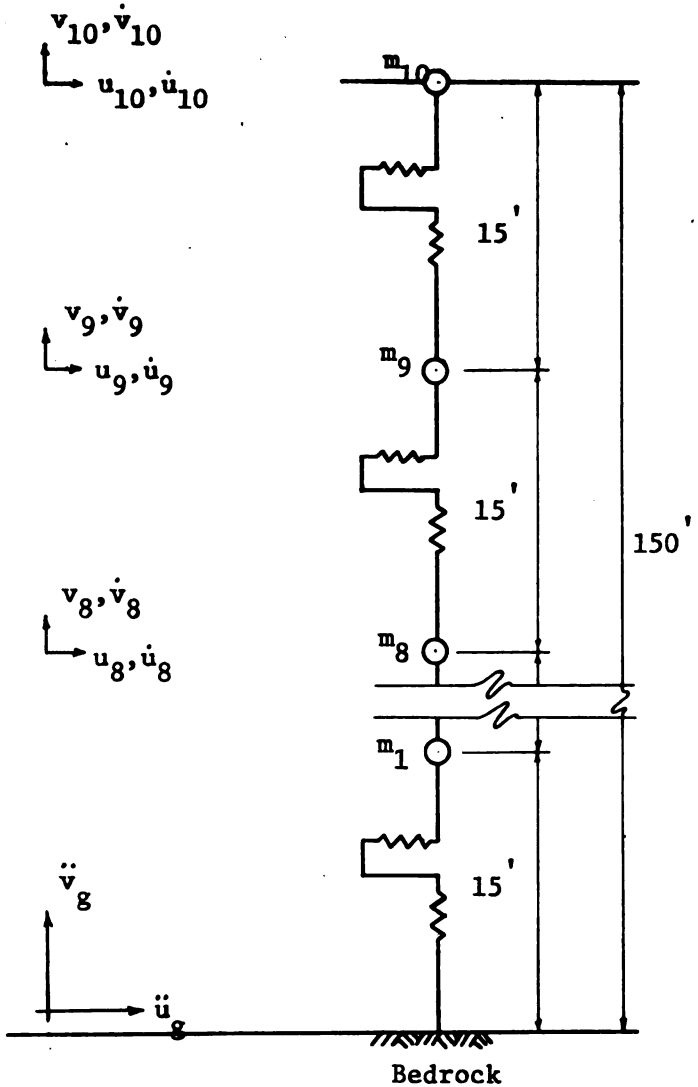

The six velocities, six displacements and two accelerations that are inputs for the cylinder-soil composite.

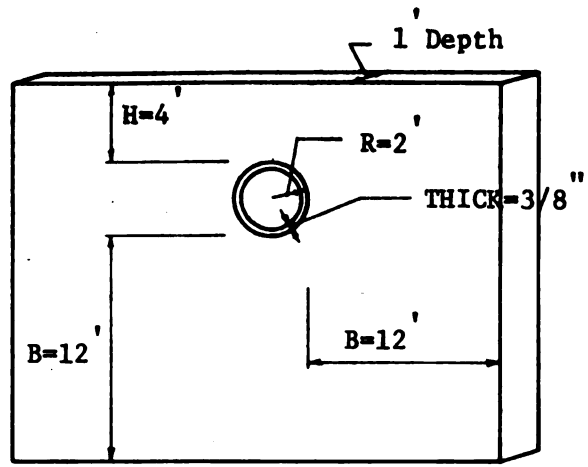

Number of cylinder nodes = 12
Soil density = 120 lb./ft.^{3}
Soil Elasticity modulus = 185000 lb./ft.^{2}
Soil Poisson's ratio = 0.4
Cylinder material density = 488 lb./ft.^{3}

Geometric and Material Data

Figure 5.5 Example for Response Analysis

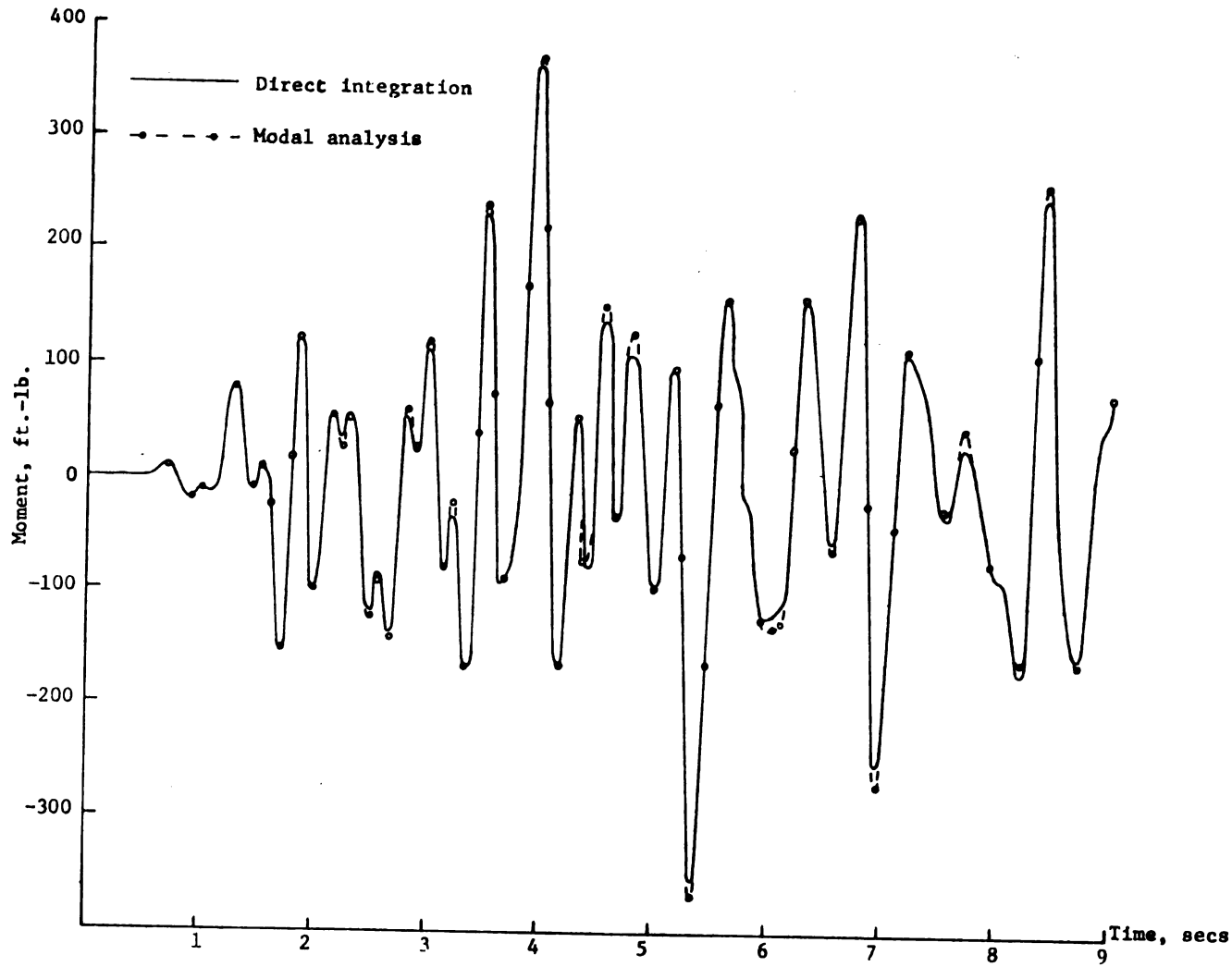

(a) Moment at Node 1

Figure 5.6 Responses

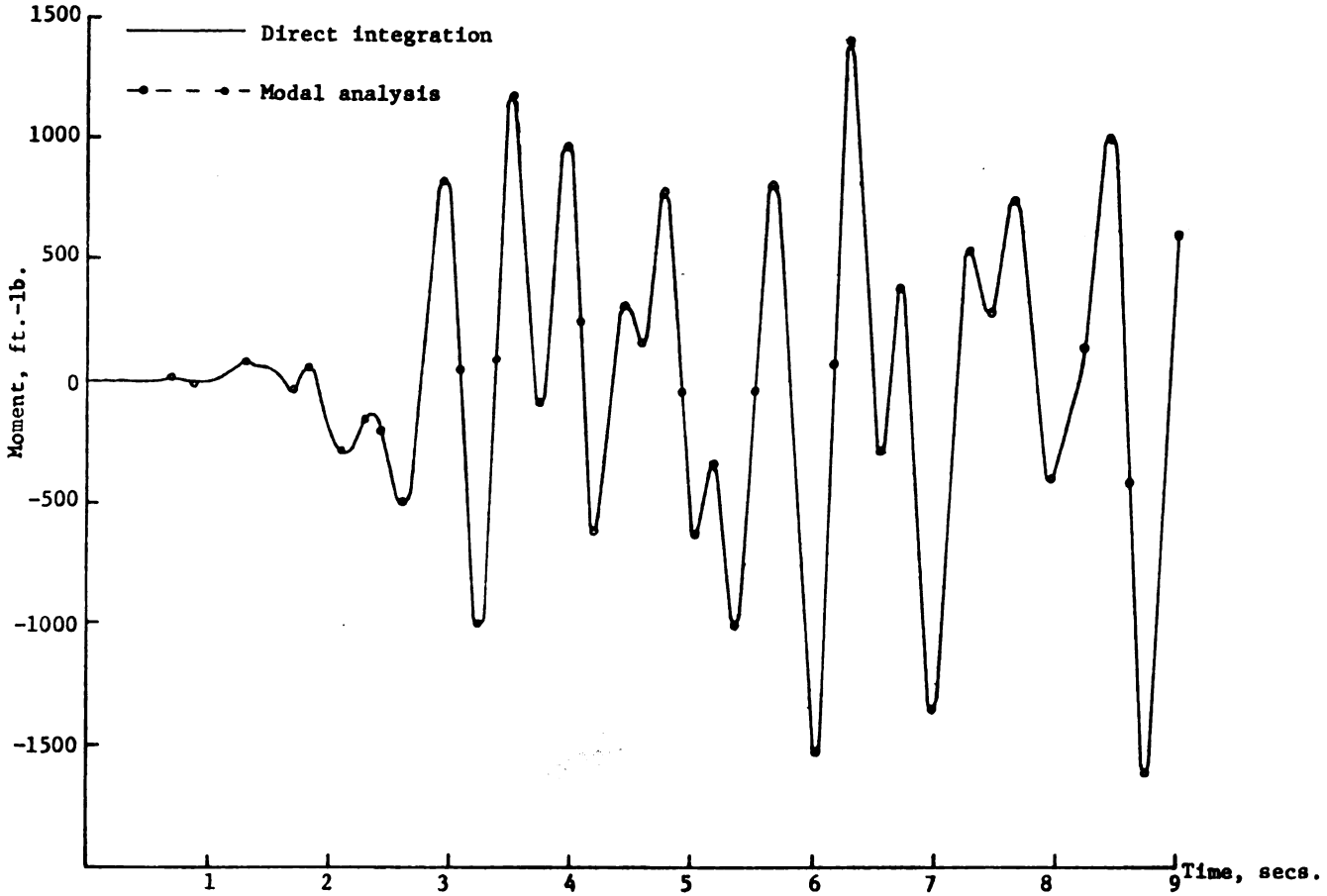

(b) Moment at Node 2

Figure 5.6 (cont'd)

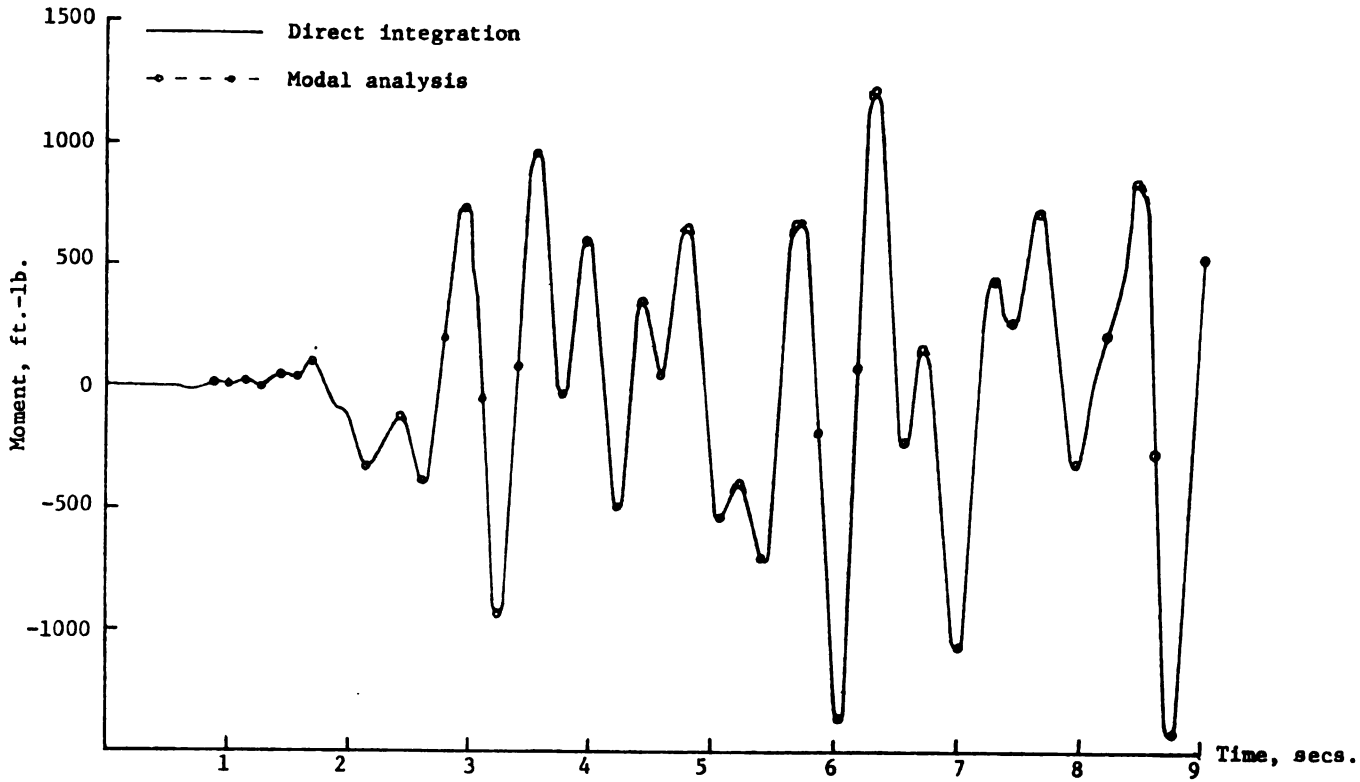

(c) Moment at Node 3

Figure 5.6 (cont'd)

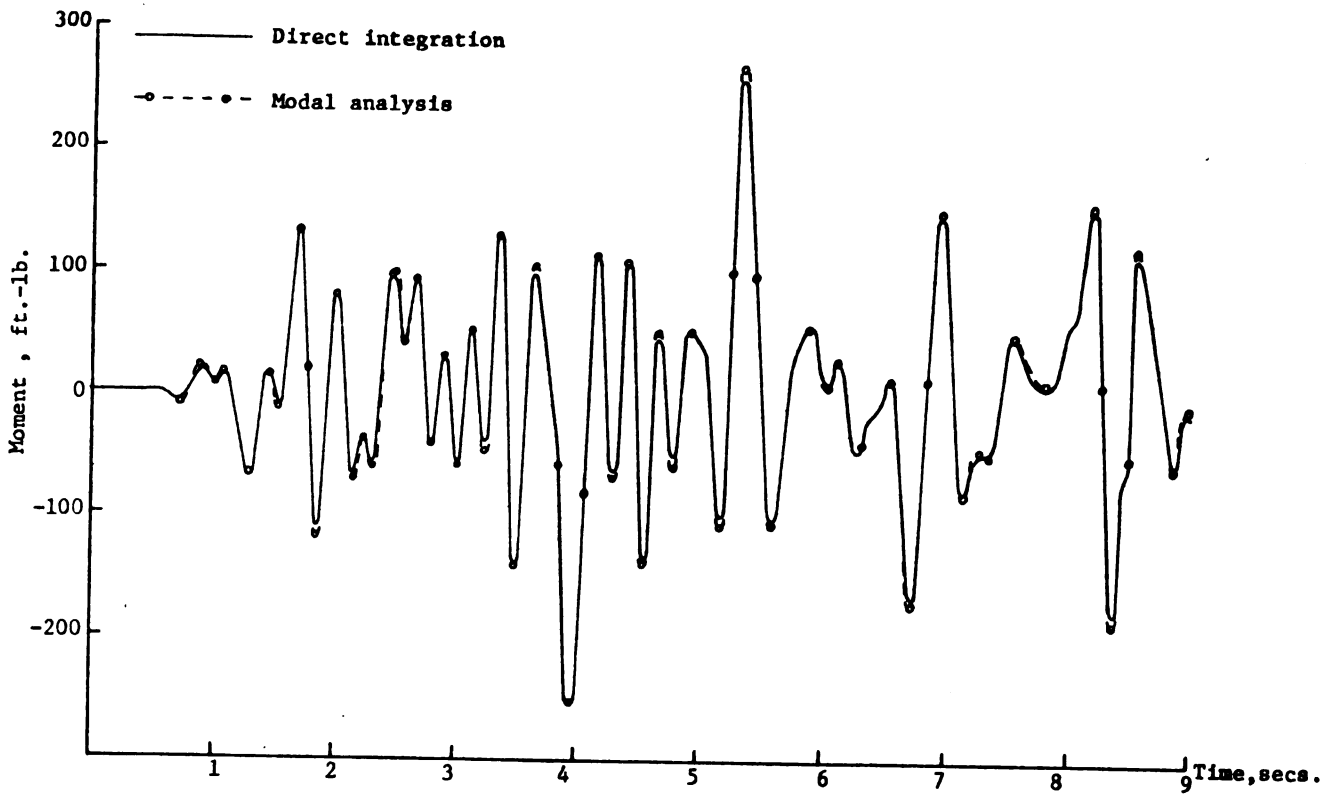

(d) Moment at Node 4

Figure 5.6 (cont'd)

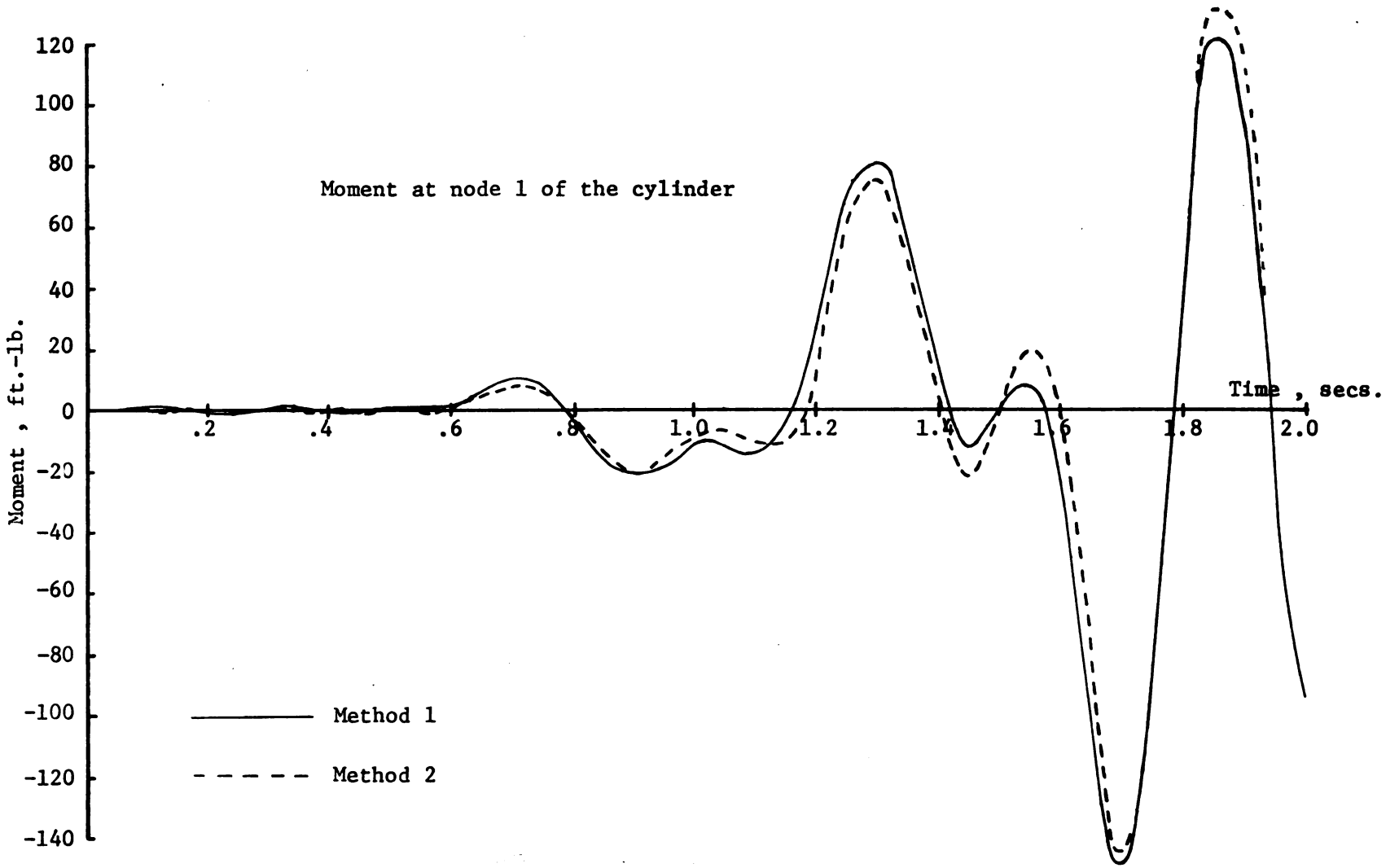

Figure 5.7 Method 1 and Method 2

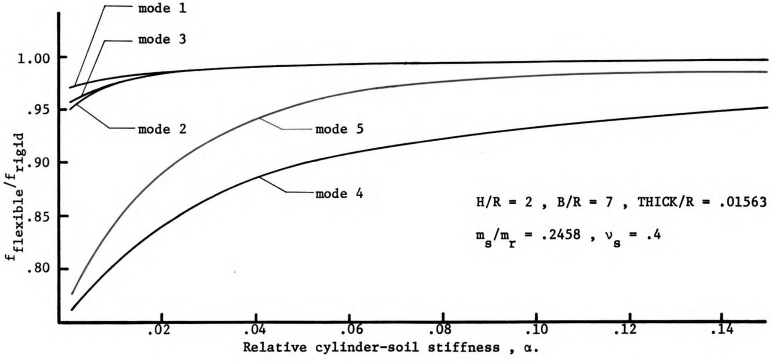

(a)

Figure 5.8 Effects of Relative Cylinder-Soil Stiffness

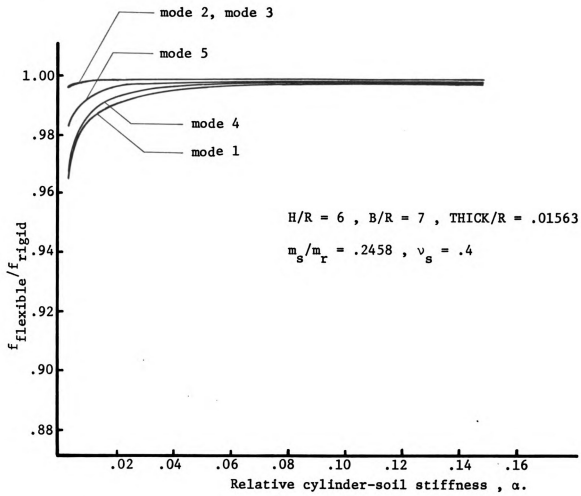

(b)

Figure 5.8 (cont'd)

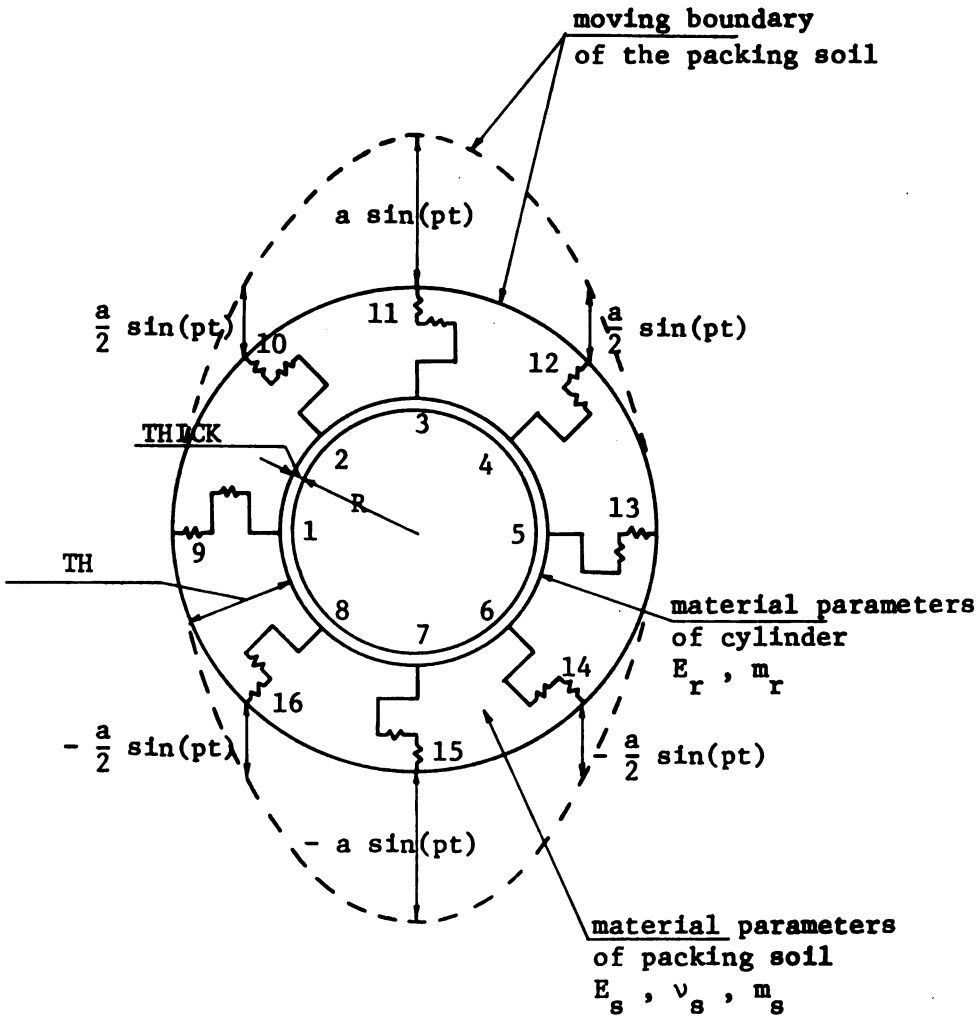

(a) Problem Definition

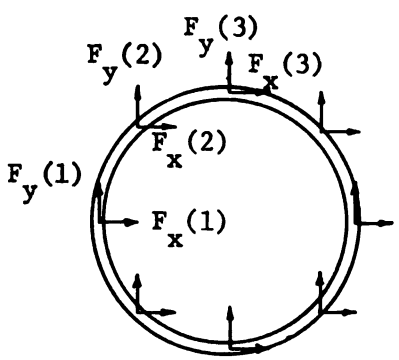

(b) Forces on the Cylinder Nodes

Figure 5.9 Simplified Problem

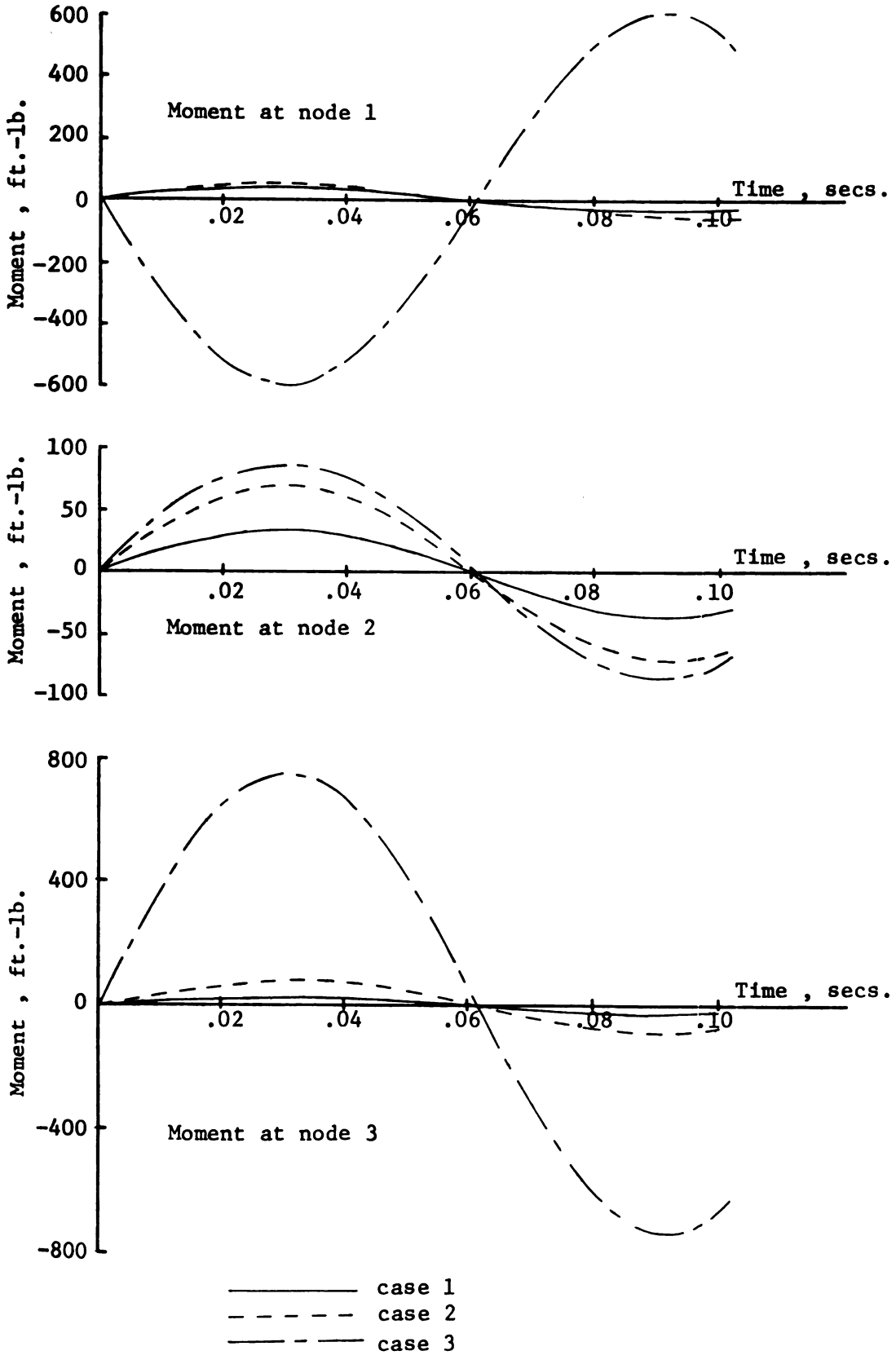

Figure 5.10 Moments for Simplified Problem

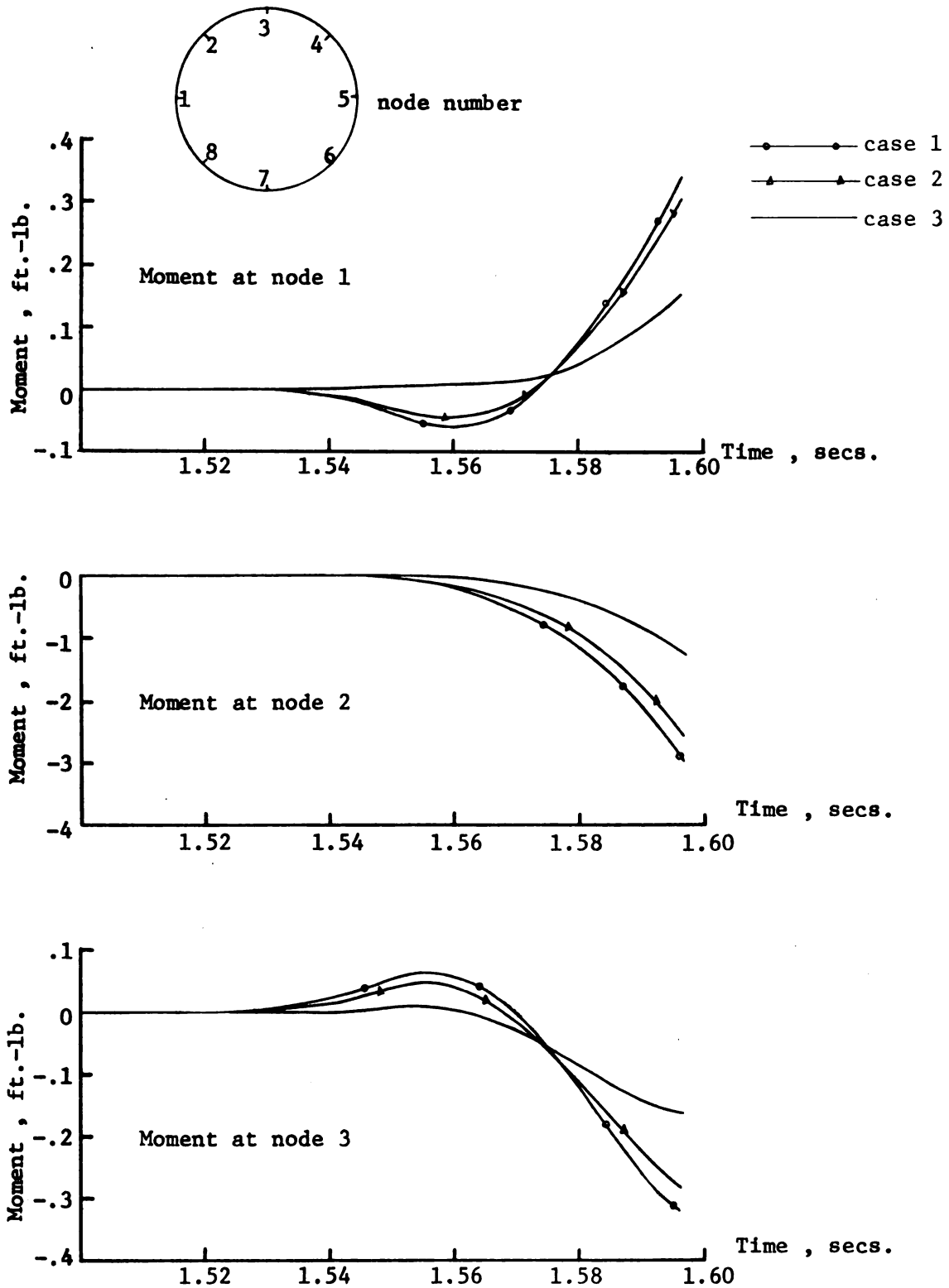

Figure 5.11 Problem With Prescribed Top Boundary

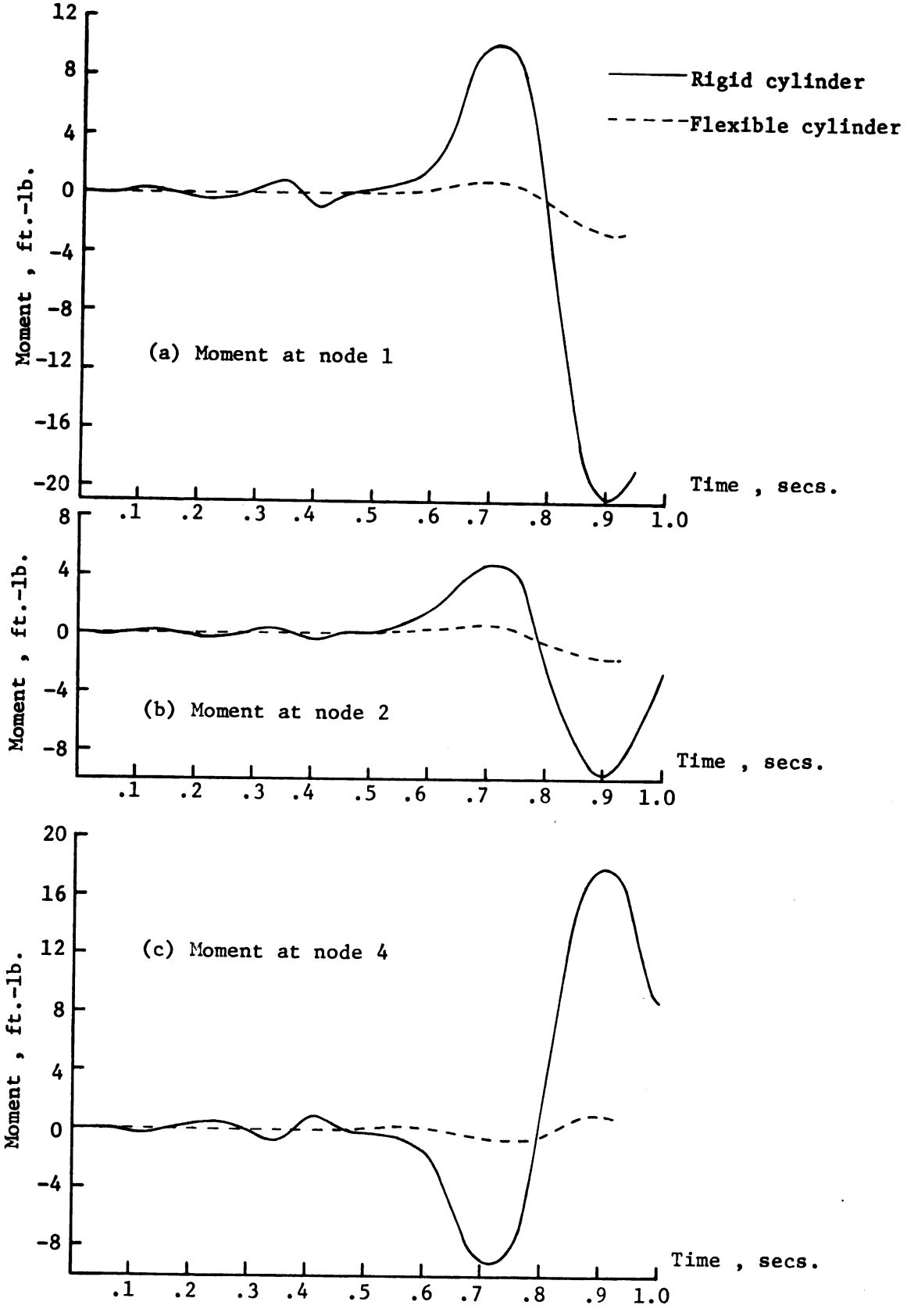

Figure 5.12 Rigid and Flexible Cylinder Solutions

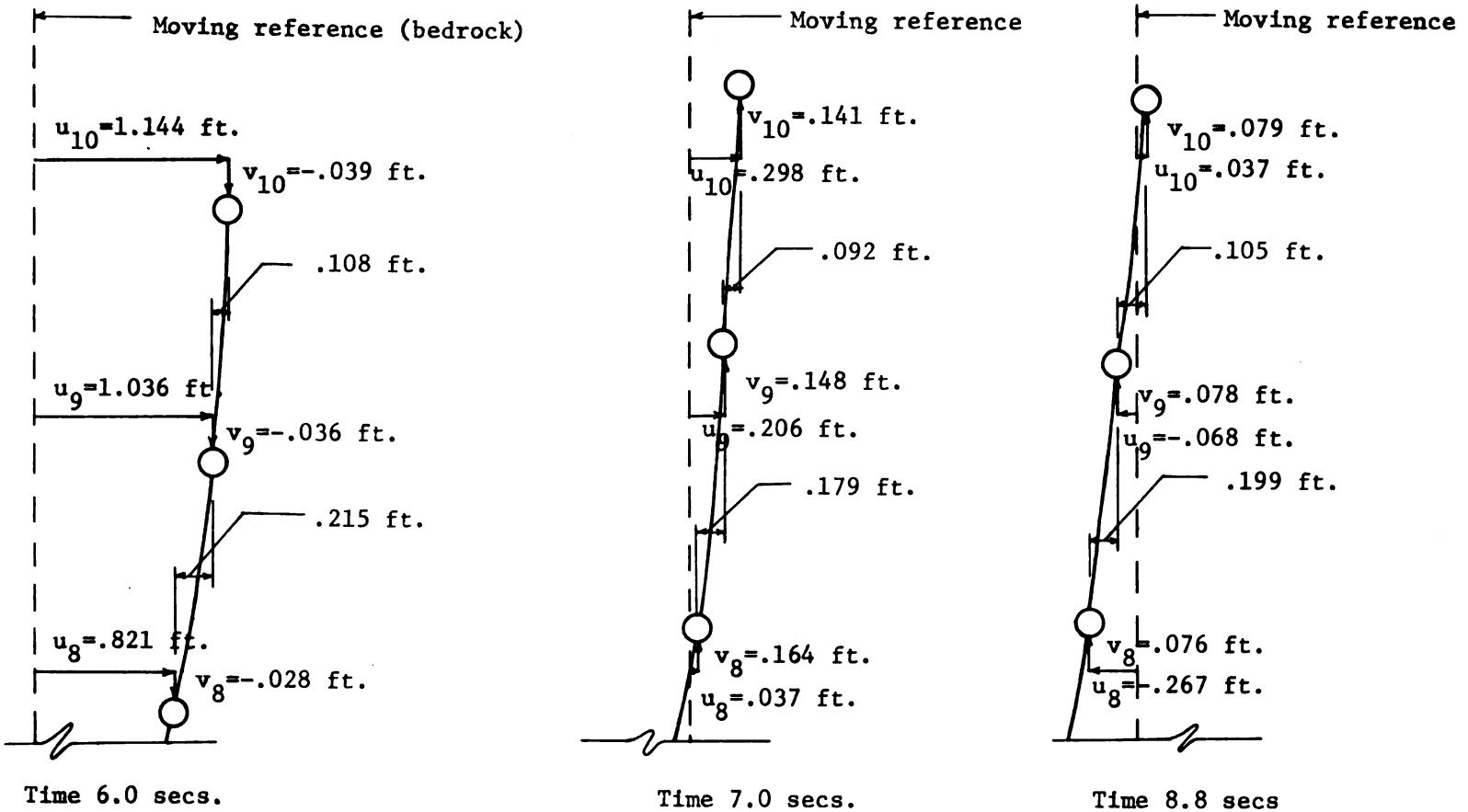

Figure 5.13 Free Field Displacements

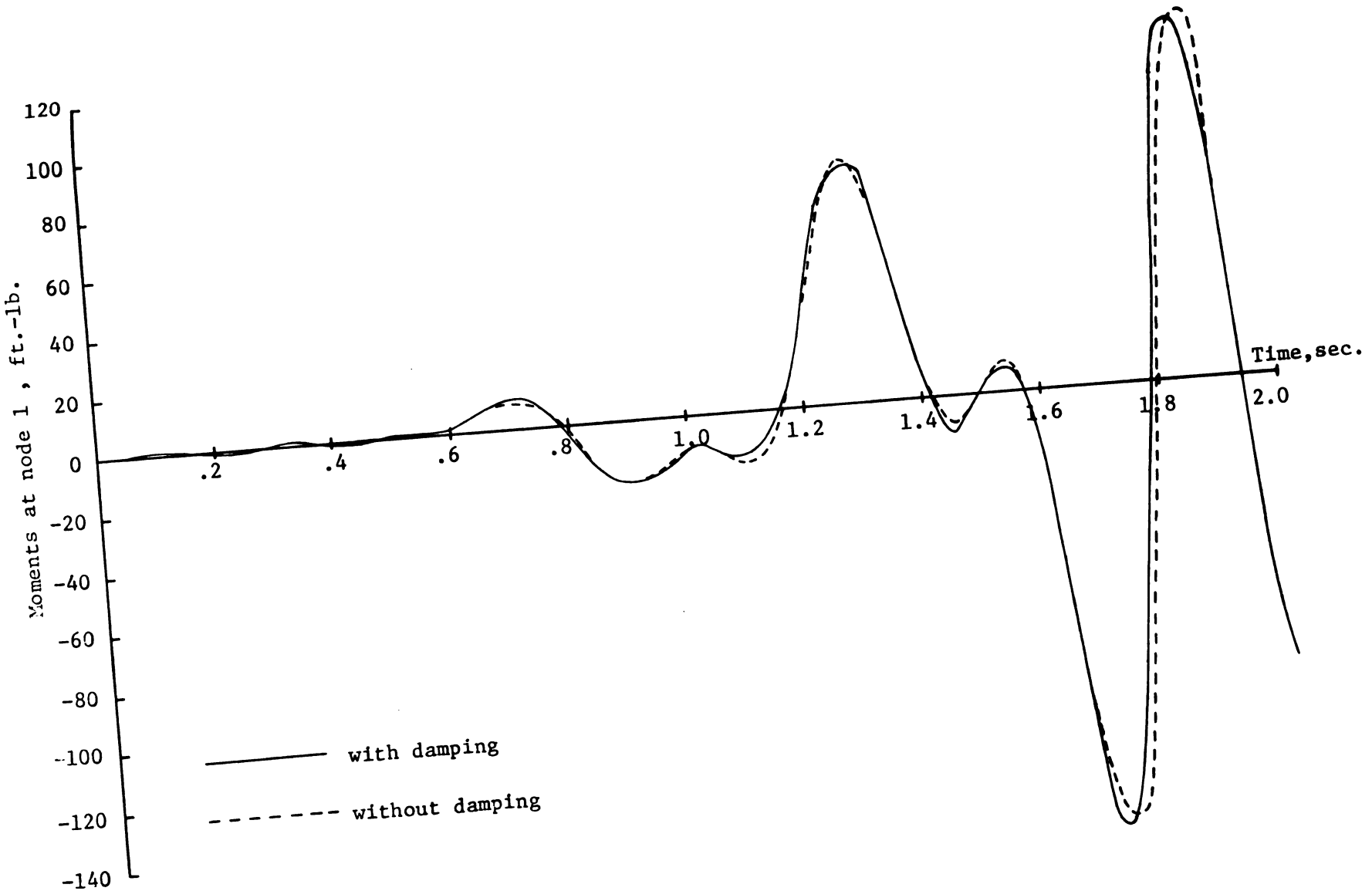

Figure 5.14 Effects of Damping

BIBLIOGRAPHY

1. Marston, A. "The Theory of External Loads on Closed Conduits in the Light of the Latest Experiments," Proceedings of th 9 th Annual Meeting, Highway Research Board, December 1929.

2. Spangler, M.G. "The Structural Design of Flexible Pipe Culverts," Iowa State College Bulletin, No. 153, 1941.

3. "Earth Loads on Steel Pipe, Chapter 8, Design and Installation of Steel Water Pipe," Journal of the American Waterworks Association, Vol. 53, No. 8, August 1961, p. 1053.

4. Allgood, J.R. "The Behavior of Shallow Buried Cylinders," Proceedings of the Symposium on Soil Structure Interaction, University of Arizona, September 1964, pp. 189-210.

5. Mow, C.C. and McCabe, W.L. "Dynamic Stresses in an Elastic Cylinder," Journal of the Engineering Mechanics Division, ASCE, Vol. 89, No. EM3, June 1963, pp. 21-41.

6. Robinson, R.R. "The Investigation of Silo and Tunnel Linings," IIT Research Institute, for AFWL, Contract No. AF 29(601)-2596, Report No. AFSWC-TDR-62-1, March 1962.

7. Ang, A.H.S. and Chang, G.C. "Numerical Calculation of Inelastic Plane Structure-Soil Interaction," Proceedings of the International Symposium on Wave Propagation and Dynamic Properties of Earth Materials, The University of New Mexico, August 1967, pp. 393-410.

8. Costantino, C.J., Wachowski, A. and Barnwell, U.L. "Finite Element Solution for Wave Propagation in Layered Media Caused by a Nuclear Detonation," Proceedings of the International Symposium on Wave Propagation and Dynamic Properties of Earth Materials, The University of New Mexico, August 1967, pp. 59-70.

9. Yamada, Y. "Dynamic Analysis of Civil Engineering Structures," Recent Advances in Matrix Methods of Structural Analysis and Design, Edited by R.H. Gallagher, Y. Yamada and J.T. Oden, The University of Alabama Press, 1971, pp. 487-513.

10. Yamada, Y. "Dynamic Analysis of Structures," Advances in Computational Methods in Structural Mechanics and Design, UAH Press, 1972, pp. 181-199.

11. Idriss, I.M. and Seed, H.B. "Response of Horizontal Soil Layers during Earthquakes," Research Report, Soil Mechanics and Bituminous Materials Laboratory, University of California, Berkeley, August 1967.

12. Penzien, J., Scheffey, C. and Parmelee, R. "Seismic Analysis of Bridges on Long Piles," Journal of the Engineering Mechanics Division, ASCE, Vol. 90, No. EM3, June 1964, pp. 223-254.

13. Dawkins, W.P. "Analysis of Tunnel Liner-Packing Systems," Journal of the Engineering Mechanics Division, ASCE, Vol. 95, No. EM3, June 1969, pp. 679-693.

14. Zienkiewicz, O.C. and Cheung, Y.K. The Finite Element Method in Structural and Continuum Mechanics, McGraw-Hill Publishing Co., Ltd., London, 1967.

15. Yuzugullu, O. and Schnobrich, W.C. "Finite Element Approach for the Prediction of Inelastic Behavior of Shear Wall-Frame Systems," Civil Engineering Studies, Structural Research Series No. 386, University of Illinois, Urbana, Illinois, May 1972.

16. Clough, R.W. "Analysis of Structural Vibrations and Dynamic Response," Recent Advances in Matrix Methods of Structural Analysis and Design, The University of Alabama Press,1971, p. 441.

17. Newmark, N.M. "A Method of Computation for Structural Dynamics," Transactions, ASCE, Vol. 127, 1962, p. 1406.

18. Clarke, N.W.B. Buried Pipelines, Maclaren and Sons, London, 1968.

19. ASTM, Standard Specifications for Reinforced Concrete Culvert, Storm Drain and Sewer Pipe, C76-70.

APPENDIX A

COMPUTER PROGRAMS

Presented in this appendix are the computer programs used in this study. There are a total of 12 programs (or packages): NSTIFF, MSOLVE, RIG20, WACC, FQTA1, EIG1, SRIGFQ1, SRIGFQ2, EIGRIG2, PA, TNORM4, DINORM4; all of which are shown in Figure 4.1 with a brief description of their main functions. See also Section 4.5 for a discussion on relevant aspects of these programs.

```
      PROGRAM NSTIFF(INPUT,OUTPUT,TAPE1)
      COMMON/STIFF/NELR,NEW,NCOUNT,NI(250),NJ(250),STIFF(250,2,2),WM(85)
     1 ,TEMPOR(2,2),N1
      COMMON/READ1/R,E1,V1,ZI,A,W1
      COMMON/READ2/P1,P2,W2,R1
      COMMON/READ3/CORD(85,2),NLO(50,5),W3,E2,V2,NEL,NND,METHOD
      COMMON/ROT/ROT(13,3,3)
      COMMON/POOL/SM1(3,3),SM2(3,3),SM3(3,3),SM4(3,3),STEMP1(12,24),
     1 GARB(1656)
      DATA WM,STIFF/1085*0/,NCOUNT/0/
      DATA ((NLO(I,J),J=1,4),I=13,36)/25,13,14,26,26,14,15,27,15,16,28,
     1 27,16,17,29,28,17,18,30,29,19,31,30,18,20,32,31,19,33,32,20,21,
     1 34,33,21,22,35,34,22,23,36,35,23,24,36,24,13,25,42,25,26,41,26,
     1 27,37,41,27,28,38,37,28,29,39,38,30,45,39,29,31,46,45,30,32,47,
     1 46,31,33,48,47,32,40,48,33,34,44,40,34,35,44,35,36,43,43,36,25,
     1 42/
C READ DATA FOR RING
C READ $ CALCULATE PARAMETERS FOR RING
      READ 101,R,E1,THICK,WM1
 101  FORMAT(F10.5,E10.4,3F10.5)
      NELR=12
      ZI=1.*(THICK**3)/12.
      A=THICK*1.
      W1=1.*1.*THICK*WM1
C READ $ CALCULATE PARAMETERS FOR SOIL
      READ 102,E2,V2,WM2,B,H
 102  FORMAT(5F10.2)
      PL=(2.*3.1415927*(R+R/4.))/NELR
      P1=(E2/(2.*(1.+V2)))*1.*PL/(R/2.)
      P2=(E2*1.*PL)/((R/2.)*(1.-V2**2))
      W2=WM2
      R1=R+(R/2.)
C CALCULATE CONNECTIVITY AROUND RING
      DO 115 I=1,NELR
      NLO(I,1)=I
 115  NLO(I,2)=I+NELR
```

```
      W3=WM2
      NEL=36
      NND=48
      METHOD=1
C CALCULATE COORDINATES OF NODES
      ALP=2.*3.1415927/NELR
      DO 110 J=1,3
      GO TO(105,106,107)J
 105  RAD=R
      GO TO 108
 106  RAD=R+R/2.
      GO TO 108
 107  RAD=R+(R/2.)+(3.*R/4.)
 108  DO 104 I=1,6
      CORD(6-(I-1)+(12*(J-1)),1)=RAD*COS(I*ALP)
 104  CORD(6-(I-1)+(12*(J-1)),2)=RAD*SIN(I*ALP)
      DO 109 I=1,6
      CORD(12-(I-1)+(12*(J-1)),1)=RAD*COS(3.1415927+I*ALP)
 109  CORD(12-(I-1)+(12*(J-1)),2)=RAD*SIN(3.1415927+I*ALP)
 110  CONTINUE
      DO 111 I=1,3
 111  CORD(37+(I-1),2)=R+H
      CORD(37,1)=-(R+H)*TAN(ALP)
      CORD(38,1)=0.
      CORD(39,1)=-CORD(37,1)
      CORD(40,1)=0.
      CORD(40,2)=-R-B
      DO 112 I=1,2
      CORD(41+4*(I-1),2)=R+H
      CORD(42+4*(I-1),2)=0.
      CORD(43+4*(I-1),2)=-R-H
 112  CORD(44+4*(I-1),2)=-R-B
      DO 113 I=1,2
      DO 113 J=1,4
 113  CORD(40+J+4*(I-1),1)=(-1.)**I*(R+B)
      WRITE(1)R,E1,V1,ZI,A,((CORD(I,J),J=1,2),I=1,85)
```

```
      GAM=(E1*ZI)/(E2*R**3*H/(1.-V2**2))
      BR=B/R
      HR=H/R
      PRINT 114,GAM,BR,HR
114   FORMAT(* GAM,RING TO SOIL PLAIN STRAIN STIFF RATIO=*F12.8,*  B/R=*
     1 F10.5,*  H/R=*F10.5)
      PRINT 401,NELR,R,E1,ZI,A,W1
401   FORMAT(/*  NO. OF RING ELEMENT=*I3,*   R=*F6.3,*   E1=*E12.6,
     1 *   ZI=*F12.10,*   A=*F10.8,*   W1=*F10.7)
      PRINT 403,P1,P2,W2,R1
403   FORMAT(/*  FOR PACKING, SHEAR SPRING P1=*F14.4,*  COMPRESSION SPRI
     1NG P2=*F16.4,*  MASS/UNIT AREA W2=*F10.7,/,*  OUTER RADIUS OF PACK
     1ING R1=*F10.4)
      PRINT 314
314   FORMAT(4X*I*1X*NLO1*1X*NLO2*)
      DO 404 I=1,NELR
404   PRINT 405,I,(NLO(I,J),J=1,2)
405   FORMAT(3I5)
      N1=NELR+1
      PRINT 406,W3,E2,V2,NEL,NND,METHOD
406   FORMAT(*  MASS DENSITY OF FEM=*F10.7,*  E2=*F14.4,*  V2=*F10.5,/,
     1 *   TOTAL NO OF ELEMENT=*I5,*   TOTAL NO OF NODE=*I5,*   METHOD=*
     2 I5)
      PRINT 409
409   FORMAT(* NODE*5X*CORD1*5X*CORD2*)
      DO 407 I=1,NND
407   PRINT 408,I,(CORD(I,J),J=1,2)
408   FORMAT(I5,2F10.4)
      PRINT 410
410   FORMAT(4X*MEMBER*3X*NLO1*3X*NLO2*3X*NLO3*3X*NLO4*)
      DO 411 I=N1,NEL
411   PRINT 412,I,(NLO(I,J),J=1,4)
412   FORMAT(I10,4I7)
      CALL RING
      CALL PACK
      CALL FEM
```

```
      DO 413 I=1,NCOUNT
413   PRINT 414,I,NI(I),NJ(I),((STIFF(I,K,L),L=1,2),K=1,2)
414   FORMAT(* N=*I5,* NI=*I5,* NJ=*I5,*  STIFF=*5X,2F15.3,/39X,2F15.3)
      DO 415 I=1,NEW
415   PRINT 416,I,WM(I)
416   FORMAT(* NODE*I5,*   MASS=*F12.6)
      PRINT 417
417   FORMAT(//* ROTATION MATRIX*)
      DO 418 I=1,N1,4
418   PRINT 419,(((ROT(I,J,K),K=1,3),(ROT(I+1,J,K),K=1,3),(ROT(I+2,J,K),
     1 K=1,3),(ROT(I+3,J,K),K=1,3)),J=1,3)
419   FORMAT(//(10X3F7.4,10X3F7.4,10X3F7.4,10X3F7.4))
      PRINT 420,NEW,NCOUNT
420   FORMAT(/* NEW=*I5,*  NCOUNT=*I5)
      PRINT 421
421   FORMAT(//15X*SM1*28X*SM2*28X*SM3*28X*SM4*)
      PRINT 500,(((SM1(I,J),J=1,3),(SM2(I,J),J=1,3),(SM3(I,J),J=1,3),,
     1 (SM4(I,J),J=1,3)),I=1,3)
500   FORMAT(//(3X3E10.4,3X3E10.4,3X3E10.4,3X3E10.4))
      PRINT 422
422   FORMAT(//*  STEMP1*)
      N2=2*NELR
      CALL MATPRT(12,24,NELR,N2,STEMP1)
      WRITE(1)NEW,NCOUNT
      WRITE(1)(NI(I),NJ(I),((STIFF(I,J,K),K=1,2),J=1,2),I=1,250)
      WRITE(1)(((ROT(I,J,K),K=1,3),J=1,3),I=1,13)
      WRITE(1)(WM(I),I=1,85)
      WRITE(1)((SM1(I,J),SM2(I,J),SM3(I,J),SM4(I,J),J=1,3),I=1,3)
      WRITE(1)((STEMP1(I,J),J=1,24),I=1,12)
      END
```

```
      SUBROUTINE RING
      COMMON/POOL/SM1(3,3),SM2(3,3),SM3(3,3),SM4(3,3),STEMP1(12,24),SR1(
     13,3),SR2(3,3),SR3(3,3),SR4(3,3),S11(24,24),S12(24,12),S22(12,12),
     2 STEMP2(24,24),RS1(3,3),RS2(3,3),RS3(3,3),RS4(3,3)
      COMMON/ROT/ROT(13,3,3)
      COMMON/READ1/R,E,V1,ZI,A,W1
      COMMON/STIFF/NELR,NEW,NCOUNT,NI(250),NJ(250),STIFF(250,2,2),WM(85)
     1 ,TEMPOR(2,2),N1
      DATA S11,S12,S22/1008*0./
      ALP=2*3.14159/NELR
C SM1=3$3 ONE END FLEXIBILITY MATRIX,TYPICAL ELEMENT
      SM4(1,1)=R**3*(6*ALP-8*SIN(ALP)+SIN(2*ALP))/(4*E*ZI)+R*(2*ALP+SIN(
     12*ALP))/(4*A*E)
      SM4(1,2)=-1*R**3*(1-COS(ALP))**2/(2*E*ZI)+R*(1-COS(2*ALP))/(4*A*E)
      SM4(1,3)=-1*R**2*(ALP-SIN(ALP))/(E*ZI)
      SM4(2,2)=R**3*(2*ALP-SIN(2*ALP))/(4*E*ZI)+R*(2*ALP-SIN(2*ALP))/(4
     1  *A*E)
      SM4(2,3)=R**2*(1-COS(ALP))/(E*ZI)
      SM4(3,3)=R*ALP/(E*ZI)
      SM4(2,1)=SM4(1,2)
      SM4(3,1)=SM4(1,3)
      SM4(3,2)=SM4(2,3)
C SM1**-1 =ONE END STIFFNESS MATRIX
      CALL INVERT(3,3,SM4)
C SM=6$6 LOCAL STIFFNESS MATRIX FOR A TYPICAL ELEMENT
      SM2(1,1)=-1*SM4(1,1)*COS(ALP)-SM4(2,1)*SIN(ALP)
      SM2(1,2)=-1*SM4(1,2)*COS(ALP)-SM4(2,2)*SIN(ALP)
      SM2(1,3)=-1*SM4(1,3)*COS(ALP)-SM4(2,3)*SIN(ALP)
      SM2(2,1)=SM4(1,1)*SIN(ALP)-SM4(2,1)*COS(ALP)
      SM2(2,2)=SM4(1,2)*SIN(ALP)-SM4(2,2)*COS(ALP)
      SM2(2,3)=SM4(1,3)*SIN(ALP)-SM4(2,3)*COS(ALP)
      SM2(3,1)=-1*SM4(3,1)+SM4(1,1)*R*(1-COS(ALP))-SM4(2,1)*R*SIN(ALP)
      SM2(3,2)=-1*SM4(3,2)+SM4(1,2)*R*(1-COS(ALP))-SM4(2,2)*R*SIN(ALP)
      SM2(3,3)=-1*SM4(3,3)+SM4(1,3)*R*(1-COS(ALP))-SM4(2,3)*R*SIN(ALP)
      DO 3 I=1,3
      DO 3 J=1,3
```

```
      SM3(I,J)=SM2(J,I)
 3    SM1(I,J)=SM4(I,J)
      SM1(1,2)=-SM1(1,2)
      SM1(2,1)=-SM1(2,1)
      SM1(2,3)=-SM1(2,3)
      SM1(3,2)=-SM1(3,2)
C GENERATE ROTATION MATRIX ROT
      DO 4 I=1,NELR
      DO 5 J=1,3
      DO 5 K=1,3
 5    ROT(I,J,K)=0.
      DEL=1.570795-(I-1)*ALP
      ROT(I,1,1)=COS(DEL)
      ROT(I,1,2)=SIN(DEL)
      ROT(I,2,1)=-ROT(I,1,2)
      ROT(I,2,2)=ROT(I,1,1)
      ROT(I,3,3)=1.
 4    CONTINUE
      DO 6 J=1,3
      DO 6 K=1,3
 6    ROT(N1,J,K)=ROT(1,J,K)
C CALCULATE OVERALL RING STIFFNESS MATRIX
      DO 7 M=1,NELR
C SM*R=SR
      DO 8 I=1,3
      DO 8 J=1,3
      SR1(I,J)=SR2(I,J)=SR3(I,J)=SR4(I,J)=0.
      DO 8 K=1,3
      SR1(I,J)=SR1(I,J)+SM1(I,K)*ROT(M,K,J)
      SR2(I,J)=SR2(I,J)+SM2(I,K)*ROT(M+1,K,J)
      SR3(I,J)=SR3(I,J)+SM3(I,K)*ROT(M,K,J)
 8    SR4(I,J)=SR4(I,J)+SM4(I,K)*ROT(M+1,K,J)
C RT*SM*R=RT*SR =SM
      DO 9 I=1,3
      DO 9 J=1,3
      RS1(I,J)=RS2(I,J)=RS3(I,J)=RS4(I,J)=0.
```

```
      DO 9 K=1,3
      RS1(I,J)=RS1(I,J)+ROT(M,K,I)*SR1(K,J)
      RS2(I,J)=RS2(I,J)+ROT(M,K,I)*SR2(K,J)
      RS3(I,J)=RS3(I,J)+ROT(M+1,K,I)*SR3(K,J)
 9    RS4(I,J)=RS4(I,J)+ROT(M+1,K,I)*SR4(K,J)
C ASSIGN RS=RT*SM*R TO APPROPRIATE PLACE IN THE PARTITIONED MATRIX
C S11, S12 OR S22
      IF(M.EQ.NELR)GO TO 15
      DO 10 I=1,2
      DO 10 J=1,2
      S11(2*(M-1)+I,2*(M-1)+J)=S11(2*(M-1)+I,2*(M-1)+J)+RS1(I,J)
      S11(2*(M-1)+I,2*M+J)=S11(2*(M-1)+I,2*M+J)+RS2(I,J)
      S11(2*M+I,2*M+J)=S11(2*M+I,2*M+J)+RS4(I,J)
 10   S11(2*M+I,2*(M-1)+J)=S11(2*M+I,2*(M-1)+J)+RS3(I,J)
      DO 11 I=1,2
      S12(2*(M-1)+I,M)=S12(2*(M-1)+I,M)+RS1(I,3)
      S12(2*(M-1)+I,M+1)=S12(2*(M-1)+I,M+1)+RS2(I,3)
      S12(2*M+I,M)=S12(2*M+I,M)+RS3(I,3)
 11   S12(2*M+I,M+1)=S12(2*M+I,M+1)+RS4(I,3)
      S22(M,M)=S22(M,M)+RS1(3,3)
      S22(M,M+1)=S22(M,M+1)+RS2(3,3)
      S22(M+1,M)=S22(M+1,M)+RS3(3,3)
      S22(M+1,M+1)=S22(M+1,M+1)+RS4(3,3)
      GO TO 7
C FOR THE LAST ELEMENT
 15   DO 16 I=1,2
      DO 16 J=1,2
      S11(2*(NELR-1)+I,2*(NELR-1)+J)=S11(2*(NELR-1)+I,2*(NELR-1)+J)
     1  +RS1(I,J)
      S11(2*(NELR-1)+I,J)=S11(2*(NELR-1)+I,J)+RS2(I,J)
      S11(I,2*(NELR-1)+J)=S11(I,2*(NELR-1)+J)+RS3(I,J)
 16   S11(I,J)=S11(I,J)+RS4(I,J)
      DO 17 I=1,2
      S12(2*(NELR-1)+I,NELR)=S12(2*(NELR-1)+I,NELR)+RS1(I,3)
      S12(2*(NELR-1)+I,1)=S12(2*(NELR-1)+I,1)+RS2(I,3)
      S12(I,NELR)=S12(I,NELR)+RS3(I,3)
```

```
 17     S12(I,1)=S12(I,1)+RS4(I,3)
        S22(NELR,NELR)=S22(NELR,NELR)+RS1(3,3)
        S22(NELR,1)=S22(NELR,1)+RS2(3,3)
        S22(1,NELR)=S22(1,NELR)+RS3(3,3)
        S22(1,1)=S22(1,1)+RS4(3,3)
 7      CONTINUE
C THE FULL STIFFNESS MATRIX HAS BEEN COMPLETED, NOW IT IS MODIFIED
C FOR ZERO MOMENT LOAD
C INVERT S22=S22**-1
        CALL INVERT(12,NELR,S22)
C STEMP1=S22**-1*S21
        N2=2*NELR
        DO 12 I=1,NELR
        DO 12 J=1,N2
        STEMP1(I,J)=0.
        DO 12 K=1,NELR
 12     STEMP1(I,J)=STEMP1(I,J)+S22(I,K)*S12(J,K)
C STEMP2=S12*S22**-1*S21
        DO 13 I=1,N2
        DO 13 J=1,N2
        STEMP2(I,J)=0.
        DO 13 K=1,NELR
 13     STEMP2(I,J)=STEMP2(I,J)+S12(I,K)*STEMP1(K,J)
C GET UPPER TRIANGULAR PART OF PIPE STIFFNESS MATRIX S11-STEMP2
        DO 14 I=1,NELR
        DO 14 J=I,NELR
        DO 18 K=1,2
        DO 18 L=1,2
        K2=2*(I-1)+K
        L2=2*(J-1)+L
        TEMPOR(K,L)=S11(K2,L2)-STEMP2(K2,L2)
 18     CONTINUE
        CALL LOC(I,J)
 14     CONTINUE
C INCREMENT MASS
        ALP=ALP*R
```

```
      W1=W1*ALP
      DO 19 I=1,NELR
19    WM(I)=W1
      RETURN
      END


      SUBROUTINE INVERT(M,N,B)
C THIS INVERTS N*N B MATRIX, M*M IS THE STORAGE ALLOCATED TO B IN THE
C CALLING PROGRAM
      DIMENSION B(M,M)
      DO 1 I=1,N
      X=B(I,I)
      B(I,I)=1.0
      DO 2 J=1,N
2     B(I,J)=B(I,J)/X
      DO 1 K=1,N
      IF(K-I)3,1,3
3     X=B(K,I)
      B(K,I)=0.0
      DO 4 J=1,N
4     B(K,J)=B(K,J)-X*B(I,J)
1     CONTINUE
      RETURN
      END


      SUBROUTINE PACK
      COMMON/POOL/USE(324),RK(4,4),PK(4,4),S(4,4),R(4,4),GARB(1592)
      COMMON/ROT/ROT(13,3,3)
      COMMON/READ1/RR,E1,V1,ZI,A,W1
      COMMON/READ2/P1,P2,W2,R1
      COMMON/READ3/CORD(85,2),NLO(50,5),W3,E2,V2,NEL,NND,METHOD
      COMMON/STIFF/NELR,NEW,NCOUNT,NI(250),NJ(250),STIFF(250,2,2),WM(85)
```

```
     1 ,TEMPOR(2,2),N1
C GET A TYPICAL ELEMENT STIFFNESS MATRIX PK
      DO 1 I=1,4
      DO 1 J=1,4
 1    PK(I,J)=0.
      PK(1,1)=PK(3,3)=P1
      PK(2,2)=PK(4,4)=P2
      PK(1,3)=PK(3,1)=-P1
      PK(2,4)=PK(4,2)=-P2
      DO 7 M=1,NELR
C R=4*4 ROTATION MATRIX FOR EACH ELEMENT
      DO 2 I=1,4
      DO 2 J=1,4
 2    R(I,J)=0.
      DO 3 I=1,2
      DO 3 J=1,2
 3    R(I,J)=R(I+2,J+2)=ROT(M,I,J)
C RK=PK*R
      DO 4 I=1,4
      DO 4 J=1,4
      RK(I,J)=0.
      DO 4 K=1,4
 4    RK(I,J)=RK(I,J)+PK(I,K)*R(K,J)
C S=RT*PK*R
      DO 5 I=1,4
      DO 5 J=1,4
      S(I,J)=0.
      DO 5 K=1,4
 5    S(I,J)=S(I,J)+R(K,I)*RK(K,J)
C ASSIGN S TO APPROPRIATE PLACE
      DO 6 I=1,2
      DO 6 J=1,2
      IF(NLO(M,I).GT.NLO(M,J))GO TO 6
 8    DO 9 K=1,2
      DO 9 L=1,2
      TEMPOR(K,L)=S(2*(I-1)+K,2*(J-1)+L)
```

```
 9      CONTINUE
        CALL LOC(NLO(M,I),NLO(M,J))
 6      CONTINUE
        DO 10 I=1,2
        WM(NLO(M,I))=WM(NLO(M,I))+.5*W2*3.14159*(R1**2-RR**2)/NELR
 10     CONTINUE
 7      CONTINUE
        RETURN
        END


        SUBROUTINE FEM
        COMMON/POOL/USE(324),SL1,SL2,CINT(2),NS(3),SM11(8,8),SM12(8,2),
       1 SM22(2,2),STEMP1(8,8),STEMP2(8,8),GARB(1437)
        COMMON/TRIAN/XI,YI,XJ,YJ,XM,YM,S1(3,2,2),S2(3,2,2),S3(3,2,2),AREA
        COMMON/READ3/CORD(85,2),NLO(50,5),W3,E2,V2,NEL,NND,METHOD
        COMMON/STIFF/NELR,NEW,NCOUNT,NI(250),NJ(250),STIFF(250,2,2),WM(85)
       1 ,TEMPOR(2,2),N1
        NEW =NND
        DO 7 M=N1,NEL
C ADD NEW JOINT NO TO INTERIER NODE IF METHOD=2
        IF(METHOD.NE.2)GO TO 24
        NEW=NEW+1
        GO TO 1
 24     CONTINUE
        DO 11 I=1,8
        DO 12 J=1,8
 12     SM11(I,J)=0.
 11     SM12(I,1)=SM12(I,2)=0.
        SM22(1,1)=SM22(1,2)=SM22(2,1)=SM22(2,2)=0.
C CALC CORD OF INTERIER NODES
 1      SL1=(CORD(NLO(M,3),2)-CORD(NLO(M,1),2))/(CORD(NLO(M,3),1)-CORD(NLO
       1(M,1),1))
        SL2=(CORD(NLO(M,2),2)-CORD(NLO(M,4),2))/(CORD(NLO(M,2),1)-CORD(NLO
       1(M,4),1))
```

```
      CINT(1)=(SL1*CORD(NLO(M,1),1)-CORD(NLO(M,1),2)-SL2*CORD(NLO(M,4),1
     6)+CORD(NLO(M,4),2))/(SL1-SL2)
      CINT(2)=CORD(NLO(M,1),2)+SL1*(CINT(1)-CORD(NLO(M,1),1))
      NLO(M,5)=NLO(M,1)
      DO 8 N=1,4
      XI=CORD(NLO(M,N),1) $ YI=CORD(NLO(M,N),2)
      XJ=CORD(NLO(M,N+1),1) $ YJ=CORD(NLO(M,N+1),2)
      XM=CINT(1) $ YM=CINT(2)
      CALL TRI(E2,V2)
      IF(METHOD.EQ.1)GO TO 9
C FOR METHOD=2, TREAT INTERIER NODE AS A REGULAR NODE
      NS(1)=NLO(M,N)
      NS(2)=NLO(M,N+1)
      NS(3)=NEW
      DO 23 I=1,3
      DO 23 J=1,3
C INCREMENT APPROPRIATE STIFFNESS ELEMENT
      IF(NS(I).GT.NS(J))GO TO 23
      DO 3 K=1,2
      DO 3 L=1,2
      GO TO (4,5,6)I
 4    TEMPOR(K,L)=S1(J,K,L)
      GO TO 3
 5    TEMPOR(K,L)=S2(J,K,L)
      GO TO 3
 6    TEMPOR(K,L)=S3(J,K,L)
 3    CONTINUE
      CALL LOC(NS(I),NS(J))
 23   CONTINUE
      DO 10 I=1,3
      WM(NS(I))=WM(NS(I))+AREA*W3/3
 10   CONTINUE
      GO TO 8
C BELOW FOR METHOD =1, MODIFIED STIFFNESS IS FOUND FOR THE QUADRILATERAL
C ELEMENT
```

```
 9     CONTINUE
C INCREMENT MASS
       WM(NLO(M,N))=WM(NLO(M,N))+AREA*W3/2.
       WM(NLO(M,N+1))=WM(NLO(M,N+1))+AREA*W3/2.
C SM ARE FULL 5*5 STIFFNESS MATRIX INCLUDING THE INTERIER NODE
       DO 14 I=1,2
       DO 14 J=1,2
       SM11(2*(N-1)+I,2*(N-1)+J)=SM11(2*(N-1)+I,2*(N-1)+J)+S1(1,I,J)
       IF(N.EQ.4)GO TO 15
       SM11(2*(N-1)+I,2*N+J)=SM11(2*(N-1)+I,2*N+J)+S1(2,I,J)
       SM11(2*N+I,2*(N-1)+J)=SM11(2*N+I,2*(N-1)+J)+S2(1,I,J)
       SM11(2*N+I,2*N+J)=SM11(2*N+I,2*N+J)+S2(2,I,J)
       SM12(2*(N-1)+I,J)=SM12(2*(N-1)+I,J)+S1(3,I,J)
       SM12(2*N+I,J)=SM12(2*N+I,J)+S2(3,I,J)
       SM22(I,J)=SM22(I,J)+S3(3,I,J)
       GO TO 14
C FOR THE LAST OF THE FOUR TRIANGLE
 15    SM11(6+I,J)=SM11(6+I,J)+S1(2,1,J)
       SM11(I,6+J)=SM11(I,6+J)+S2(1,I,J)
       SM11(I,J)=SM11(I,J)+S2(2,I,J)
       SM12(6+I,J)=SM12(6+I,J)+S1(3,I,J)
       SM12(I,J)=SM12(I,J)+S2(3,I,J)
       SM22(I,J)=SM22(I,J)+S3(3,I,J)
 14    CONTINUE
       IF(N.EQ.4)GO TO 16
 8     CONTINUE
       GO TO 7
CK22**-1
 16    CONTINUE
       CALL INVERT(2,2,SM22)
C K22**-1*K21=STEMP1
       DO 17 I=1,2
       DO 17 J=1,8
       STEMP1(I,J)=0.
       DO 17 K=1,2
 17    STEMP1(I,J)=STEMP1(I,J)+SM22(I,K)*SM12(J,K)
```

```
C K12*K22**-1*K21=STEMP2
      DO 18 I=1,8
      DO 18 J=1,8
      STEMP2(I,J)=0.
      DO 18 K=1,2
 18   STEMP2(I,J)=STEMP2(I,J)+SM12(I,K)*STEMP1(K,J)
C TO CHECK THE VALUE OF THE FULL QUAD STIFF MATRIX
      DO 100 I=1,8
      DO 100 J=1,8
 100  STEMP1(I,J)=SM11(I,J)-STEMP2(I,J)
C C QUADRILATERAL STIFFNESS K11-STEMP2 PUT IN APPROPRIATE PLACE IN STIFF
      DO 19 I=1,4
      DO 19 J=1,4
      IF(NLO(M,I).GT.NLO(M,J))GO TO 19
 20   DO 21 K=1,2
      DO 21 L=1,2
      TEMPOR(K,L)=SM11(2*(I-1)+K,2*(J-1)+L)-STEMP2(2*(I-1)+K,2*(J-1)+L)
 21   CONTINUE
      CALL LOC(NLO(M,I),NLO(M,J))
 19   CONTINUE
 7    CONTINUE
      RETURN
      END


      SUBROUTINE TRI(E2,V2)
      COMMON/TRIAN/XI,YI,XJ,YJ,XM,YM,S1(3,2,2),S2(3,2,2),S3(3,2,2),AREA
C THIS CALCULATE THE 6*6 TRIANGLE STIFFNESS MATRIX SM
      AREA =0.5*(XJ*YM+XM*YI+XI*YJ-XJ*YI-XI*YM-XM*YJ)
      C=E2/(4*AREA*(1+V2)*(1-2*V2))
      C1=.5*(1-2*V2)
       C2=1-V2
      BI=YJ-YM
      CI=XM-XJ
      BJ=YM-YI
```

```
      CJ=XI-XM
      BM=YI-YJ
      CM=XJ-XI
      S1(1,1,1)=(C2*BI**2+C1*CI**2)*C
      S1(1,1,2)=(V2*BI*CI+C1*BI*CI)*C
      S1(1,2,1)=S1(1,1,2)
      S1(1,2,2)=(C2*CI**2+C1*BI**2)*C
      S1(2,1,1)=(C2*BI*BJ+C1*CI*CJ)*C
      S1(2,1,2)=(V2*BI*CJ+C1*BJ*CI)*C
      S1(2,2,1)=(V2*BJ*CI+C1*BI*CJ)*C
      S1(2,2,2)=(C2*CI*CJ+C1*BI*BJ)*C
      S1(3,1,1)=(C2*BI*BM+C1*CI*CM)*C
      S1(3,1,2)=(V2*BI*CM+C1*BM*CI)*C
      S1(3,2,1)=(V2*BM*CI+C1*BI*CM)*C
      S1(3,2,2)=(C2*CI*CM+C1*BI*BM)*C
      S2(2,1,1)=(C2*BJ**2+C1*CJ**2)*C
      S2(2,1,2)=(V2*BJ*CJ+C1*BJ*CJ)*C
      S2(2,2,1)=(V2*BJ*CJ+C1*BJ*CJ)*C
      S2(2,2,2)=(C2*CJ**2+C1*BJ**2)*C
      S2(3,1,1)=(C2*BJ*BM+C1*CJ*CM)*C
      S2(3,1,2)=(V2*BJ*CM+C1*BM*CJ)*C
      S2(3,2,1)=(V2*BM*CJ+C1*BJ*CM)*C
      S2(3,2,2)=(C2*CJ*CM+C1*BJ*BM)*C
      S3(3,1,1)=(C2*BM**2+C1*CM**2)*C
      S3(3,1,2)=(V2*BM*CM+C1*BM*CM)*C
      S3(3,2,1)=(V2*BM*CM+C1*BM*CM)*C
      S3(3,2,2)=(C2*CM**2+C1*BM**2)*C
      DO 1 I=1,2
      DO 1 J=1,2
      S2(1,I,J)=S1(2,J,I)
      S3(1,I,J)=S1(3,J,I)
1     S3(2,I,J)=S2(3,J,I)
      RETURN
      END
```

```
      SUBROUTINE LOC(NODEI,NODEJ)
      COMMON/STIFF/NELR,NEW,NCOUNT,NI(250),NJ(250),STIFF(250,2,2),WM(85)
     1 ,TEMPOR(2,2),N1
      IF(NCOUNT.NE.0)GO TO 16
C FOR THE VERY FIRST ENTRY
      DO 17 I=1,2
      DO 17 J=1,2
 17   STIFF(1,I,J)=TEMPOR(I,J)
      NCOUNT=1
      NI(1)=NODEI
      NJ(1)=NODEJ
      GO TO 4
C FOR REGULER ENTRY
 16   NSLOT=0
      DO 1 NN=1,NCOUNT
      IF(NI(NN).GT.NODEI)GO TO 8
      IF(NI(NN).EQ.NODEI)GO TO 2
C BELOW IS FOR NI(NN).LT.NODEI
      NSLOT=NN
      GO TO 1
 2    NSLOT=NN
      IF(NJ(NN).LT.NODEJ)GO TO 1
      IF(NJ(NN).EQ.NODEJ)GO TO 3
C BELOW FOR NJ(NN).GT.NODEJ
      NSLOT=NN-1
      GO TO 8
 3    DO 13 I=1,2
      DO 13 J=1,2
 13   STIFF(NN,I,J)=STIFF(NN,I,J)+TEMPOR(I,J)
      GO TO 4
 1    CONTINUE
C A NEW ADDITION TO STIFF ARRAY , PUT IN APPROPRIATE PLACE
C NOW SHIFT THE LATTER PART OF THE ARRAY
 8    NTEMP=NCOUNT-NSLOT
      IF(NTEMP.EQ.0)GO TO 18
      DO 10 I=1,NTEMP
```

```
      K=NCOUNT-I+1
      DO 14 J=1,2
      DO 14 L=1,2
      NI(K+1)=NI(K)
      NJ(K+1)=NJ(K)
 14   STIFF(K+1,J,L)=STIFF(K,J,L)
 10   CONTINUE
C NOW INSERT THE NEW STIFF
 18   NSLOT1=NSLOT+1
      DO 15 J=1,2
      DO 15 L=1,2
 15   STIFF(NSLOT1,J,L)=TEMPOR(J,L)
      NI(NSLOT1)=NODEI
      NJ(NSLOT1)=NODEJ
      NCOUNT=NCOUNT+1
 4    RETURN
      END


      SUBROUTINE MATPRT(M1,N1,M,N,A)
C THIS ROUTINE PRINT M*N MATRIX A BY COLUMN, STARTING OVER EVERY 10 COLUMI
C M1*N1 IS THE STORAGE ALLOCATED TO A IN THE CALLING PROGRAM
      INTEGER RTCOL
      DIMENSION A(M1,N1)
 601  FORMAT(*0*)
 602  FORMAT(* *,1P10E13.5)
      NPAGES=(N-1)/10 + 1
      DO 101 I=1,NPAGES
      PRINT 601
      LTCOL =10*(I-1) + 1
      RTCOL = 10*I
      IF(RTCOL.GT.N) RTCOL=N
      DO 101 J=1,M
 101  PRINT 602,(A(J,K),K=LTCOL,RTCOL)
      RETURN
      END
```

```
      PROGRAM MSOLVE(INPUT,OUTPUT,TAPE60=INPUT,TAPE61=OUTPUT,TAPE1)
      COMMON/READ1/R,E1,V1,ZI,A,W1
      COMMON/DUMP/NUMB
      COMMON/STIFF/NELR,NEW,NCOUNT,NI(250),NJ(250),STIFF(250,2,2),TEMPOR
     1(2,2),N1,WM(85)
      COMMON/READ2/P1,P2,W2,R1
      COMMON/READ3/CORD(85,2),NLO(50,5),W3,E2,V2,NEL,NND,METHOD
      COMMON/READ4/N,DELTAT,NC1,NC2,AMP,RMASS(15),RLENG(15),S1(15,2),
     1 DAMP(15,2),DATA T(200,2),DATA A(200,2)
      COMMON/INP/D(15,2),VA(15,2),VV(15,2),V(15,2),VAOLD(15,2),INDEX(2),
     1 DNUM,MARK,UA(2)
      COMMON/F/F(15,2),US(15,2),USOLD(15,2)
      COMMON/BOUND/ACC(85,2),VEL(85,2),DIS(85,2),ACCOLD(85,2)
      COMMON/READ5/NNDT,NNDB,NNDS,FTR
      COMMON/PARA/TBEGIN,PBEGIN,PINTER,TEND,L1,K1,L2,K2,IEND,NA,NB
      COMMON/T/NT
      COMMON/POOL/SM1(3,3),SM2(3,3),SM3(3,3),SM4(3,3),STEMP1(12,24),
     1 ROS(13),DISM(6)
      COMMON/ROT/ROT(13,3,3)
      DATA WM,STIFF/1085*0./,NCOUNT/0/
C READ DATA FOR RING
      READ 101,NELR,R,E1,V1,ZI,A,W1
 101  FORMAT(I5,F10.5,E10.2,4F10.5)
      PRINT 401,NELR,R,E1,V1,ZI,A,W1
 401  FORMAT(/*  NO. OF RING ELEMENT=*I5,*   R=*F10.3,*   E1=*E10.2,*
     1V1=*F10.4,*   ZI=*F10.5,*   A=*F10.5,*   W1=*F10.5)
C DATA FOR PACKING MATERIAL AND CONNECTIVITY
      READ 102,P1,P2,W2,R1
 102  FORMAT(4F10.3)
      READ 202,((NLO(I,J),J=1,2),I=1,NELR)
```

```
202  FORMAT(5X,2I5)
     PRINT 403,P1,P2,W2,R1
403  FORMAT(/*  FOR PACKING, SHEAR SPRING P1=*F10.2,*  COMPRESSION SPRI
    1NG P2=*F10.2,*  MASS PER UNIT AREA W2=*F10.4,/,*   OUTER RADIUS OF
    2 PACKING R1=*F10.4)
     PRINT 314
314  FORMAT(4X*I*1X*NLO1*1X*NLO2*)
     DO 404 I=1,NELR
404  PRINT 405,I,(NLO(I,J),J=1,2)
405  FORMAT(3I5)
     READ 103,W3,E2,V2,NEL,NND,METHOD
103  FORMAT(3F10.2,3I5)
     READ 203,((CORD(I,J),J=1,2),I=1,NND)
203  FORMAT(8F10.5)
     N1=NELR+1
     READ 303,((NLO(I,J),J=1,4),I=N1,NEL)
303  FORMAT(4I5,10X,4I5,10X,4I5)
     PRINT 406,W3,E2,V2,NEL,NND,METHOD
406  FORMAT(*  MASS DENSITY OF FEM=*F10.5,*  E2=*F10.2,*  V2=*F10.5,/,
    1 *   TOTAL NO OF ELEMENT=*I5,*   TOTAL NO OF NODE=*I5,*   METHOD=*
    2 I5)
     PRINT 409
409  FORMAT(* NODE*5X*CORD1*5X*CORD2*)
     DO 407 I=1,NND
407  PRINT 408,I,(CORD(I,J),J=1,2)
408  FORMAT(I5,2F10.2)
     PRINT 410
410  FORMAT(4X*MEMBER*3X*NLO1*3X*NLO2*3X*NLO3*3X*NLO4*)
     DO 411 I=N1,NEL
411  PRINT 412,I,(NLO(I,J),J=1,4)
412  FORMAT(I10,4I7)
      READ(1)NEW,NCOUNT
      READ(1)(NI(I),NJ(I),((STIFF(I,J,K),K=1,2),J=1,2),I=1,250)
      READ(1)(((ROT(I,J,K),K=1,3),J=1,3),I=1,13)
      READ(1)(WM(I),I=1,85)
      READ(1)((SM1(I,J),SM2(I,J),SM3(I,J),SM4(I,J),J=1,3),I=1,3)
```

```
      READ(1)((STEMP1(I,J),J=1,24),I=1,12)
      READ 1,N,DELTAT,AMP,NC1,NC2
 1    FORMAT(I5,2F10.5,2I5)
      PRINT 19,N,DELTAT,AMP,NC1,NC2
 19   FORMAT(//*  N=*I5,*   DELTAT=*F10.5,*   AMP=*F10.5,*   NC1=*I5,
     1 *   NC2=*I5)
      PRINT 4
 4    FORMAT(/4X*I*10X*RMASS*10X*RLENG*13X*S1*11X*DAMP*)
      DO 2 I=1,N
      READ 3,RMASS(I),RLENG(I),S1(I,1),DAMP(I,1),S1(I,2),DAMP(I,2)
 3    FORMAT(6F10.4)
      PRINT 5,I,RMASS(I),RLENG(I),(S1(I,J),DAMP(I,J),J=1,2)
 5    FORMAT(I5,4F15.4,/35X,2F15.4)
 2    CONTINUE
      READ 14,FTR,TBEGIN,PBEGIN,PINTER,TEND,NNDT,NNDB,NNDS
 14   FORMAT(5F10.5,3I5)
      PRINT 20,FTR,TBEGIN,PBEGIN,PINTER,TEND,NNDT,NNDB,NNDS
 20   FORMAT(/* FTR=*F7.4,* TBEGIN=*F7.4,* PBEGIN=*F7.4,* PINTER=*F7.4,
     1 * TEND=*F7.4,* NNDT=*I5,* NNDB=*I5,* NNDS=*I5)
C INITIAL VALUES FOR SUBROUTINE FSI
      DO 6 I=1,N
      DO 6 J=1,2
 6    US(I,J)=F(I,J)=0.
C INITIAL VALUES FOR SUBROUTINE FREE
      DO 7 I=1,N
      DO 7 J=1,2
 7    V(I,J)=VV(I,J)=0.
C INITIAL VALUES FOR SUBROUTINE INTERP
      DO 8 I=1,NEW
      DO 8 J=1,2
 8    VEL(I,J)=DIS(I,J)=0.
      DO 9 I=1,NC1
      II=4*(I-1)
 9    READ26,(DATA T(II+J,1),DATA A(II+J,1),J=1,4)
      DO 10 I=1,NC2
      II=4*(I-1)
```

```
 10    READ26,(DATA T(II+J,2),DATA A(II+J,2),J=1,4)
 26    FORMAT((3X,4(F8.0,F9.0)))
C GET THE PARAMETERS USED IN SUBROUTINE
       NT=PINTER*2./DELTAT
       NUMB=PBEGIN/DELTAT
       IF(NUMB.EQ.0)NUMB=1
       NB=NND-2*NNDS+1
       NA=NB+NNDS-1
       L2=NND-NNDB-2*NNDS+1
       K2=L2+NNDB-1
       IEND=NND-NNDB-2*NNDS
C GET THE INITIAL ACCELERATION FOR ALL MASS AT T=0
       DO 11 I=1,N
       DO 11 J=1,2
       VA(I,J)=-DATA A(1,J)*AMP
 11    VAOLD(I,J)=-DATA A(1,J)*AMP
       DO 12 I=1,NEW
       DO 12 J=1,2
       ACC(I,J)=-DATA A(1,J)*AMP
 12    ACCOLD(I,J)=-DATA A(1,J)*AMP
       MARK=0
       INDEX(1)=INDEX(2)=2
C ***********************************************************************
C BEGIN THE STEP BY STEP SOLUTION
C ***********************************************************************
 700   DNUM=DELTAT*NUMB
        IF(DNUM.GE.TEND)CALL EXIT
       DO 701 J=1,2
 1720  IF(DNUM.LE.DATA T(INDEX(J),J))GO TO 1730
       INDEX(J)=INDEX(J)+1
       GO TO 1720
C GROUND ACCELERATION INTERPOLATED BY TWO SUITABLE CONSECUTIVE READINGS
 1730  UA(J)=(DNUM-DATA T(INDEX(J)-1,J))*(DATA A(INDEX(J),J)-DATA A(INDEX
      1(J)-1,J))/(DATA T(INDEX(J),J)-DATA T(INDEX(J)-1,J))
       UA(J)=(DATA A(INDEX(J)-1,J)+UA(J))*AMP
       MARK=MARK+1
```

```
      IF(MARK.LE.NT)GO TO 25
 25   CONTINUE
      CALL FREE(J)
C INTERP IS TO GET THE FREE FIELD SOLUTION AT THE BOUNDARY
      CALL INTERP(J)
 701  CONTINUE
      CALL SOLVE
      NUMB=NUMB+1
      GO TO 700
      END


      SUBROUTINE FREE(J)
      COMMON/READ4/N,DELTAT,NC1,NC2,AMP,RMASS(15),RLENG(15),S1(15,2),
     1 DAMP(15,2),DATA T(200,2),DATA A(200,2)
      COMMON/INP/D(15,2),VA(15,2),VV(15,2),V(15,2),VAOLD(15,2),INDEX(2),
     1 DNUM,MARK,UA(2)
      COMMON/F/F(15,2),US(15,2),USOLD(15,2)
      COMMON/T/NT
C BEGIN THE BETA INTEGRATION
      DO 9 I=1,N
 9    V(I,J)=V(I,J)+DELTAT*VV(I,J)+.5*DELTAT**2*VA(I,J)
      DO 10 I=2,N
      USOLD(I,J)=US(I,J)
      D(I,J)=DAMP(I,J)*(VV(I,J)-VV(I-1,J))
 10   US(I,J)=V(I,J)-V(I-1,J)
      USOLD(1,J)=US(1,J)
      D(1,J)=DAMP(1,J)*VV(1,J)
      US(1,J)=V(1,J)
      DO 1 I=1,N
 1    F(I,J)=S1(I,J)*US(I,J)
      M=N-1
      DO 11 I=1,M
 11   VA(I,J)=(F(I+1,J)-F(I,J)+D(I+1,J)-D(I,J)-RMASS(I)   *UA(J))/
     1 RMASS(I)
      VA(N,J)=(-F(N,J)-D(N,J)-RMASS(N)   *UA(J))/RMASS(N)
```

```
      DO 12 I=1,N
      VV(I,J)=VV(I,J)+.5*DELTAT*(VAOLD(I,J)+VA(I,J))
 12   VAOLD(I,J)=VA(I,J)
      IF(MARK.LE.NT)GO TO 25
 25   CONTINUE
      RETURN
      END


      SUBROUTINE INTERP(J)
      COMMON/READ3/CORD(85,2),NLO(50,5),W3,E2,V2,NEL,NND,METHOD
      COMMON/READ4/N,DELTAT,NC1,NC2,AMP,RMASS(15),RLENG(15),S1(15,2),
     1 DAMP(15,2),DATA T(200,2),DATA A(200,2)
      COMMON/INP/D(15,2),VA(15,2),VV(15,2),V(15,2),VAOLD(15,2),INDEX(2),
     1 DNUM,MARK,UA(2)
      COMMON/BOUND/ACC(85,2),VEL(85,2),DIS(85,2),ACCOLD(85,2)
      COMMON/READ5/NNDT,NNDB,NNDS,FTR
      COMMON/T/NT
      COMMON/PARA/TBEGIN,PBEGIN,PINTER,TEND,L1,K1,L2,K2,IEND,NA,NB
C THIS SUBPROG INTERPOLATE FREE FIELD RESULT TO GET THE BOUNDARY VALUE
C FOR THE FINITE ELEMENT PROBLEM
C INITIAL VALUES AT TOP SURFACE
      MM=NB
      NN=N
      RL2=RLENG(N) $ RL1=0. $ RN=0.
 1720 IF(RN.LE.RL2)GO TO 1730
      NN=NN-1
      RL1=RL2
      RL2=RL2+RLENG(NN)
      GO TO 1720
C GENERAL INTERPOLATION
 1730 CON=(RN-RL1)/(RL2-RL1)
      ACC(MM,J)=VA(NN,J)+(VA(NN-1,J)-VA(NN,J))*CON
      VEL(MM,J)=VV(NN,J)+(VV(NN-1,J)-VV(NN,J))*CON
      DIS(MM,J)=V(NN,J)+(V(NN-1,J)-V(NN,J))*CON
```

```
      MM=MM+1
      RN=ABS(CORD(MM,2)-CORD(NB,2))
      IF(MM.GT.NA)GO TO 1721
      GO TO 1720
C NOW ASSIGN THE INTERPOLATED SIDE VALUES TO T8E REST OF THE BOUNDARY
 1721 CONTINUE
      DO 1723 I=L2,K2
      ACC(I,J)=ACC(NA,J)
      VEL(I,J)=VEL(NA,J)
      DIS(I,J)=DIS(NA,J)
 1723 CONTINUE
      DO 1724 I=1,NNDS
      ACC(NND-NNDS+I,J)=ACC(NB+I-1,J)
      VEL(NND-NNDS+I,J)=VEL(NB+I-1,J)
 1724 DIS(NND-NNDS+I,J)=DIS(NB+I-1,J)
C PRINT RESULT
      IF(MARK.LE.NT)GO TO 25
 25   CONTINUE
      RETURN
      END


      SUBROUTINE SOLVE
      COMMON/ADD2/FX(12),FY(12)
      COMMON/STIFF/NELR,NEW,NCOUNT,NI(250),NJ(250),STIFF(250,2,2),TEMPOR
     1(2,2),N1,WM(85)
      COMMON/INP/D(15,2),VA(15,2),VV(15,2),V(15,2),VAOLD(15,2),
     1 INDEX(2),DNUM,MARK,UA(2)
      COMMON/BOUND/ACC(85,2),VEL(85,2),DIS(85,2),ACCOLD(85,2)
      COMMON/READ5/NNDT,NNDB,NNDS,FTR
      COMMON/READ3/CORD(85,2),NLO(50,5),W3,E2,V2,NEL,NND,METHOD
      COMMON/READ4/N,DELTAT,NC1,NC2,AMP,RMASS(15),RLENG(15),S1(15,2),
     1 DAMP(15,2),DATA T(200,2),DATA A(200,2)
      COMMON/T/NT
      COMMON/PARA/TBEGIN,PBEGIN,PINTER,TEND,L1,K1,L2,K2,IEND,NA,NB
```

```
      DO 1 I=1,IEND
      DO 1 J=1,2
 1    DIS(I,J)=DIS(I,J)+DELTAT*VEL(I,J)+.5*DELTAT**2*ACC(I,J)
      IF(METHOD.NE.2)GO TO 3
C FOR INTERIER NODE
      NN=NND+1
      DO 2 I=NN,NEW
      DO 2 J=1,2
 2    DIS(I,J)=DIS(I,J)+DELTAT*VEL(I,J)+.5*DELTAT**2*ACC(I,J)
C NOW BEGIN EQUATION OF MOTION TO CALCULATE ACCELERATION
 3    FORCEX=FORCEY=0.
      NCO=1
      DO 300 I=1,NELR
      FX(I)=FY(I)=0.
      NELRI=NELR+I
 302  IF(NI(NCO).EQ.I.AND.NJ(NCO).EQ.NELRI)GO TO 303
      NCO=NCO+1
      GO TO 302
 303  DO 300 J=1,2
      FX(I)=FX(I)-STIFF(NCO,1,J)*(DIS(NELRI,J)-DIS(I,J))-FTR*STIFF(NCO,
     1 1,J)*(VEL(NELRI,J)-VEL(I,J))
      FY(I)=FY(I)-STIFF(NCO,2,J)*(DIS(NELRI,J)-DIS(I,J))-FTR*STIFF(NCO,2
     1,J)*(VEL(NELRI,J)-VEL(I,J))
 300  CONTINUE
      I=0
      NCO=1
 10   I=I+1
      CON1=CON2=C1=C2=0.
      IF(NI(NCO).GT.I)GO TO 13
C BELOW ARE FOR LOWER DIAGONAL PART OF STIFF
      IF(I.EQ.1)GO TO 9
      NCO1=NCO-1
      DO 11 J=1,NCO1
      IF(NJ(J).NE.I)GO TO 11
      CON1=CON1+STIFF(J,1,1)*DIS(NI(J),1)+STIFF(J,2,1)*DIS(NI(J),2)
      CON2=CON2+STIFF(J,1,2)*DIS(NI(J),1)+STIFF(J,2,2)*DIS(NI(J),2)
```

```
      C1=C1+FTR*(STIFF(J,1,1)*VEL(NI(J),1)+STIFF(J,2,1)*VEL(NI(J),2))
      C2=C2+FTR*(STIFF(J,1,2)*VEL(NI(J),1)+STIFF(J,2,2)*VEL(NI(J),2))
 11    CONTINUE
 9    DO 4 J=I,NEW
      IF(NI(NCO).GT.I)GO TO 13
      IF(NJ(NCO).NE.J)GO TO 4
      CON1=CON1+STIFF(NCO,1,1)*DIS(J,1)+STIFF(NCO,1,2)*DIS(J,2)
      CON2=CON2+STIFF(NCO,2,1)*DIS(J,1)+STIFF(NCO,2,2)*DIS(J,2)
      C1=C1+FTR*(STIFF(NCO,1,1)*VEL(J,1)+STIFF(NCO,1,2)*VEL(J,2))
      C2=C2+FTR*(STIFF(NCO,2,1)*VEL(J,1)+STIFF(NCO,2,2)*VEL(J,2))
      NCO=NCO+1
 4    CONTINUE
 13   ACC(I,1)=(-CON1-C1)/WM(I) -UA(1)
      ACC(I,2)=(-CON2-C2)/WM(I) -UA(2)
C NOW CALCULATE VELOCITY
      IF(I.LT.IEND)GO TO 10
      IF(METHOD.NE.2)GO TO 7
C RESET I=NND FOR THE FIRST INTERIER NODE ONLY
      IF(I.EQ.IEND)GO TO 20
      GO TO 21
 20   I=NND
 22   IF(NI(NCO).EQ.NND+1)GO TO 21
      NCO=NCO+1
      GO TO 22
 21   IF(I.LT.NEW)GO TO 10
C CALCULATE VELOCITY
 7    DO 12 I=1,IEND
      DO 12 J=1,2
      VEL(I,J)=VEL(I,J)+.5*DELTAT*(ACCOLD(I,J)+ACC(I,J))
 12   ACCOLD(I,J)=ACC(I,J)
      IF(METHOD.NE.2)GO TO 14
      DO 15 I=NN,NEW
      DO 15 J=1,2
      VEL(I,J)=VEL(I,J)+.5*DELTAT*(ACCOLD(I,J)+ACC(I,J))
 15   ACCOLD(I,J)=ACC(I,J)
 14   IF(MARK.LE.NT)GO TO 25
```

```
      IF(DNUM.LE.PBEGIN)GO TO 25
      PRINT 8,DNUM
 8    FORMAT(/*  FOR TIME*F10.5)
      DO 304 I=1,NELR
      FX(I)=FX(I)-WM(I)*(ACC(I,1)+UA(1))
 304  FY(I)=FY(I)-WM(I)*(ACC(I,2)+UA(2))
      PRINT 305
 305  FORMAT(/* NODE*8X*FX*8X*FY*6X*ACC1*6X*VEL1*6X*DIS1*6X*ACC2*6X*VEL2
     1*6X*DIS2*)
      N2=2*NELR
      DO 306 I=1,NELR
 306  PRINT 307,I,FX(I),FY(I),(ACC(I,J),VEL(I,J),DIS(I,J),J=1,2)
 307  FORMAT(I5,4F10.4,F10.7,2F10.4,F10.7)
      DO 308 I=N1,N2
 308  PRINT 309,I,(ACC(I,J),VEL(I,J),DIS(I,J),J=1,2)
 309  FORMAT(I5,20X,2F10.4,F10.7,2F10.4,F10.7)
      MARK=0
      CALL MOMENT
 25   CONTINUE
      RETURN
      END


      SUBROUTINE MOMENT
      COMMON/BOUND/ACC(85,2),VEL(85,2),DIS(85,2),ACCOLD(85,2)
      COMMON/POOL/SM1(3,3),SM2(3,3),SM3(3,3),SM4(3,3),STEMP1(12,24),
     1 ROS(13),DISM(6)
      COMMON/ROT/ROT(13,3,3)
      COMMON/STIFF/NELR,NEW,NCOUNT,NI(250),NJ(250),STIFF(250,2,2),TEMPOR
     1(2,2),N1,WM(85)
C THIS SUBROUTINE BACK CALCULATE MOMENT
C ROS =S22**-1*S21 *DIS =ROTATION AT EACH RING NODE
      DO 1 I=1,NELR
      ROS(I)=0.
      DO 1 K=1,NELR
```

```
      ROS(I)=ROS(I)-STEMP1(I,2*K-1)*DIS(K,1)-STEMP1(I,2*K)*DIS(K,2)
 1    CONTINUE
      DO 7 M=1,NELR
C ROTATE DIS BACK TO DISM, LOCAL COORD
      DO 2 J=1,2
      DISM(J)=DISM(J+3)=0.
      DO 2 K=1,2
      DISM(J)=DISM(J)+ROT(M,J,K)*DIS(M,K)
      IF(M.EQ.NELR)GO TO 5
      DISM(J+3)=DISM(J+3)+ROT(M+1,J,K)*DIS(M+1,K)
      GO TO 2
 5    DISM(J+3)=DISM(J+3)+ROT(M+1,J,K)*DIS(1,K)
 2    CONTINUE
      DISM(3)=ROS(M)
      IF(M.EQ.NELR)DISM(6)=ROS(1)
      IF(M.EQ.NELR)GO TO 6
      DISM(6)=ROS(M+1)
C NOW BACK CALCULATE MOMENT=RM
 6    RM1=RM2=0.
      DO 3 K=1,3
      RM1=RM1+SM1(3,K)*DISM(K)+SM2(3,K)*DISM(K+3)
      RM2=RM2+SM3(3,K)*DISM(K)+SM4(3,K)*DISM(K+3)
 3    CONTINUE
      PRINT 4,M,RM1,RM2
 4    FORMAT(* MEMBER*I5,*     MOMENT 1=*F20.5,*     MOMENT 2=*F20.5)
 7    CONTINUE
      RETURN
      END
```

Package RIG20 This package also includes subroutines FREE and INTERP given in package MSOLVE earlier.

```
      PROGRAM RIG20(INPUT,OUTPUT,TAPE60=INPUT,TAPE61=OUTPUT,TAPE1)
      COMMON/READ1/R,E1,V1,ZI,A,W1
      COMMON/DUMP/NUMB,TR(3,3)
      COMMON/STIFF/NELR,NEW,NCOUNT,NI(250),NJ(250),STIFF(250,2,2),TEMPOR
     1(2,2),N1,WM(85)
      COMMON/READ2/P1,P2,W2,R1
      COMMON/READ3/CORD(85,2),NLO(50,5),W3,E2,V2,NEL,NND,METHOD
      COMMON/READ4/N,DELTAT,NC1,NC2,AMP,RMASS(15),RLENG(15),S1(15,2),
     1 DAMP(15,2),DATA T(480,2),DATA A(480,2)
      COMMON/INP/D(15,2),VA(15,2),VV(15,2),V(15,2),VAOLD(15,2),INDEX(2),
     1 DNUM,MARK,UA(2)
      COMMON/F/F(15,2),US(15,2),USOLD(15,2)
      COMMON/BOUND/ACC(85,2),VEL(85,2),DIS(85,2),ACCOLD(85,2)
      COMMON/READ5/NNDT,NNDB,NNDS,FTR
      COMMON/PARA/TBEGIN,PBEGIN,PINTER,TEND,L1,K1,L2,K2,IEND,NA,NB
      COMMON/T/NT
      COMMON/POOL/SM1(3,3),SM2(3,3),SM3(3,3),SM4(3,3),STEMP1(12,24),
     1 ROS(13),DISM(6)
      COMMON/ROT/ROT(13,3,3)
      COMMON/ADD2/FX(12),FY(12),FLEX(12,3,3),TRF(12,3,2)
      COMMON/DUHAM/RMAX(12),TMAX(12)
      DATA WM,STIFF/1085*0./,NCOUNT/0/
C READ DATA FOR RING
      READ 101,NELR,R,E1,V1,ZI,A,W1
 101  FORMAT(I5,F10.5,E10.2,4F10.5)
      DO 996 I=1,NELR
 996  RMAX(I)=TMAX(I)=0.
      PRINT 401,NELR,R,E1,V1,ZI,A,W1
 401  FORMAT(/*  NO. OF RING ELEMENT=*I5,*   R=*F10.3,*   E1=*E10.2,*
     1V1=*F10.4,*   ZI=*F10.5,*   A=*F10.5,*   W1=*F10.5)
C DATA FOR PACKING MATERIAL AND CONNECTIVITY
      READ 102,P1,P2,W2,R1
 102  FORMAT(4F10.3)
      READ 202,((NLO(I,J),J=1,2),I=1,NELR)
 202  FORMAT(5X,2I5)
      PRINT 403,P1,P2,W2,R1
```

```
403  FORMAT(/*  FOR PACKING, SHEAR SPRING P1=*F10.2,*  COMPRESSION SPRI
    1NG P2=*F10.2,*  MASS PER UNIT AREA W2=*F10.4,/,*   OUTER RADIUS OF
    2 PACKING R1=*F10.4)
     PRINT 314
314  FORMAT(4X*I*1X*NLO1*1X*NLO2*)
     DO 404 I=1,NELR
404  PRINT 405,I,(NLO(I,J),J=1,2)
405  FORMAT(3I5)
     READ 103,W3,E2,V2,NEL,NND,METHOD
103  FORMAT(3F10.2,3I5)
     READ 203,((CORD(I,J),J=1,2),I=1,NND)
203  FORMAT(8F10.5)
     N1=NELR+1
     READ 303,((NLO(I,J),J=1,4),I=N1,NEL)
303  FORMAT(4I5,10X,4I5,10X,4I5)
     PRINT 406,W3,E2,V2,NEL,NND,METHOD
406  FORMAT(*  MASS DENSITY OF FEM=*F10.5,*  E2=*F10.2,*  V2=*F10.5,/,
    1 *   TOTAL NO OF ELEMENT=*I5,*   TOTAL NO OF NODE=*I5,*   METHOD=*
    2 I5)
     PRINT 409
409  FORMAT(* NODE*5X*CORD1*5X*CORD2*)
     DO 407 I=1,NND
407  PRINT 408,I,(CORD(I,J),J=1,2)
408  FORMAT(I5,2F10.2)
     PRINT 410
410  FORMAT(4X*MEMBER*3X*NLO1*3X*NLO2*3X*NLO3*3X*NLO4*)
     DO 411 I=N1,NEL
411  PRINT 412,I,(NLO(I,J),J=1,4)
412  FORMAT(I10,4I7)
      READ(1)NEW,NCOUNT
      READ(1)(NI(I),NJ(I),((STIFF(I,J,K),K=1,2),J=1,2),I=1,250)
      READ(1)(((ROT(I,J,K),K=1,3),J=1,3),I=1,13)
      READ(1)(WM(I),I=1,85)
      READ(1)((SM1(I,J),SM2(I,J),SM3(I,J),SM4(I,J),J=1,3),I=1,3)
      READ(1)((STEMP1(I,J),J=1,24),I=1,12)
     READ 1,N,DELTAT,AMP,NC1,NC2
```

```
 1     FORMAT(I5,2F10.5,2I5)
       PRINT 19,N,DELTAT,AMP,NC1,NC2
 19    FORMAT(//*  N=*I5,*   DELTAT=*F10.5,*   AMP=*F10.5,*   NC1=*I5,
      1 *   NC2=*I5)
       PRINT 4
 4     FORMAT(/4X*I*10X*RMASS*10X*RLENG*13X*S1*11X*DAMP*)
       DO 2 I=1,N
       READ 3,RMASS(I),RLENG(I),S1(I,1),DAMP(I,1),S1(I,2),DAMP(I,2)
 3     FORMAT(6F10.4)
       PRINT 5,I,RMASS(I),RLENG(I),(S1(I,J),DAMP(I,J),J=1,2)
 5     FORMAT(I5,4F15.4,/35X,2F15.4)
 2     CONTINUE
       READ 14,FTR,TBEGIN,PBEGIN,PINTER,TEND,NNDT,NNDB,NNDS
 14    FORMAT(5F10.5,3I5)
       PRINT 20,FTR,TBEGIN,PBEGIN,PINTER,TEND,NNDT,NNDB,NNDS
 20    FORMAT(/* FTR=*F7.4,* TBEGIN=*F7.4,* PBEGIN=*F7.4,* PINTER=*F7.4,
      1 * TEND=*F7.4,* NNDT=*I5,* NNDB=*I5,* NNDS=*I5)
C INITIAL VALUES FOR SUBROUTINE FSI
       DO 6 I=1,N
       DO 6 J=1,2
 6     US(I,J)=F(I,J)=0.
C INITIAL VALUES FOR SUBROUTINE FREE
       DO 7 I=1,N
       DO 7 J=1,2
 7     V(I,J)=VV(I,J)=0.
C INITIAL VALUES FOR SUBROUTINE INTERP
       DO 8 I=1,NEW
       DO 8 J=1,2
 8     VEL(I,J)=DIS(I,J)=0.
       DO 9 I=1,NC1
       II=4*(I-1)
 9     READ26,(DATA T(II+J,1),DATA A(II+J,1),J=1,4)
       DO 10 I=1,NC2
       II=4*(I-1)
 10    READ26,(DATA T(II+J,2),DATA A(II+J,2),J=1,4)
 26    FORMAT((3X,4(F8.0,F9.0)))
```

```
C GET THE PARAMETERS USED IN SUBROUTINE
      NT=PINTER*2./DELTAT
      NUMB=PBEGIN/DELTAT
      IF(NUMB.EQ.0)NUMB=1
      NB=NND-2*NNDS+1
      NA=NB+NNDS-1
      L2=NND-NNDB-2*NNDS+1
      K2=L2+NNDB-1
      IEND=NND-NNDB-2*NNDS
C FLEX(I,J,K)=FLEXIBILITY MATRIX FOR POINT I,WHERE LOAD IS APPLIED, USED
C IN SUBROUTINE RMOM
      ALP=2.*3.14159/NELR
      DO 27 I=1,NELR
      AL=ALP*I
      FLEX(I,1,1)=R**3.*(6.*AL-8.*SIN(AL)+SIN(2.*AL))/(4.*E1*ZI)+R*(2.*
     1 AL+SIN(2.*AL))/(4.*A*E1)
      FLEX(I,1,2)=-1.*R**3.*(1.-COS(AL))**2./(2.*E1*ZI)+R*(1.-COS(2.*AL)
     1)/(4.*A*E1)
      FLEX(I,1,3)=-1.*R**2.*(AL-SIN(AL))/(E1*ZI)
      FLEX(I,2,2)=R**3.*(2.*AL-SIN(2.*AL))/(4.*E1*ZI)+R*(2.*AL-SIN(2.*AL
     1))/(4.*A*E1)
      FLEX(I,2,3)=R**2.*(1.-COS(AL))/(E1*ZI)
      FLEX(I,3,3)=R*AL/(E1*ZI)
      FLEX(I,2,1)=FLEX(I,1,2)
      FLEX(I,3,1)=FLEX(I,1,3)
      FLEX(I,3,2)=FLEX(I,2,3)
C NOW ROTATE THE FLEXIBILITY MATRIX TO GLOBAL COORDINATE, TR=FLEX*ROT
      DO 30 J=1,3
      DO 30 K=1,3
      TR(J,K)=0.
      DO 30 L=1,3
 30   TR(J,K)=TR(J,K)+FLEX(I,J,L)*ROT(I+1,L,K)
C FLEX=ROT**-1*TR
      DO 31 J=1,3
      DO 31 K=1,3
      FLEX(I,J,K)=0.
```

```
      DO 31 L=1,3
 31   FLEX(I,J,K)=FLEX(I,J,K)+ROT(I+1,L,J)*TR(L,K)
      IF(I.EQ.NELR)GO TO 27
C FOR NODE 1,SKIP PROCEDURE BELOW $ USE FLEX (NELR,3,3) IN EQ LATER ON
      DO 28 J=1,3
      DO 28 K=1,3
 28   TR(J,K)=0.
      TR(1,1)=TR(2,2)=TR(3,3)=1.
      TR(1,3)=-1.*(CORD(1,2)-CORD(I+1,2))
      TR(2,3)=CORD(1,1)-CORD(I+1,1)
C TRF(3,2)=TR(3,3)*FLEX(3,2)  USING ONLY 3*2 PORTION OF FLEX
      DO 29 J=1,3
      DO 29 K=1,2
      TRF(I,J,K)=0.
      DO 29 L=1,3
 29   TRF(I,J,K)=TRF(I,J,K)+TR(J,L)*FLEX(I,L,K)
 27   CONTINUE
C NOW PUT FLEX(NELR,3,3) IN TR(3,3)
      DO 32 I=1,3
      DO 32 J=1,3
 32   TR(I,J)=FLEX(NELR,I,J)
C GET THE INITIAL ACCELERATION FOR ALL MASS AT T=0
      DO 11 I=1,N
      DO 11 J=1,2
      VA(I,J)=-DATA A(1,J)*AMP
 11   VAOLD(I,J)=-DATA A(1,J)*AMP
      DO 12 I=1,NEW
      DO 12 J=1,2
      ACC(I,J)=-DATA A(1,J)*AMP
 12   ACCOLD(I,J)=-DATA A(1,J)*AMP
      MARK=0
      INDEX(1)=INDEX(2)=2
C ***********************************************************************
C BEGIN THE STEP BY STEP SOLUTION
C ***********************************************************************
 700  DNUM=DELTAT*NUMB
```

```
      IF(DNUM.GE.TEND)GO TO 999
      DO 701 J=1,2
 1720 IF(DNUM.LE.DATA T(INDEX(J),J))GO TO 1730
      INDEX(J)=INDEX(J)+1
      GO TO 1720
C GROUND ACCELERATION INTERPOLATED BY TWO SUITABLE CONSECUTIVE READINGS
 1730 UA(J)=(DNUM-DATA T(INDEX(J)-1,J))*(DATA A(INDEX(J),J)-DATA A(INDEX
     1(J)-1,J))/(DATA T(INDEX(J),J)-DATA T(INDEX(J)-1,J))
      UA(J)=(DATA A(INDEX(J)-1,J)+UA(J))*AMP
      MARK=MARK+1
      IF(MARK.LE.NT)GO TO 25
 25   CONTINUE
      CALL FREE(J)
C INTERP IS TO GET THE FREE FIELD SOLUTION AT THE BOUNDARY
      CALL INTERP(J)
 701  CONTINUE
      CALL SOLVE
      NUMB=NUMB+1
      GO TO 700
 999  DO 998 I=1,NELR
 998  PRINT 997,I,RMAX(I),TMAX(I)
 997  FORMAT(/*  NODE*I5,*  MAX MOMENT =*F15.6,*  AT TIME*F10.5)
      END


      SUBROUTINE SOLVE
      COMMON/ADD2/FX(12),FY(12),FLEX(12,3,3),TRF(12,3,2)
      COMMON/STIFF/NELR,NEW,NCOUNT,NI(250),NJ(250),STIFF(250,2,2),TEMPOR
     1(2,2),N1,WM(85)
      COMMON/INP/D(15,2),VA(15,2),VV(15,2),V(15,2),VAOLD(15,2),
     1 INDEX(2),DNUM,MARK,UA(2)
      COMMON/BOUND/ACC(85,2),VEL(85,2),DIS(85,2),ACCOLD(85,2)
      COMMON/READ5/NNDT,NNDB,NNDS,FTR
      COMMON/READ3/CORD(85,2),NLO(50,5),W3,E2,V2,NEL,NND,METHOD
      COMMON/READ4/N,DELTAT,NC1,NC2,AMP,RMASS(15),RLENG(15),S1(15,2),
     1 DAMP(15,2),DATA T(200,2),DATA A(200,2)
```

```
      COMMON/T/NT
      COMMON/PARA/TBEGIN,PBEGIN,PINTER,TEND,L1,K1,L2,K2,IEND,NA,NB
      DO 1 I=1,IEND
      DO 1 J=1,2
 1    DIS(I,J)=DIS(I,J)+DELTAT*VEL(I,J)+.5*DELTAT**2*ACC(I,J)
      IF(METHOD.NE.2)GO TO 3
C FOR INTERIER NODE
      NN=NND+1
      DO 2 I=NN,NEW
      DO 2 J=1,2
 2    DIS(I,J)=DIS(I,J)+DELTAT*VEL(I,J)+.5*DELTAT**2*ACC(I,J)
C NOW BEGIN EQUATION OF MOTION TO CALCULATE ACCELERATION
 3    FORCEX=FORCEY=0.
      NCO=1
      DO 300 I=1,NELR
      FX(I)=FY(I)=0.
      NELRI=NELR+I
 302  IF(NI(NCO).EQ.I.AND.NJ(NCO).EQ.NELRI)GO TO 303
      NCO=NCO+1
      GO TO 302
 303  DO 300 J=1,2
      FX(I)=FX(I)-STIFF(NCO,1,J)*(DIS(NELRI,J)-DIS(I,J))-FTR*STIFF(NCO,
     1 1,J)*(VEL(NELRI,J)-VEL(I,J))
      FY(I)=FY(I)-STIFF(NCO,2,J)*(DIS(NELRI,J)-DIS(I,J))-FTR*STIFF(NCO,2
     1,J)*(VEL(NELRI,J)-VEL(I,J))
 300  CONTINUE
      DO 400 I=1,NELR
      FORCEX=FORCEX+FX(I)
 400  FORCEY=FORCEY+FY(I)
      ACCX=FORCEX/(NELR*WM(1))-UA(1)
      ACCY=FORCEY/(NELR*WM(1))-UA(2)
C NOW DISTRIBUTE THE X Y ACCELERATION TO OTHER RIGID RING NODES
      DO 301 I=1,NELR
      ACC(I,1)=ACCX
      ACC(I,2)=ACCY
 301  CONTINUE
```

```
      I=NELR
      NCO=1
 16   IF(NI(NCO).EQ.NELR+1)GO TO 17
      NCO=NCO+1
      GO TO 16
 17   CONTINUE
 10   I=I+1
      CON1=CON2=C1=C2=0.
      IF(NI(NCO).GT.I)GO TO 13
C BELOW ARE FOR LOWER DIAGONAL PART OF STIFF
      IF(I.EQ.1)GO TO 9
      NCO1=NCO-1
      DO 11 J=1,NCO1
      IF(NJ(J).NE.I)GO TO 11
      CON1=CON1+STIFF(J,1,1)*DIS(NI(J),1)+STIFF(J,2,1)*DIS(NI(J),2)
      CON2=CON2+STIFF(J,1,2)*DIS(NI(J),1)+STIFF(J,2,2)*DIS(NI(J),2)
      C1=C1+FTR*(STIFF(J,1,1)*VEL(NI(J),1)+STIFF(J,2,1)*VEL(NI(J),2))
      C2=C2+FTR*(STIFF(J,1,2)*VEL(NI(J),1)+STIFF(J,2,2)*VEL(NI(J),2))
 11    CONTINUE
 9    DO 4 J=I,NEW
      IF(NI(NCO).GT.I)GO TO 13
      IF(NJ(NCO).NE.J)GO TO 4
      CON1=CON1+STIFF(NCO,1,1)*DIS(J,1)+STIFF(NCO,1,2)*DIS(J,2)
      CON2=CON2+STIFF(NCO,2,1)*DIS(J,1)+STIFF(NCO,2,2)*DIS(J,2)
      C1=C1+FTR*(STIFF(NCO,1,1)*VEL(J,1)+STIFF(NCO,1,2)*VEL(J,2))
      C2=C2+FTR*(STIFF(NCO,2,1)*VEL(J,1)+STIFF(NCO,2,2)*VEL(J,2))
      NCO=NCO+1
 4    CONTINUE
 13   ACC(I,1)=(-CON1-C1)/WM(I) -UA(1)
      ACC(I,2)=(-CON2-C2)/WM(I) -UA(2)
C NOW CALCULATE VELOCITY
      IF(I.LT.IEND)GO TO 10
      IF(METHOD.NE.2)GO TO 7
C RESET I=NND FOR THE FIRST INTERIER NODE ONLY
      IF(I.EQ.IEND)GO TO 20
      GO TO 21
```

```
 20    I=NND
 22    IF(NI(NCO).EQ.NND+1)GO TO 21
       NCO=NCO+1
       GO TO 22
 21    IF(I.LT.NEW)GO TO 10
C CALCULATE VELOCITY
 7     DO 12 I=1,IEND
       DO 12 J=1,2
       VEL(I,J)=VEL(I,J)+.5*DELTAT*(ACCOLD(I,J)+ACC(I,J))
 12    ACCOLD(I,J)=ACC(I,J)
       IF(METHOD.NE.2)GO TO 14
       DO 15 I=NN,NEW
       DO 15 J=1,2
       VEL(I,J)=VEL(I,J)+.5*DELTAT*(ACCOLD(I,J)+ACC(I,J))
 15    ACCOLD(I,J)=ACC(I,J)
 14    IF(DNUM.LE..02)GO TO 27
       IF(MARK.LE.NT)GO TO 25
       IF(DNUM.LE.PBEGIN)GO TO 25
 27    PRINT 8,DNUM
 8     FORMAT(/*  FOR TIME*F10.5)
       PRINT 26,((DIS(I,J),J=1,2),I=1,IEND)
 26    FORMAT(* DIS=*(12F10.6))
       DO 304 I=1,NELR
       FX(I)=FX(I)-WM(I)*(ACC(I,1)+UA(1))
 304   FY(I)=FY(I)-WM(I)*(ACC(I,2)+UA(2))
        IF(DNUM.LE..02)GO TO 28
       MARK=0
 28    CALL RMOM
 25    CONTINUE
       RETURN
       END
```

```
      SUBROUTINE RMOM
      COMMON/INP/D(15,2),VA(15,2),VV(15,2),V(15,2),VAOLD(15,2),INDEX(2),
     1 DNUM,MARK,UA(2)
      COMMON/ADD2/FX(12),FY(12),FLEX(12,3,3),TRF(12,3,2)
      DIMENSION U(3),Y(3),FO(3),RM(12)
      COMMON/STIFF/NELR,NEW,NCOUNT,NI(250),NJ(250),STIFF(250,2,2),TEMPOR
     1(2,2),N1,WM(85)
      COMMON/READ1/R,E,V1,ZI,A,W1
      COMMON/BOUND/ACC(85,2),VEL(85,2),DIS(85,2),ACCOLD(85,2)
      COMMON/READ3/CORD(85,2),NLO(50,5),W3,E2,V2,NEL,NND,METHOD
      COMMON/DUMP/NUMB,TR(3,3)
      COMMON/ROT/ROT(13,3,3)
      COMMON/DUHAM/RMAX(12),TMAX(12)
      EMOM=0.
C ROTATE TO MEMBER COORD
      DO 14 I=1,NELR
      FMX=ROT(I,1,1)*FX(I)+ROT(I,1,2)*FY(I)
      FMY=ROT(I,2,1)*FX(I)+ROT(I,2,2)*FY(I)
C FIND UNEQUAL MOMENT
      EMOM=EMOM+FMX*R
 14   CONTINUE
C ADD FORCE AT NODES TO TAKE CARE OF UNEQUAL MOMENT
      EFORCE=-EMOM/(NELR*R)
      DO 404 I=1,NELR
      FX(I)=ROT(I,1,1)*EFORCE+FX(I)
      FY(I)=ROT(I,1,2)*EFORCE+FY(I)
 404  CONTINUE
      N2=2*NELR
C NOW CALCULATE DISP INFLUNCE MATRIX TR*FLEX WHERE TR=TRANSFORMATION,
C FLEX=FLEXIBILITY MATRIX FOR THE POINT WHERE LOAD IS APPLIED
      U(1)=U(2)=U(3)=0.
      DO 2 I=1,NELR
      IF(I.EQ.NELR)GO TO 2
C FOR NODE 1,SKIP PROCEDURE BELOW $ USE FLEX IN THE SOLUTION OF SIMULTAN
C EQUATION
C U(3)=TRF(3,2)*F(2) AND ADD THIS TO U(3) FROM PREVOUS NODE
```

```
      DO 5 J=1,3
      U(J)=U(J)+TRF(I,J,1)*FX(I+1)+TRF(I,J,2)*FY(I+1)
 5    CONTINUE
 2    CONTINUE
 7    DO 9 I=1,3
 9    Y(I)=-U(I)
C PUT FLEX(NELR,3,3) IN TR(3,3)
      DO 32 I=1,3
      DO 32 J=1,3
 32   TR(I,J)=FLEX(NELR,I,J)
      CALL E@(TR,FO,Y,3,3)
C NOW THAT FO ARE KNOWN, SOLVE FOR MOMENT RM AT THE NODES
      NU=0
      DO 10 I=2,NELR
      II=NELR-(I-2)
      NU=NU+1
      RM(II)=-FO(3)+FO(1)*(CORD(1,2)-CORD(II,2))-FO(2)*(CORD(1,1)-
     1  CORD(II,1))
      IF(NU.EQ.1)GO TO 10
      DO 13 J=2,NU
      NODE=NELR-(J-2)
      RM(II)=RM(II)+FX(NODE)*(CORD(NODE,2)-CORD(II,2))-FY(NODE)*
     1  (CORD(NODE,1)-CORD(II,1))
 13   CONTINUE
 10   CONTINUE
      RM(1)=-FO(3)
      DO 11 I=1,NELR
 11   PRINT 12,I,RM(I)
 12   FORMAT(*  NODE*I5,*   MOMENT=*F15.6)
C CHECK FOR MAX
      DO 994 I=1,NELR
      CHECK=ABS(RM(I))-RMAX(I)
      IF(CHECK.GT.0.)GO TO 993
      GO TO 994
 993  RMAX(I)=ABS(RM(I))
      TMAX(I)=DNUM
```

```
994   CONTINUE
      RETURN
      END


      SUBROUTINE EQ(A,X,Y,NS,N)
      DIMENSION A(NS,NS),X(NS),Y(NS)
      M=N-1
      DO 10 I=1,M
      L=I+1
      DO 10 J=L,N
      IF(A(J,I))6,10,6
6     DO 8 K=L,N
8     A(J,K)=A(J,K)-A(I,K)*A(J,I)/A(I,I)
      Y(J)=Y(J)-Y(I)*A(J,I)/A(I,I)
10    CONTINUE
      X(N)=Y(N)/A(N,N)
      DO 30 I=1,M
      K=N-I
      L=K+1
      DO 20 J=L,N
20    Y(K)=Y(K)-X(J)*A(K,J)
      X(K)=Y(K)/A(K,K)
30    CONTINUE
      RETURN
      END
```

```
      PROGRAM WACC(INPUT,OUTPUT,TAPE3)
      COMMON/READ1/R,E1,V1,ZI,A,W1
      COMMON/DUMP/NUMB
      COMMON/STIFF/NELR,NEW,NCOUNT,NI(250),NJ(250),STIFF(250,2,2),TEMPOR
     1(2,2),N1,WM(85)
      COMMON/READ2/P1,P2,W2,R1
      COMMON/READ3/CORD(85,2),NLO(50,5),W3,E2,V2,NEL,NND,METHOD
      COMMON/READ4/N,DELTAT,NC1,NC2,AMP,RMASS(15),RLENG(15),S1(15,2),
     1 DAMP(15,2),DATA T(472,2),DATA A(472,2)
      COMMON/INP/D(15,2),VA(15,2),VV(15,2),V(15,2),VAOLD(15,2),INDEX(2),
     1 DNUM,MARK,UA(2)
      COMMON/F/F(15,2),US(15,2),USOLD(15,2)
      COMMON/BOUND/ACC(85,2),VEL(85,2),DIS(85,2),ACCOLD(85,2)
      COMMON/READ5/NNDT,NNDB,NNDS,FTR
      COMMON/PARA/TBEGIN,PBEGIN,PINTER,TEND,L1,K1,L2,K2,IEND,NA,NB
      COMMON/T/NT
      COMMON/POOL/SM1(3,3),SM2(3,3),SM3(3,3),SM4(3,3),STEMP1(12,24),
     1 ROS(13),DISM(6)
      COMMON/ROT/ROT(13,3,3)
      COMMON/NEW/NSPG,WA(2,50),WV(3,2,50),WVV(3,2,50)
      DATA WM,STIFF/1085*0./,NCOUNT/0/
      READ 101,NND,NSPG
101   FORMAT(2I5)
      PRINT 102,NND,NSPG
102   FORMAT(* NO OF NODES=*I5,*  LOWEST LEVEL OF S-D MASS HAVING AN EFF
     1ECT ON FEM=*I5)
      NEW=NND
      READ 203,((CORD(I,J),J=1,2),I=1,NND)
203   FORMAT(8F10.5)
      N1=NELR+1
      PRINT 409
409   FORMAT(* NODE*5X*CORD1*5X*CORD2*)
      DO 407 I=1,NND
407   PRINT 408,I,(CORD(I,J),J=1,2)
408   FORMAT(I5,2F10.2)
      READ 1,N,DELTAT,AMP,NC1,NC2
```

```
 1    FORMAT(I5,2F10.5,2I5)
      PRINT 19,N,DELTAT,AMP,NC1,NC2
 19   FORMAT(//*  N=*I5,*   DELTAT=*F10.5,*   AMP=*F10.5,*   NC1=*I5,
     1 *   NC2=*I5)
      PRINT 4
 4    FORMAT(/4X*I*10X*RMASS*10X*RLENG*13X*S1*11X*DAMP*)
      DO 2 I=1,N
      READ 3,RMASS(I),RLENG(I),S1(I,1),DAMP(I,1),S1(I,2),DAMP(I,2)
 3    FORMAT(6F10.4)
      PRINT 5,I,RMASS(I),RLENG(I),(S1(I,J),DAMP(I,J),J=1,2)
 5    FORMAT(I5,4F15.4,/35X,2F15.4)
 2    CONTINUE
      READ 14,FTR,TBEGIN,PBEGIN,PINTER,TEND,NNDT,NNDB,NNDS
 14   FORMAT(5F10.5,3I5)
      PRINT 20,FTR,TBEGIN,PBEGIN,PINTER,TEND,NNDT,NNDB,NNDS
 20   FORMAT(/* FTR=*F7.4,* TBEGIN=*F7.4,* PBEGIN=*F7.4,* PINTER=*F7.4,
     1 * TEND=*F7.4,* NNDT=*I5,* NNDB=*I5,* NNDS=*I5)
C INITIAL VALUES FOR SUBROUTINE FSI
      DO 6 I=1,N
      DO 6 J=1,2
 6    US(I,J)=F(I,J)=0.
C INITIAL VALUES FOR SUBROUTINE FREE
      DO 7 I=1,N
      DO 7 J=1,2
 7    V(I,J)=VV(I,J)=0.
C INITIAL VALUES FOR SUBROUTINE INTERP
      DO 8 I=1,NEW
      DO 8 J=1,2
 8    VEL(I,J)=DIS(I,J)=0.
      DO 9 I=1,NC1
      II=4*(I-1)
 9    READ26,(DATA T(II+J,1),DATA A(II+J,1),J=1,4)
      DO 10 I=1,NC2
      II=4*(I-1)
 10   READ26,(DATA T(II+J,2),DATA A(II+J,2),J=1,4)
 26   FORMAT((3X,4(F8.0,F9.0)))
```

```
C GET THE PARAMETERS USED IN SUBROUTINE
      NT=PINTER*2./DELTAT
      NUMB=PBEGIN/DELTAT
      IF(NUMB.EQ.0)NUMB=1
      NB=NND-2*NNDS+1
      NA=NB+NNDS-1
      L2=NND-NNDB-2*NNDS+1
      K2=L2+NNDB-1
      IEND=NND-NNDB-2*NNDS
C NSPG IS THE DEEPEST(SMALLEST)MASS LEVEL OF SPRING DASHPOT HAVING ANY
C EFFECT ON THE INTERPOLATED VALUES OF FINITE ELEMENT BOUNDARY MOVEMENT
      WRITE(3)NB,NA,NNDS,DELTAT,NT,N,NSPG
C GET THE INITIAL ACCELERATION FOR ALL MASS AT T=0
      DO 11 I=1,N
      DO 11 J=1,2
      VA(I,J)=-DATA A(1,J)*AMP
 11   VAOLD(I,J)=-DATA A(1,J)*AMP
      DO 12 I=1,NEW
      DO 12 J=1,2
      ACC(I,J)=-DATA A(1,J)*AMP
 12   ACCOLD(I,J)=-DATA A(1,J)*AMP
      UA(1)=-ACC(1,1)
      UA(2)=-ACC(1,2)
      WRITE(3)UA(1),(V(I,1),I=NSPG,N),(VV(I,1),I=NSPG,N)
      WRITE(3)UA(2),(V(I,2),I=NSPG,N),(VV(I,2),I=NSPG,N)
      MARK=0
      INDEX(1)=INDEX(2)=2
C ***********************************************************************
C BEGIN THE STEP BY STEP SOLUTION
C ***********************************************************************
 700  DNUM=DELTAT*NUMB
      MARK=MARK+1
       IF(DNUM.GE.TEND)CALL EXIT
      DO 701 J=1,2
 1720 IF(DNUM.LE.DATA T(INDEX(J),J))GO TO 1730
      INDEX(J)=INDEX(J)+1
```

```
      GO TO 1720
C GROUND ACCELERATION INTERPOLATED BY TWO SUITABLE CONSECUTIVE READINGS
 1730 UA(J)=(DNUM-DATA T(INDEX(J)-1,J))*(DATA A(INDEX(J),J)-DATA A(INDEX
     1(J)-1,J))/(DATA T(INDEX(J),J)-DATA T(INDEX(J)-1,J))
      UA(J)=(DATA A(INDEX(J)-1,J)+UA(J))*AMP
      CALL FREE(J)
C INTERP IS TO GET THE FREE FIELD SOLUTION AT THE BOUNDARY
 701  CONTINUE
      IF(MARK.LT.50)GO TO 25
      WRITE(3)(((WA(J,L),((WV(I,J,L),WVV(I,J,L)),I=1,3)),J=1,2),L=1,50)
      MARK=0
 25   CONTINUE
      NUMB=NUMB+1
      GO TO 700
      END


      SUBROUTINE FREE(J)
      COMMON/READ4/N,DELTAT,NC1,NC2,AMP,RMASS(15),RLENG(15),S1(15,2),
     1 DAMP(15,2),DATA T(200,2),DATA A(200,2)
      COMMON/INP/D(15,2),VA(15,2),VV(15,2),V(15,2),VAOLD(15,2),INDEX(2),
     1 DNUM,MARK,UA(2)
      COMMON/F/F(15,2),US(15,2),USOLD(15,2)
      COMMON/T/NT
      COMMON/NEW/NSPG,WA(2,50),WV(3,2,50),WVV(3,2,50)
C BEGIN THE BETA INTEGRATION
      DO 9 I=1,N
 9    V(I,J)=V(I,J)+DELTAT*VV(I,J)+.5*DELTAT**2*VA(I,J)
      DO 10 I=2,N
      USOLD(I,J)=US(I,J)
      D(I,J)=DAMP(I,J)*(VV(I,J)-VV(I-1,J))
 10   US(I,J)=V(I,J)-V(I-1,J)
      USOLD(1,J)=US(1,J)
      D(1,J)=DAMP(1,J)*VV(1,J)
      US(1,J)=V(1,J)
```

```
      DO 1 I=1,N
1     F(I,J)=S1(I,J)*US(I,J)
      M=N-1
      DO 11 I=1,M
11    VA(I,J)=(F(I+1,J)-F(I,J)+D(I+1,J)-D(I,J)-RMASS(I)   *UA(J))/
     1 RMASS(I)
      VA(N,J)=(-F(N,J)-D(N,J)-RMASS(N)   *UA(J))/RMASS(N)
      DO 12 I=1,N
      VV(I,J)=VV(I,J)+.5*DELTAT*(VAOLD(I,J)+VA(I,J))
12    VAOLD(I,J)=VA(I,J)
      WA(J,MARK)=UA(J)
      DO 26 I=NSPG,N
      WV(I-NSPG+1,J,MARK)=V(I,J)
26    WVV(I-NSPG+1,J,MARK)=VV(I,J)
      IF(MARK.LT.50)GO TO 25
      IF(J.EQ.2)GO TO 3
      PRINT 2,DNUM
2     FORMAT(/* TIME*F8.3)
3     PRINT 4,J,UA(J),J,(V(I,J),I=1,N)
4     FORMAT(* UA*I1,*=*F10.5,* V*I1,*=*(10F10.5))
      PRINT 5,J,(VV(I,J),I=1,N)
5     FORMAT(* VV*I1,*=*(10F10.5))
      PRINT 27,(WV(I,J,50),I=1,3),(WVV(I,J,50),I=1,3)
27    FORMAT(* WV=*3F10.5,* WVV=*3F10.5)
25    CONTINUE
      RETURN
      END
```

```
      PROGRAM FQTA1(INPUT,OUTPUT,TAPE1,TAPE12)
C THIS PROGRAM SOLVES THE EIGENPROBLEM AX=LAMDA*BX,THE MATRIX B MUST
C BE DIAGONAL AND IS INPUTED AS THE ONE DIMENSIONAL ARRAY AMASS , IT IS
C DIMENSIONED FOR 78*78 DEG OF FREEDOM,DIMENSION A(N,N),D(N*(N+1)/2)
C R(N*N)
      DIMENSION NI(250),NJ(250),STIFF(250,2,2),WM(85),ROT(13,3,3)
      DIMENSION PERIOD(78),AMASS(78),FQCY(78),VALU(78),X(78)
      COMMON/EIGEN/A(78,78),D(3081),N
      DIMENSION R(6084)
      EQUIVALENCE(A(1,1),R(1))
      READ(1)RADIUS,Z,Z,Z,Z,((Z,J=1,2),I=1,85)
      IR=12
      IS=27
      PRINT 2,IR,IS,RADIUS
 2    FORMAT(*  NO OF RING NODE =*I5,*  NO OF SOIL NODE =*I5,*  RING RAD
     1IUS =*F10.5)
      N=2*(IR+IS)
      READ(1)NEW,NCOUNT
      READ(1)(NI(I),NJ(I),((STIFF(I,J,K),K=1,2),J=1,2),I=1,250)
      READ(1)(((ROT(I,J,K),K=1,3),J=1,3),I=1,13)
      READ(1)(WM(I),I=1,85)
C GENERATE STIFFNESS MATRIX A
      DO 107 I=1,N
      DO 107 J=1,N
 107  A(I,J)=0.
      I=0
      N1=N/2
      NCO=1
 103  I=I+1
      IF(NI(NCO).GT.I)GO TO 102
      DO 104 J=I,NEW
      IF(NI(NCO).GT.I)GO TO 102
      IF(NJ(NCO).GT.N1)GO TO 105
      NII=2*(NI(NCO)-1)
      NIJ=2*(NJ(NCO)-1)
      DO 106 II=1,2
```

```
      DO 106 IJ=1,2
 106  A(NII+II,NIJ+IJ)=STIFF(NCO,II,IJ)
 105  NCO=NCO+1
 104  CONTINUE
 102  IF(I.LT.N1)GO TO 103
      DO 202 I=1,N
      DO 202 J=I,N
 202  A(J,I)=A(I,J)
      PRINT 49
      DO 101 I=1,N1
      AMASS(2*I-1)=WM(I)
      AMASS(2*I)=WM(I)
 101  CONTINUE
      DO 23 I=1,N
      DO 23 J=1,N
 23   A(I,J)=A(I,J)/(ABS(SQRT(AMASS(I)*AMASS(J))))
C PUT LOWER DIAGONAL OF A INTO 1 DIMENSIONAL ARRAY D BY ROW
      MARK=0
      DO 108 I=1,N
      DO 108 J=1,I
      MARK=MARK+1
      D(MARK)=A(I,J)
 108  CONTINUE
      CALL EIGEN(D,R,N,0)
C NOW GET THE EIGENVALUE $ PUT IN ARRAY VALU
      DO 32 J=1,N
      JJ=(J*J+J)/2
 32   VALU(J)=D(JJ)
      TWOPI=6.28318
      DO 24 I=1,N
 24   FQCY(I)=(ABS(SQRT(VALU(I))))/TWOPI
      DO 100 I=1,N
  100 PERIOD(I)=1./FQCY(I)
      PRINT 56
      DO 25 I=1,N
   25 PRINT 52,VALU(I),FQCY(I),PERIOD(I)
```

```
C NOW GET THE EIGEN VECTOR OUT FROM ONE DIMENSIONAL ARRAY R
      JMOM=N
      IMOM=N
      WRITE(12)IMOM,JMOM
      WRITE(12)(FQCY(I),I=1,N)
      KMAX=0
      DO 35 J=1,N
      KMIN=KMAX+1
      KMAX=KMAX+N
      I=0
      DO 36 K=KMIN,KMAX
      I=I+1
      X(I)=R(K)
 36   X(I)=X(I)/(ABS(SQRT(AMASS(I))))
      JJ=N-J+1
      PRINT 63,JJ,(X(I),I=1,N)
 63   FORMAT(*  MODE*I5,/(10F12.5))
C NOW WRITE ON TAPE2 THE FIRST 3*IR EIGEN VECTORS FOR MOMENT ANALYSIS
      IF(JJ.GT.JMOM)GO TO 35
      WRITE(12)(X(I),I=1,IMOM)
 35   CONTINUE
 49   FORMAT(*  RESULT FOR AX =LAMDA BX FOR FLEXIBLE RING CASE*///)
   50 FORMAT(///* MASS ELEMENTS*/)
   52 FORMAT(F12.4,2F14.5)
   56 FORMAT(///*  EIGENVALUE*5X*FREQUENCY*8X*PERIOD*/)
   58 FORMAT(///* MODES NORMALIZED WITH RESPECT TO MASS AS ROW VECTOR*/)
 60   FORMAT((10E12.5))
      END


      SUBROUTINE EIGEN(A,R,N,MV)
      DIMENSION A(1),R(1)
C        GENERATE IDENTITY MATRIX
      IF(MV-1) 10,25,10
   10 IQ=-N
      DO 20 J=1,N
```

```
      IQ=IQ+N
      DO 20 I=1,N
      IJ=IQ+I
      R(IJ)=0.0
      IF(I-J) 20,15,20
   15 R(IJ)=1.0
   20 CONTINUE
C        COMPUTE INITIAL AND FINAL NORMS (ANORM AND ANORMX)
   25 ANORM=0.0
      DO 35 I=1,N
      DO 35 J=I,N
      IF(I-J) 30,35,30
   30 IA=I+(J*J-J)/2
      ANORM=ANORM+A(IA)*A(IA)
   35 CONTINUE
      IF(ANORM) 165,165,40
   40 ANORM=1.414*SQRT(ANORM)
      ANRMX=ANORM*1.0E-6/FLOAT(N)
C        INITIALIZE INDICATORS AND COMPUTE THRESHOLD, THR
      IND=0
      THR=ANORM
   45 THR=THR/FLOAT(N)
   50 L=1
   55 M=L+1
C        COMPUTE SIN AND COS
   60 MQ=(M*M-M)/2
      LQ=(L*L-L)/2
      LM=L+MQ
   62 IF( ABS(A(LM))-THR) 130,65,65
   65 IND=1
      LL=L+LQ
      MM=M+MQ
      X=0.5*(A(LL)-A(MM))
   68 Y=-A(LM)/ SQRT(A(LM)*A(LM)+X*X)
      IF(X) 70,75,75
   70 Y=-Y
```

```
   75 SINX=Y/ SQRT(2.0*(1.0+( SQRT(1.0-Y*Y))))
      SINX2=SINX*SINX
   78 COSX= SQRT(1.0-SINX2)
      COSX2=COSX*COSX
      SINCS =SINX*COSX
C        ROTATE L AND M COLUMNS
      ILQ=N*(L-1)
      IMQ=N*(M-1)
      DO 125 I=1,N
      IQ=(I*I-I)/2
      IF(I-L) 80,115,80
   80 IF(I-M) 85,115,90
   85 IM=I+MQ
      GO TO 95
   90 IM=M+IQ
   95 IF(I-L) 100,105,105
  100 IL=I+LQ
      GO TO 110
  105 IL=L+IQ
  110 X=A(IL)*COSX-A(IM)*SINX
      A(IM)=A(IL)*SINX+A(IM)*COSX
      A(IL)=X
  115 IF(MV-1) 120,125,120
  120 ILR=ILQ+I
      IMR=IMQ+I
      X=R(ILR)*COSX-R(IMR)*SINX
      R(IMR)=R(ILR)*SINX+R(IMR)*COSX
      R(ILR)=X
  125 CONTINUE
      X=2.0*A(LM)*SINCS
      Y=A(LL)*COSX2+A(MM)*SINX2-X
      X=A(LL)*SINX2+A(MM)*COSX2+X
      A(LM)=(A(LL)-A(MM))*SINCS+A(LM)*(COSX2-SINX2)
      A(LL)=Y
      A(MM)=X
C        TESTS FOR COMPLETION
```

```
C         TEST FOR M = LAST COLUMN
  130 IF(M-N) 135,140,135
  135 M=M+1
      GO TO 60
C         TEST FOR L = SECOND FROM LAST COLUMN
  140 IF(L-(N-1)) 145,150,145
  145 L=L+1
      GO TO 55
  150 IF(IND-1) 160,155,160
  155 IND=0
      GO TO 50
C         COMPARE THRESHOLD WITH FINAL NORM
  160 IF (THR-ANRMX) 165,165,45
C         SORT EIGENVALUES AND EIGENVECTORS
  165 IQ=-N
      DO 185 I=1,N
      IQ=IQ+N
      LL=I+(I*I-I)/2
      JQ=N*(I-2)
      DO 185 J=I,N
      JQ=JQ+N
      MM=J+(J*J-J)/2
      IF(A(LL)-A(MM)) 170,185,185
  170 X=A(LL)
      A(LL)=A(MM)
      A(MM)=X
      IF(MV-1) 175,185,175
  175 DO 180 K=1,N
      ILR=IQ+K
      IMR=JQ+K
      X=R(ILR)
      R(ILR)=R(IMR)
  180 R(IMR)=X
  185 CONTINUE
      RETURN
      END
```

```
      PROGRAM EIG1(INPUT,OUTPUT,TAPE1,TAPE12)
      COMMON/POOL/SM1(3,3),SM2(3,3),SM3(3,3),SM4(3,3),STEMP1(12,24)
      COMMON/ROT/ROT(13,3,3)
      COMMON/SOLVE/X(78),DIS(85,2),ROS(13),DISM(6),NELR
C THIS PROGRAM READ STIFFNESS DATA FROM TAPE1, EIGENVECTORS FROM TAPE12 AND
C SOLVE FOR THE MOMENTS CORRESPONDING TO EACH MODE OF THE RING
      READ(1)A,A,A,A,A,((A,J=1,2),I=1,85)
      READ(1)A,A
      READ(1)(A,A,((A,K=1,2),J=1,2),I=1,250)
      READ(1)(((ROT(I,J,K),K=1,3),J=1,3),I=1,13)
      READ(1)(A,I=1,85)
      READ(1)((SM1(I,J),SM2(I,J),SM3(I,J),SM4(I,J),J=1,3),I=1,3)
      READ(1)((STEMP1(I,J),J=1,24),I=1,12)
      PRINT 3
 3    FORMAT(*  MOMENT CONFIGURATION OF THE MODE*)
      READ(12)IMOM,JMOM
      READ(12)(A,I=1,IMOM)
      NELR=12
      DO 1 K=1,JMOM
      READ(12)(X(I),I=1,IMOM)
      JJ=JMOM-K+1
      PRINT 4,JJ
 4    FORMAT(//*  MODE*I5)
      DO 2 I=1,NELR
      DIS(I,1)=X(2*I-1)
 2    DIS(I,2)=X(2*I)
      CALL MOMENT
 1    CONTINUE
      END


      SUBROUTINE MOMENT
      COMMON/SOLVE/X(78),DIS(85,2),ROS(13),DISM(6),NELR
      COMMON/ROT/ROT(13,3,3)
      COMMON/POOL/SM1(3,3),SM2(3,3),SM3(3,3),SM4(3,3),STEMP1(12,24)
C THIS SUBROUTINE BACK CALCULATE MOMENT
```

```
C ROS =S22**-1*S21 *DIS =ROTATION AT EACH RING NODE
      DO 1 I=1,NELR
      ROS(I)=0.
      DO 1 K=1,NELR
      ROS(I)=ROS(I)-STEMP1(I,2*K-1)*DIS(K,1)-STEMP1(I,2*K)*DIS(K,2)
 1    CONTINUE
      DO 7 M=1,NELR
C ROTATE DIS BACK TO DISM, LOCAL COORD
      DO 2 J=1,2
      DISM(J)=DISM(J+3)=0.
      DO 2 K=1,2
      DISM(J)=DISM(J)+ROT(M,J,K)*DIS(M,K)
      IF(M.EQ.NELR)GO TO 5
      DISM(J+3)=DISM(J+3)+ROT(M+1,J,K)*DIS(M+1,K)
      GO TO 2
 5    DISM(J+3)=DISM(J+3)+ROT(M+1,J,K)*DIS(1,K)
 2    CONTINUE
      DISM(3)=ROS(M)
      IF(M.EQ.NELR)DISM(6)=ROS(1)
      IF(M.EQ.NELR)GO TO 6
      DISM(6)=ROS(M+1)
C NOW BACK CALCULATE MOMENT=RM
 6    RM1=RM2=0.
      DO 3 K=1,3
      RM1=RM1+SM1(3,K)*DISM(K)+SM2(3,K)*DISM(K+3)
      RM2=RM2+SM3(3,K)*DISM(K)+SM4(3,K)*DISM(K+3)
 3    CONTINUE
      PRINT 4,M,RM1,RM2
 4    FORMAT(* MEMBER*I5,*    MOMENT 1=*F20.5,*    MOMENT 2=*F20.5)
 7    CONTINUE
      RETURN
      END
```

```
      PROGRAM SRIGFQ1(INPUT,OUTPUT,TAPE1,TAPE4)
C THIS PROGRAM TRANSFORMS THE STIFFNESS AND MASS MATRIX READ FROM TAPE1 INTO
C RIGID CYLINDER STIFFNESS AND MASS MATRIX

C DIMENSIONED HERE IS FOR A MAX OF IR=RING NODE=20 ,IS=SOIL NODE=45
C DIMENSION DEPENDENT ON IR $ IS ARE AS BELOW
C ROT(IR+1,3,3),A(2*IS+3,2*IS+3),B(2*(IR+IS),2*(IR+IS)),D(2*IS+3)*(2*IS
C +4)/2),R(2*IS+3)*(2*IS+3)),T(2*IR,3),KT(2*IR,3),TK(3,2*IS),PERIOD,
C AMASS FQCY, VALU,X ALL DIMENSIONED 2*IS+3
      DIMENSION NI(600),NJ(600),STIFF(600,2,2),WM(85),ROT(21,3,3)
      DIMENSION T(40,3),KT(40,3),TKT(3,3),TK(3,90),B(130,130)
      DIMENSION A(93,93),AMASS(93)
      READ 1,IR,IS,RADIUS
 1    FORMAT(2I5,F10.5)
      PRINT 2,IR,IS,RADIUS
 2    FORMAT(*  NO OF RING NODE=*I5,*   NO OF SOIL NODE=*I5,*   RING RAD
     1IUS=*F10.5)
      READ(1)NEW,NCOUNT
      READ(1)(NI(I),NJ(I),((STIFF(I,J,K),K=1,2),J=1,2),I=1,600)
      READ(1)(((ROT(I,J,K),K=1,3),J=1,3),I=1,21)
      READ(1)(WM(I),I=1,85)
C GENERATE STIFFNESS MATRIX A
      N=2*(IR+IS)
      DO 107 I=1,N
      DO 107 J=1,N
 107  B(I,J)=0.
      I=0
      N1=IR+IS
      NCO=1
 103  I=I+1
      IF(NI(NCO).GT.I)GO TO 102
      DO 104 J=I,NEW
      IF(NI(NCO).GT.I)GO TO 102
      IF(NJ(NCO).GT.N1)GO TO 105
      NII=2*(NI(NCO)-1)
      NIJ=2*(NJ(NCO)-1)
```

```
      DO 106 II=1,2
      DO 106 IJ=1,2
 106  B(NII+II,NIJ+IJ)=STIFF(NCO,II,IJ)
 105  NCO=NCO+1
 104  CONTINUE
 102  IF(I.LT.N1)GO TO 103
      DO 202 I=1,N
      DO 202 J=I,N
 202  B(J,I)=B(I,J)
C GENERATE TRANSFORMATION MATRIX T FOR CHANGING FROM RIGID 3 DEG OF FREE
C DISPLACEMENT TO RING NODE DISPLACEMENT
      IR2=2*IR
      IS2=2*IS
      DO 3 I=1,IR2
      DO 3 J=1,3
 3    T(I,J)=0.
      DO 4 I=1,IR
      T(2*I-1,1)=1.
      T(2*I,2)=1.
      T(2*I-1,3)=-ROT(I,1,1)*RADIUS
 4    T(2*I,3)=-ROT(I,1,2)*RADIUS
C NOW GET T TRNPOSED* KRR * T
      DO 5 I=1,IR2
      DO 5 J=1,3
      KT(I,J)=0.
      DO 5 K=1,IR2
      KT(I,J)=KT(I,J)+B(I,K)*T(K,J)
 5    CONTINUE
      DO 6 I=1,3
      DO 6 J=1,3
      TKT(I,J)=0.
      DO 6 K=1,IR2
 6    TKT(I,J)=TKT(I,J)+T(K,I)*KT(K,J)
C NOW GET T TRANSPOSED * KRS
      DO 7 I=1,3
      DO 7 J=1,IS2
```

```
      TK(I,J)=0.
      DO 7 K=1,IR2
 7    TK(I,J)=TK(I,J)+T(K,I)*B(K,J+IR2)
C NOW GET THE  REAL RIGID RING SOIL STIFFNESS MATRIX ,A
      DO 8 I=1,3
      DO 8 J=1,3
 8    A(I,J)=TKT(I,J)
      DO 9 I=1,3
      DO 9 J=1,IS2
 9    A(I,3+J)=TK(I,J)
      DO 10 I=1,IS2
      DO 10 J=1,IS2
 10   A(3+I,3+J)=B(IR2+I,IR2+J)
C N IS DEGREE OF FREEDOM FOR THE EIGEN PROBLEM
      N=3+IS2
      DO 11 I=4,N
      DO 11 J=1,3
 11   A(I,J)=A(J,I)
      AMASS(1)=IR*WM(1)
      AMASS(2)=AMASS(1)
      AMASS(3)=AMASS(1)*RADIUS**2
      DO 12 I=1,IS
      AMASS(3+2*I-1)=WM(IR+I)
 12   AMASS(3+2*I)=WM(IR+I)
      WRITE(4)N
      WRITE(4)((A(I,J),I=1,N),J=1,N),(AMASS(I),I=1,N)
      END
```

Package SRIGFQ2 This package also includes subroutine EIGEN given earlier in package FQTA1

```
      PROGRAM SRIGFQ2(INPUT,OUTPUT,TAPE4,TAPE2)
C THIS PROGRAM READS IN RIGID CYLINDER STIFFNESS AND MASS MATRIX AND
C GET THE FREQUENCIES AND MODE SHAPES

C DIMENSIONED HERE IS FOR A MAX OF IR=RING NODE=20, IS=SOIL NODE=45
C DIMENSION DEPENDENT ON IR $ IS ARE AS BELOW
C ROT(IR+1,3,3),A(2*IS+3,2*IS+3),B(2*(IR+IS),2*(IR+IS)),D(2*IS+3)*(2*IS
C +4)/2),R(2*IS+3)*(2*IS+3)),T(2*IR,3),KT(2*IR,3),TK(3,2*IS),PERIOD,
C AMASS FQCY, VALU,X ALL DIMENSIONED 2*IS+3
      COMMON/EIGEN/A(93,93),D(4371),N
      DIMENSION R(8649)
      DIMENSION PERIOD(93),AMASS(93),FQCY(93),VALU(93),X(93)
      EQUIVALENCE(A(1,1),R(1))
      READ(4)N
      READ(4)((A(I,J),I=1,N),J=1,N),(AMASS(I),I=1,N)
      PRINT 49
      DO 23 I=1,N
      DO 23 J=1,N
 23   A(I,J)=A(I,J)/(ABS(SQRT(AMASS(I)*AMASS(J))))
C PUT LOWER DIAGONAL OF A INTO 1 DIMENSIONAL ARRAY D BY ROW
      MARK=0
      DO 108 I=1,N
      DO 108 J=1,I
      MARK=MARK+1
      D(MARK)=A(I,J)
 108  CONTINUE
      CALL EIGEN(D,R,N,0)
C NOW GET THE EIGENVALUE $ PUT IN ARRAY VALU
      DO 32 J=1,N
      JJ=(J*J+J)/2
 32   VALU(J)=D(JJ)
      TWOPI=6.28318
      DO 24 I=1,N
 24   FQCY(I)=(ABS(SQRT(VALU(I))))/TWOPI
      DO 100 I=1,N
  100 PERIOD(I)=1./FQCY(I)
```

```
      PRINT 56
      DO 25 I=1,N
   25 PRINT 52,VALU(I),FQCY(I),PERIOD(I)
C NOW GET THE EIGEN VECTOR OUT FROM ONE DIMENSIONAL ARRAY R
      PRINT 58
C JMOM IS THE NO OF FREQ DESIRED ,IMOM IS NO OF ELEMENT IN THE MODE DESI
      JMOM=N
      IMOM=N
      WRITE(2)IMOM,JMOM
      KMAX=0
      LASTJ=N-JMOM+1
      WRITE(2)LASTJ,N
      WRITE(2)(FQCY(I),I=LASTJ,N)
      DO 35 J=1,N
      KMIN=KMAX+1
      KMAX=KMAX+N
      I=0
      DO 36 K=KMIN,KMAX
      I=I+1
      X(I)=R(K)
 36   X(I)=X(I)/(ABS(SQRT(AMASS(I))))
      JJ=N-J+1
      PRINT 63,JJ,(X(I),I=1,N)
 63   FORMAT(*  MODE*I5,/(10F12.5))
C NOW WRITE ON TAPE2 THE FIRST 3*IR EIGEN VECTORS FOR MOMENT ANALYSIS
      IF(JJ.GT.JMOM)GO TO 35
      WRITE(2)(X(I),I=1,IMOM)
 35   CONTINUE
 49   FORMAT(*  RESULT FOR AX= LAMDA BX RIGID RING CASE*///)
   50 FORMAT(///* MASS ELEMENTS*/)
   52 FORMAT(F12.4,2F14.5)
   56 FORMAT(///*  EIGENVALUE*5X*FREQUENCY*8X*PERIOD*/)
   58 FORMAT(///* MODES NORMALIZED WITH RESPECT TO MASS AS ROW VECTOR*/)
 60   FORMAT((10E12.5))
      END
```

Package EIGRIG2 This package also includes subroutine EQ given earlier in package RIG20

```
      PROGRAM EIGRIG 2(INPUT,OUTPUT,TAPE1,TAPE2)
C THIS PROGRAM READS STIFFNESS DATA FROM TAPE1, EIGENVECTORS FROM TAPE2
C IT THEN SOLVES FOR THE MODAL MOMENT OF THE RIGID CYLINDER

      DIMENSION DIS(24,2),X(57),WM(85),FQCY(63)
      COMMON/ADD2/FX(12),FY(12),FLEX(12,3,3),TRF(12,3,2),CORD(85,2),TR(3
     1,3)
      COMMON/STIFF/NELR,NI(250),NJ(250),STIFF(250,2,2),ROT(13,3,3)
      READ(1)R,E1,V1,ZI,A,((CORD(I,J),J=1,2),I=1,85)
      READ(1)Z,Z
      READ(1)(NI(I),NJ(I),((STIFF(I,J,K),K=1,2),J=1,2),I=1,250)
      READ(1)(((ROT(I,J,K),K=1,3),J=1,3),I=1,13)
      READ(1)(WM(I),I=1,85)
      READ(2)IMOM,JMOM
      READ(2)LASTJ,N
      READ(2)(FQCY(I),I=LASTJ,N)
      NELR=12
      PRINT 3,R,E1,V1,ZI,A
 3    FORMAT(*  RING PROPERTY  R=*F6.3,*   E1=*E12.6,*   V1=*F5.3,
     1 *   ZI=*F12.10,*   A=*F10.8)
      PRINT 409
 409  FORMAT(* NODE*5X*CORD1*5X*CORD2*)
      DO 407 I=1,NELR
 407  PRINT 408,I,(CORD(I,J),J=1,2)
 408  FORMAT(I5,2F10.2)
C FLEX(I,J,K)=FLEXIBILITY MATRIX FOR POINT I,WHERE LOAD IS APPLIED, USED
C IN SUBROUTINE RMOM
      ALP=2.*3.14159/NELR
      DO 27 I=1,NELR
      AL=ALP*I
      FLEX(I,1,1)=R**3.*(6.*AL-8.*SIN(AL)+SIN(2.*AL))/(4.*E1*ZI)+R*(2.*
     1 AL+SIN(2.*AL))/(4.*A*E1)
      FLEX(I,1,2)=-1.*R**3.*(1.-COS(AL))**2./(2.*E1*ZI)+R*(1.-COS(2.*AL)
     1)/(4.*A*E1)
      FLEX(I,1,3)=-1.*R**2.*(AL-SIN(AL))/(E1*ZI)
      FLEX(I,2,2)=R**3.*(2.*AL-SIN(2.*AL))/(4.*E1*ZI)+R*(2.*AL-SIN(2.*AL
```

```
     1))/(4.*A*E1)
      FLEX(I,2,3)=R**2.*(1.-COS(AL))/(E1*ZI)
      FLEX(I,3,3)=R*AL/(E1*ZI)
      FLEX(I,2,1)=FLEX(I,1,2)
      FLEX(I,3,1)=FLEX(I,1,3)
      FLEX(I,3,2)=FLEX(I,2,3)
C NOW ROTATE THE FLEXIBILITY MATRIX TO GLOBAL COORDINATE, TR=FLEX*ROT
      DO 30 J=1,3
      DO 30 K=1,3
      TR(J,K)=0.
      DO 30 L=1,3
 30   TR(J,K)=TR(J,K)+FLEX(I,J,L)*ROT(I+1,L,K)
C FLEX=ROT**-1*TR
      DO 31 J=1,3
      DO 31 K=1,3
      FLEX(I,J,K)=0.
      DO 31 L=1,3
 31   FLEX(I,J,K)=FLEX(I,J,K)+ROT(I+1,L,J)*TR(L,K)
      IF(I.EQ.NELR)GO TO 27
C FOR NODE 1,SKIP PROCEDURE BELOW $ USE FLEX (NELR,3,3) IN EQ LATER ON
      DO 28 J=1,3
      DO 28 K=1,3
 28   TR(J,K)=0.
      TR(1,1)=TR(2,2)=TR(3,3)=1.
      TR(1,3)=-1.*(CORD(1,2)-CORD(I+1,2))
      TR(2,3)=CORD(1,1)-CORD(I+1,1)
C TRF(3,2)=TR(3,3)*FLEX(3,2)  USING ONLY 3*2 PORTION OF FLEX
      DO 29 J=1,3
      DO 29 K=1,2
      TRF(I,J,K)=0.
      DO 29 L=1,3
 29   TRF(I,J,K)=TRF(I,J,K)+TR(J,L)*FLEX(I,L,K)
 27   CONTINUE
C NOW PUT FLEX(NELR,3,3) IN TR(3,3)
      DO 32 I=1,3
      DO 32 J=1,3
```

```
 32    TR(I,J)=FLEX(NELR,I,J)
C FIRST GET THE FREQUENCY IN RADIAN /SEC
       DO 40 I=LASTJ,N
 40    FQCY(I)=FQCY(I)*2.*3.14159
C NOW BEGIN CALCULATE MOMENT. LOOP K=1,JMOM EACH K FOR CORRESPONDING MOD
       DO 4 K=1,JMOM
       READ(2)(X(I),I=1,IMOM)
       JJ=JMOM-K+1
       PRINT 6,JJ,(X(I),I=1,IMOM)
 6     FORMAT(//*  MODE*I5,*  EIGENVECTOR AS BELOW*/(10F12.5))
C TRANSFER THE 3 DEGREE FREEDOM RIGID RING DISPLACEMENT TO NODE DISPLACE
       DO 5 I=1,NELR
       DIS(I,1)=X(1)-ROT(I,1,1)*R*X(3)
 5     DIS(I,2)=X(2)-ROT(I,1,2)*R*X(3)
C GET THE OUTER PACKING DISPLACEMENT FROM THE ELEMENT OF THE EIGENVECTOR
       N2=2*NELR
       N1=NELR+1
       DO 7 I=N1,N2
       DIS(I,1)=X(2*(I-NELR)+2)
 7     DIS(I,2)=X(2*(I-NELR)+3)
C NOW GET FORCES IN X $ Y DIRECTION, FX FY,AT EACH NODE
       NCO=1
       DO 300 I=1,NELR
       FX(I)=FY(I)=0.
       NELRI=NELR+I
 302   IF(NI(NCO).EQ.I.AND.NJ(NCO).EQ.NELRI)GO TO 303
       NCO=NCO+1
       GO TO 302
 303   DO 300 J=1,2
       FX(I)=FX(I)-STIFF(NCO,1,J)*(DIS(NELRI,J)-DIS(I,J))
       FY(I)=FY(I)-STIFF(NCO,2,J)*(DIS(NELRI,J)-DIS(I,J))
 300   CONTINUE
C NOW ADD THE TRANSLATIONAL DALEMBERT FORCE AT EACH NODE
       DO 304 I=1,NELR
       FX(I)=FX(I)+WM(I)*FQCY(LASTJ+K-1)**2*DIS(I,1)
 304   FY(I)=FY(I)+WM(I)*FQCY(LASTJ+K-1)**2*DIS(I,2)
```

```
C NOW ADD THE ROTATIONAL DALEMBERT FORCE
      EMOM=0.
C ROTATE TO MEMBER COORDINATE
      DO 14 I=1,NELR
      FMX=ROT(I,1,1)*FX(I)+ROT(I,1,2)*FY(I)
      FMY=ROT(I,2,1)*FX(I)+ROT(I,2,2)*FY(I)
C FIND UNEQULIBRATED MOMENT
      EMOM=EMOM+FMX*R
 14   CONTINUE
C ADD FORCE AT NODES TO TAKE CARE OF UNEQUILIBRATED MOMENT
      EFORCE=-EMOM/(NELR*R)
      DO 404 I=1,NELR
      FX(I)=ROT(I,1,1)*EFORCE+FX(I)
      FY(I)=ROT(I,1,2)*EFORCE+FY(I)
 404  CONTINUE
      CALL RMOM
 4    CONTINUE
      END


      SUBROUTINE RMOM
      DIMENSION U(3),Y(3),FO(3),RM(12)
      COMMON/ADD2/FX(12),FY(12),FLEX(12,3,3),TRF(12,3,2),CORD(85,2),TR(3
     1,3)
      COMMON/STIFF/NELR,NI(250),NJ(250),STIFF(250,2,2),ROT(13,3,3)
      U(1)=U(2)=U(3)=0.
      DO 2 I=1,NELR
      IF(I.EQ.NELR)GO TO 2
C FOR NODE 1,SKIP PROCEDURE BELOW $ USE FLEX IN THE SOLUTION OF SIMULTAN
C EQUATION
C U(3)=TRF(3,2)*F(2) AND ADD THIS TO U(3) FROM PREVOUS NODE
      DO 5 J=1,3
      U(J)=U(J)+TRF(I,J,1)*FX(I+1)+TRF(I,J,2)*FY(I+1)
 5    CONTINUE
 2    CONTINUE
```

```
 7     DO 9 I=1,3
 9     Y(I)=-U(I)
C PUT FLEX(NELR,3,3) IN TR(3,3)
       DO 32 I=1,3
       DO 32 J=1,3
 32    TR(I,J)=FLEX(NELR,I,J)
       CALL EQ(TR,FO,Y,3,3)
C NOW THAT FO ARE KNOWN, SOLVE FOR MOMENT RM AT THE NODES
       NU=0
       DO 10 I=2,NELR
       II=NELR-(I-2)
       NU=NU+1
       RM(II)=-FO(3)+FO(1)*(CORD(1,2)-CORD(II,2))-FO(2)*(CORD(1,1)-
      1  CORD(II,1))
       IF(NU.EQ.1)GO TO 10
       DO 13 J=2,NU
       NODE=NELR-(J-2)
       RM(II)=RM(II)+FX(NODE)*(CORD(NODE,2)-CORD(II,2))-FY(NODE)*
      1  (CORD(NODE,1)-CORD(II,1))
 13    CONTINUE
 10    CONTINUE
       RM(1)=-FO(3)
       DO 11 I=1,NELR
 11    PRINT 12,I,RM(I)
 12    FORMAT(*  NODE*I5,*    MOMENT =*F20.5)
       RETURN
       END
```

```
      PROGRAM PA(INPUT,OUTPUT,TAPE4,TAPE2,TAPE6)
      DIMENSION A(102,102),AMASS(102),FQCY(77),X(77),D(77,25),CX(77),CY(
     177),DDAT(77,6),T(25,6)
C DIMENSIONED ABOVE FOR A MAX OF NFULL=OVERALL DEG OF FREEDOM INCLUDING
C RIGID RING =102, IS=INTERIOR SOIL NODE =37 DIMENSION SHOULD BE
C A(NFULL*2,NFULL*2),AMASS(NFULL*2),FQCY $ X(3+2*IS),D(3+2*IS,NFULL-N)
C DDAT(3+2*IS,DEG OF INDEP VARIABLE THE BOUNDARY IS INTERPOLATED FROM)
C T(NFUL-N,DEG OF INDEP VARIABLE)
C READ STIFFNESS $ MASS $ NFULL
      READ(4)NFULL
      READ(4)((A(I,J),I=1,NFULL),J=1,NFULL),(AMASS(I),I=1,NFULL)
      PRINT 9
 9    FORMAT(*  BELOW IS THE FIRST 5 ROWS OF K MATRIX FOR CHECK*)
      DO 8 I=1,5
 8    PRINT 10,(A(I,J),J=1,NFULL)
 10   FORMAT(10F12.3)
C READ INFREQ AND MODE SHAPE, N IS DEG OF FREEDOM NOT INCLUDING
C BOUNDARY NODES ,NBOUN IS DEG OF FREEDOM OF BOUNDARY NODES
C READ OR PUT IN BY ANY MEAN THE TRANSFORMATION MATRIX T
      DO 7 I=1,18
      DO 7 J=1,6
 7    T(I,J)=0.
      T(1,1)=T(9,1)=T(17,1)=T(2,2)=T(10,2)=T(18,2)=1./3.
      T(1,3)=T(9,3)=T(17,3)=T(2,4)=T(10,4)=T(18,4)=2./3.
      T(5,3)=T(13,3)=T(6,4)=T(14,4)=2./5.
      T(7,3)=T(15,3)=T(8,4)=T(16,4)=14./15.
      T(3,5)=T(11,5)=T(4,6)=T(12,6)=1.
      T(5,5)=T(13,5)=T(6,6)=T(14,6)=3./5.
      T(7,5)=T(15,5)=T(8,6)=T(16,6)=1./15.
      READ(2)IMOM,JMOM
      READ(2)LASTJ,N
      READ(2)(FQCY(I),I=LASTJ,N)
      NBOUN=NFULL-N
C GET THE MODE PARTICIPATION FACTOR D(I,J) I IS MODE NO, J REFERS TO
C BOUNDARY NODE DEG OF FREEDOM . ALSO CX(I) $ CY(I)
      WRITE(6)N,NBOUN
```

```
      PRINT 5
 5    FORMAT(/* MODE PARTICIPATION FACTOR CX,CY AND D*)
      DO 1 I=1,N
C READ IN MODE SHAPE ,JJ IS MODE NO
      READ(2)(X(K),K=1,IMOM)
C NOW GET THE BI VALUE AS A DENOMINATOR FOR CASE OF UNNORMALIZED EIGENVECTOR
      BI=0.
      DO 11 K=1,N
 11   BI=BI+X(K)**2*AMASS(K)
      JJ=N-I+1
      DO 2 J=1,NBOUN
      D(I,J)=0.
      DO 2 K=1,N
      D(I,J)=D(I,J)+X(K)*A(K,J+N)
 2    CONTINUE
      DO 6 J=1,6
      DDAT(I,J)=0.
      DO 6 K=1,18
 6    DDAT(I,J)=DDAT(I,J)+D(I,K)*T(K,J)
      CX(I)=X(1)*AMASS(1)
      CY(I)=X(2)*AMASS(2)
      NHALF=(N-3)/2
      DO 3 K=1,NHALF
      CX(I)=CX(I)+X(2*K+2)*AMASS(2*K+2)
      CY(I)=CY(I)+X(2*K+3)*AMASS(2*K+3)
 3    CONTINUE
C NOW DIVIDE EVERYTHING BY BI
      CX(I)=CX(I)/BI
      CY(I)=CY(I)/BI
      DO 12 J=1,6
 12   DDAT(I,J)=DDAT(I,J)/BI
      WRITE(6)JJ,CX(I),CY(I),(DDAT(I,J),J=1,6)
      PRINT 4,JJ,CX(I),CY(I),(DDAT(I,J),J=1,6)
 4    FORMAT(*  MODE*I5,*  CX=*F15.8,*  CY=*F15.8,*  D VECTOR IS BELOW*/
     1 (8F15.8))
 1    CONTINUE
      END
```

```
      PROGRAM TNORM4(INPUT,OUTPUT,TAPE2,TAPE3,TAPE6,TAPE8)
C THIS PROGRAM IS TO TEST NORMAL $ DIRECT INTEGRATION METHOD
C DELTAT FOR ALL MODES IS THE SAME AS DELTAT FOR DIRECT INTEGRATION
      DIMENSION CX(57),CY(57),D(57,6),FQCY(57),DAMP(57),WA(2,50)
      DIMENSION WV(3,2,50),WVV(3,2,50),AREAL(57,50),ADD(57),ADDOLD(57),
     1 A(57),AD(57)
      DIMENSION ABD(57,3,2),ABV(57,3,2),ACX(57),ACY(57),ABDMAX(57,3,2)
      DIMENSION ABVMAX(57,3,2),ACXMAX(57),ACYMAX(57)
C INITIALIZE MAXIMUM VALUE
      DO 29 L=1,57
      ACXMAX(L)=ACYMAX(L)=0.
      DO 29 J=1,3
      DO 29 K=1,2
 29   ABDMAX(L,J,K)=ABVMAX(L,J,K)=0.
      READ 2,FTR,TEND,PINTER,PINTE2
 2    FORMAT(8F10.5)
      READ(6)B,B
      DO 1 I=1,57
      II=57-I+1
 1    READ(6)B,CX(II),CY(II),(D(II,J),J=1,6)
      READ(2)IMOM,JMOM
      READ(2)LASTJ,N
C********* READ IN FQCY(I), I BEING THE REAL MODE NUMBER
      READ(2)(FQCY(N-I+1),I=LASTJ,N)
C TURN FREQ INTO RADIAN/SEC ,ALSO GET THE MODAL DAMPING RATIO
      DO 3 I=1,57
      FQCY(I)=2.*3.1415927*FQCY(I)
 3    DAMP(I)=FTR*FQCY(I)/2.
      READ(3)NB,NA,NNDS,DELTAT,NT,N,NSPG
C READ INITIAL VALUE AT TIME=0
      DO 4 J=1,2
 4    READ(3)WA(J,1),(WV(I,J,1),I=1,3),(WVV(I,J,1),I=1,3)
C INITIALIZE ACCELERATION
      NO=N-NSPG+1
      DO 5 L=1,57
      ADD(L)=0.
```

```
      DO 6 J=1,NO
      DO 6 K=1,2
      ADD(L)=ADD(L)-D(L,2*(J-1)+K)*WV(J,K,1)-FTR*D(L,2*(J-1)+K)*
     1 WVV(J,K,1)
 6    CONTINUE
      ADD(L)=ADD(L)-CX(L)*WA(1,1)-CY(L)*WA(2,1)
      ADDOLD(L)=ADD(L)
 5    CONTINUE
C INITIALIZE DISP $ VEL
      DO 7 L=1,57
 7    A(L)=AD(L)=0.
C BEGIN INTEGRATION
      NUMB=1
      NT=PINTER/DELTAT
      NT2=PINTE2/DELTAT
      MARK=50
      MARKP=0
      MARKP2=0
 700  DNUM=DELTAT*NUMB
      IF(DNUM.GE.TEND)GO TO 998
      IF(MARK.NE.50)GO TO 26
C READ 50 STEP TIME ALL AT ONCE
      READ(3)(((WA(J,L),((WV(I,J,L),WVV(I,J,L)),I=1,3)),J=1,2),L=1,50)
      IF(EOF(3))998,999
 999  MARK=0
 26   MARK=MARK+1
      DO 8 L=1,57
      U=0.
      DO 9 J=1,NO
      DO 9 K=1,2
      ABD(L,J,K)=D(L,2*(J-1)+K)*WV(J,K,MARK)
      ABV(L,J,K)=FTR*D(L,2*(J-1)+K)*WVV(J,K,MARK)
      U=U+ABD(L,J,K)+ABV(L,J,K)
 9    CONTINUE
      ACX(L)=CX(L)*WA(1,MARK)
      ACY(L)=CY(L)*WA(2,MARK)
```

```
      U=U+ACX(L)+ACY(L)
      A(L)=A(L)+DELTAT*AD(L)+.5*DELTAT**2*ADD(L)
      ADD(L)=-U-(FQCY(L)**2*A(L))-(2.*DAMP(L)*FQCY(L)*AD(L))
      AD(L)=AD(L)+.5*DELTAT*(ADDOLD(L)+ADD(L))
      ADDOLD(L)=ADD(L)
      AREAL(L,MARK)=A(L)
 8    CONTINUE
C CHECK FOR MAX
      DO 31 L=1,57
      CHECK=ABS(ACX(L))-ACXMAX(L)
      IF(CHECK.LE.0)GO TO 37
      ACXMAX(L)=ABS(ACX(L))
 37   CHECK=ABS(ACY(L))-ACYMAX(L)
      IF(CHECK.LE.0)GO TO 36
      ACYMAX(L)=ABS(ACY(L))
 36   DO 31 J=1,3
      DO 31 K=1,2
      CHECK=ABS(ABD(L,J,K))-ABDMAX(L,J,K)
      IF(CHECK.LE.0)GO TO 33
      ABDMAX(L,J,K)=ABS(ABD(L,J,K))
 33   CHECK=ABS(ABV(L,J,K))-ABVMAX(L,J,K)
      IF(CHECK.LE.0)GO TO 31
      ABVMAX(L,J,K)=ABS(ABV(L,J,K))
 31   CONTINUE
      IF(MARK.NE.50)GO TO 23
      WRITE(8)((AREAL(L,J),L=1,57),J=1,50)
 23   MARKP=MARKP+1
      IF(MARKP.LT.NT)GO TO 25
      PRINT 10,DNUM,(A(L),L=1,57)
 10   FORMAT(* TIME*F10.5,* AREAL=*/(10F13.6))
      MARKP=0
 25   CONTINUE
      MARKP2=MARKP2+1
      IF(MARKP2.LT.NT2)GO TO 43
      MARKP2=0
      DO 30 J=1,3
```

```
      DO 30 K=1,2
30    PRINT 34,J,K,(ABD(L,J,K),L=1,57)
34    FORMAT(* ABD,FINAL AREAL DUE TO BOUNDARY DISP FOR J=*I3,*  K=*I3,
     1 /(8F16.6))
      DO 32 J=1,3
      DO 32 K=1,2
32    PRINT 35,J,K,(ABV(L,J,K),L=1,57)
35    FORMAT(* ABV,FINAL AREAL DUE TO BOUNDARY VEL FOR J=*I3,*  K=*I3,
     1 /(8F16.6))
      PRINT 38,(ACX(L),L=1,57)
38    FORMAT(* ACX,FINAL AREAL DUE TO HORIZONTAL ACC*/(8F16.6))
      PRINT 39,(ACY(L),L=1,57)
39    FORMAT(* ACY,FINAL AREAL DUE TO VERTICAL ACC*/(8F16.6))
43    CONTINUE
      NUMB=NUMB+1
      GO TO 700
998   PRINT 40
40    FORMAT(//////30X*BELOW ARE MAXIMUM VALUE FOR THE WHOLE RUN*//////)
      DO 41 J=1,3
      DO 41 K=1,2
41    PRINT 34,J,K,(ABDMAX(L,J,K),L=1,57)
      DO 42 J=1,3
      DO 42 K=1,2
42    PRINT 35,J,K,(ABVMAX(L,J,K),L=1,57)
      PRINT 38,(ACXMAX(L),L=1,57)
      PRINT 39,(ACYMAX(L),L=1,57)
      END
```

```
      PROGRAM DINORM4(INPUT,OUTPUT,TAPE2,TAPE5,TAPE8)
      DIMENSION FQCY(57),X(57,57),RMO(57,12),DIS(57),DM(12),AREAL(57,50)
      DIMENSION ARMAX(57),RMOTEM(57,12)
C THIS PROGRAM READS AREAL AT EACH DELTAT FROM TAPE8 $ CALCULATE
C DISPLACEMENT $ MOMENT
      DO 12 L=1,57
 12   ARMAX(L)=0.
      READ 1,DELTAT,TEND,PINTER,PINTE2
 1    FORMAT(8F10.5)
      READ(2)IMOM,JMOM
      READ(2)LASTJ,N
      READ(2)(FQCY(N-I+1),I=LASTJ,N)
      DO2 J=1,N
 2    READ(2)(X(I,N-J+1),I=1,IMOM)
      DO 3 I=1,57
      II=57-I+1
 3    READ(5)(RMO(II,J),J=1,12)
      NUMB=1
      NT=PINTER/DELTAT
      NT2=PINTE2/DELTAT
      MARK=50
      MARKP=0
      MARKP2=0
 700  DNUM=DELTAT*NUMB
      IF(DNUM.GE.TEND)GO TO 998
      IF(MARK.NE.50)GO TO 11
      READ(8)((AREAL(L,J),L=1,57),J=1,50)
      IF(EOF(8))998,999
 999  MARK=0
 11   MARK=MARK+1
      DO 4 I=1,57
 4    DIS(I)=0.
      DO 5 I=1,12
 5    DM(I)=0.
      DO 6 L=1,57
      CHECK=ABS(AREAL(L,MARK))-ARMAX(L)
```

```
      IF(CHECK.LE.0)GO TO 14
      ARMAX(L)=ABS(AREAL(L,MARK))
14    CONTINUE
      DO 7 J=1,57
7     DIS(J)=DIS(J)+X(J,L)*AREAL(L,MARK)
      DO 8 J=1,12
      RMOTEM(L,J)=RMO(L,J)*AREAL(L,MARK)
8     DM(J)=DM(J)+RMOTEM(L,J)
6     CONTINUE
      MARKP=MARKP+1
      IF(MARKP.LT.NT)GO TO 25
      PRINT 9,DNUM,(DIS(J),J=1,57)
9     FORMAT(* TIME=*F10.5,*  DISPLACEMENT AS BELOW*/(12F11.7))
      PRINT 10,(DM(J),J=1,12)
10    FORMAT(*  MOMENT BELOW*/(12F11.4))
      MARKP=0
25    CONTINUE
      MARKP2=MARKP2+1
      IF(MARKP2.LT.NT2)GO TO 26
      DO 15 J=1,12
15    PRINT 16,J,(RMOTEM(L,J),L=1,57)
16    FORMAT(* MOMENT BROKEN DOWN BY MODE, NODE *I5,*  MODAL MOMENT BELO
     1W*/(8F16.4))
      MARKP2=0
26    CONTINUE
      NUMB=NUMB+1
      GO TO 700
998   PRINT 997
997   FORMAT(//////30X*BELOW ARE MAX MOMENT OF EACH 12 NODES FOR THE RUN
     1 *)
      DO 996 L=1,57
      DO 995 J=1,12
995   DM(J)=RMO(L,J)*ARMAX(L)
      PRINT 993,L,ARMAX(L)
993   FORMAT(* MODE*I5,*  ARMAX,IE AREAL MAX=*F16.8*  CORRESPONDING MODA
     1L MOMENT BELOW*)
```

```
      PRINT 994,(DM(J),J=1,12)
994   FORMAT(8F16.4)
996   CONTINUE
      END
```